Dissecting gene metabolite relationships in the *Medicago truncatula* terpenome after *Aphanomyces euteiches* infection

Dissertation

zur Erlangung des

Doktorgrades der Naturwissenschaften (Dr. rer.nat.)

der

Naturwissenschaftlichen Fakultät 1- Biowissenschaften

der Martin-Lurther-Universität

Halle-Wittenberg

vorgelegt

von Frau Esther Armah Harding

Gutachter

1. Prof. Dr. Bettina Hause
2. Prof. Dr. Dorothea Tholl
3. Prof. Dr. Alain Tissier

Tag der Verteidigung: 02.12.2025, Halle (Saale)

"Do all the good you can. By all the means you can. In all the ways you can. In all the places you can. At all the times you can. To all the people you can. As long as ever you can."

John Wesley

Table of contents

Abbreviations

Ae	*Aphanomyces euteiches*
bp	Base pair
CDS	Coding sequence
CYP	Cytochrome P450 enzyme
BLAST	Basic local alignment search tool
DsRed	Discosoma sp. red fluorescent protein
DEGs	Differentially expressed genes
DMAPP	Dimethylallyl diphosphate
DXP	1-deoxylulose 5-phosphate
DMSO	Dimethyl sulfoxide
ETI	Effector triggered immunity
FPP	Farnesyl diphosphate
GA-3P	Glyceraldehyde-3-phosphate
GPP	Geranyl diphosphate
GGPP	Geranylgeranyl diphosphate
GC-MS	Gas chromatography-mass spectrometry
GFP	Green fluorescent protein
GO	Gene ontology
HMGC-CoA	Hydroxymethylglutaryl-CoA
KEGG	Kyoto Encyclopedia of Genes and Genomes
LC-MS	Liquid chromatography mass spectrometry
Lj	*Lotus japonicus*
Lys-M	Lysin motif
LYK	LysM domain containing receptor-like kinases
MeJA	Methyl jasmonate
MEP	2-C-methyl-D-erythritol 4-phosphate pathway
min	Minute
MVA	Mevalonate pathway
NDP	Neryl diphosphate
PCA	Principal component analysis
PR	Pathogenesis related

PTI	Pattern triggered immunity
qRT-PCR	Quantitative reverse-transcription PCR
rRNA	Ribosomal RNA
SARDI	South Australian Research and Development Institute
TPS	Terpene synthase
VOCs	Volatile organic compounds
WT	Wildtype
IPTG	Isopropyl -β-D-thiogalacto-pyranoside

List of Figures

List of tables

1 Introduction

Plants exhibit an extraordinary importance as a source of nutrients for many organisms, including humans, animals, and microbes. Throughout human existence, plants have been a fundamental source of sustenance, from their use as a primary food source to their medicinal and industrial properties (Beattie & Freeman, 2008). Despite their fame, plants face many challenges as sessile organisms. Their immobility makes them vulnerable to biotic and abiotic stress agents, resulting in an unavoidable decrease in yield and plant growth (Fones et al., 2020; Strange & Scott, 2005). Harnessing how plant systems manipulate their environment to escape danger is undoubtedly the key to sustainable Agriculture.

Recently, the attitude among plant scientists toward plant disease management has changed. Aside from the classical yet significant strategies to control plant diseases, which include practices like the use of resistant varieties, crop rotation, and chemical application (Hassanali et al., 2008; Zhan et al., 2014), more attention is now being paid to developing and improving tools for editing plant genomes (Talakayala et al., 2022), fine-tuning plant transcriptomes, detecting plant pathogens, and risk modeling (Haq et al., 2022). The fundamental reason for this new interest among plant scientists is to meet global food demand, projected to rise by 35% to 56% between 2010 and 2050 (van Dijk et al., 2021). Therefore, the need to establish all-purpose rules to circumvent disease emergence or circumscribe the host range of microbes amid the intricate dynamics of plant-microorganism interactions become indispensable.

1.1 Plant-pathogen interaction

In natural habitats, plants are constantly subjected to a plethora of microorganisms, several of which are responsible for infecting plants and inciting devastating biotic stress. Like other higher organisms, plants display a remarkable diversity of associations with microbes (Jones & Dangl, 2006). At one end of the spectrum is mutualism, as observed between nitrogen-fixing rhizobacteria (Dodds et al., 2024) and arbuscular mycorrhizae (Hause & Fester, 2005). At the other extreme is the parasitism from detrimental microorganisms such as fungi, oomycetes, viruses, and nematodes that kill or colonize plants to obtain nutrients (Hacquard et al., 2017; Iqbal et al., 2021). Throughout human history, plant diseases have been known to have had profound effects on crop production and natural diversity. Issues such as the rust plaquing cereal crops, which required sacrifices to gods in the Roman days, and the Irish potato farming driving mass migration in the 1800s are timeless reminders of the disaster plant diseases can inflict on nature (Dodds et al., 2024).

1.1.1 Plant-pathogen interaction: oomycetes

Fungi and Oomycetes are the two most important plant pathogens threatening global food security and plant resilience (Latijnhouwers et al., 2003). Oomycetes are often inaccurately referred to as fungi due to their similar life cycle. This similarity is mainly attributed to the fact that these taxonomic groups, fungi and oomycetes, have their mycelia and spore formation through sexual or asexual reproduction (Hughes & Grau, 2007; Latijnhouwers et al., 2003). However, despite the behavioral similarities of oomycetes to true fungi (Mycota), phylogenetic studies have shown that oomycetes and fungi belong to two different eukaryotic branches. Based on ribosomal RNA (rRNA) sequences (Kumar & Rzhetsky, 1996; Paquin et al., 1997) and the combination of the deduced amino acid sequences of actin and tubulin (Latijnhouwers et al., 2003), it was shown that oomycetes are a distinct lineage of stramenopile eukaryotes, unrelated to true fungi but closely related to heterokont (golden brown algae) (Figure 1.1A). In contrast, true fungi are known to share a common ancestor with animals (Figure 1.1A) (Baldauf et al., 2000), and oomycetes have evolved to have the ability to infect plants independently of true fungi.

Oomycetes can be distinguished from fungi based on several morphological and physiological parameters. The cell walls of most oomycetes consist primarily of 1,3-β-glucans, some 1,6-β-glucans, and 1,4-β-glucans (cellulose). Chitin, a principal constituent of fungal cell walls, has been detected in small amounts in only a few oomycetes (Badreddine et al., 2008). Also, the fungal hyphae are septate, while oomycete hyphae are coenocytic with diploid nuclei in all stages (Hughes & Grau, 2013). Another striking difference is the production of bi-flagellated motile spores known as zoospores among some specific oomycete species (Beakes et al., 2012). Studies have shown that within oomycetes, the plant-infecting pathogens belong to two lineages (Cooke et al., 2000; Leclerc et al., 2000; Petersen & Rosendahl, 2000; Riethmüller et al., 2000). The first is the Pythiales and Peronsporales lineage, including the genera *Phytophthora* and *Pythium*, and the second is the Saprolegniales lineage, including *Aphanomyces* (Figure 1.1B) (Kamoun, 2001).

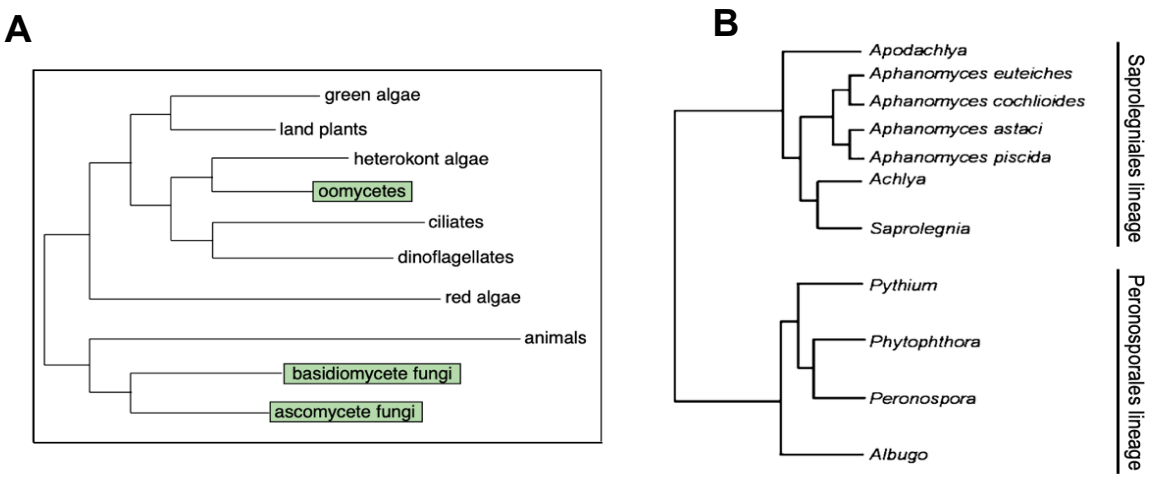

Figure 1.1: Evolutionary relationships between oomycetes and fungi.

A.Phylogenetic tree showing the evolutionary relationships between the major eukaryotic groups. Note the position of the oomycetes (highlighted green) compared with the other eukaryotic plant pathogens (filamentous fungi in the basidiomycetes and ascomycetes) (highlighted in green) (Baldauf et al., 2000). Oomycetes appear as an independent group of plant-pathogenic eukaryotes. **B**. Phylogenetic tree illustrating relationships within the oomycete lineage (Kamoun, 2001).

1.2 Oomycetes: *Phytophthora infestans*

P. infestans, a hemi-biotrophic oomycete, is the causal agent of potato late blight, a disease with a significant historical impact (Dodds et al., 2024; Gorzolka et al., 2021). This pathogen remains number one among the top 10 plant oomycetes (Kamoun et al., 2015). Potato was a central crop in European agriculture, offering twice the calories of rye and wheat per hectare until the emergence of *P. infestans* (Kamoun et al., 2015). The threat of late blight persists as it remains a major problem in potato production, the world's third-largest stable crop (Fisher et al., 2012; Haverkort et al., 2008). The life cycle of *P. infestans* includes both asexual and sexual reproduction (Figure 1.2A) (Leesutthiphonchai et al., 2018). *P. infestans* is heterothallic; sex organs only develop when isolates of opposite mating types sense the sex hormone produced by the mate (Kamoun et al., 2015). The mating types of *P. infestans* are divided into two major mating genotypes termed A1 and A2 (Fry, 2016; Judelson, 2017).

Late blight infection starts when a *P. infestans* spore lands on a leaf, germinates, and penetrates an epidermal cell. The inner cells of the epidermis become colonized, followed by hyphae growth through intercellular layers. The haustorium of the pathogen invaginates the host cell plasma membrane, and this stage is the biotrophic phase of the pathogen colonization in host plants. The pathogen switches to a necrotrophic phase in the plasma membrane, killing plant cells and forming visible necrotrophic lesions on host tissues (Kamoun et al., 2015). The hyphae escape via the stomata and produce asexual spores called sporangia, which can easily be dispersed by wind or water.

The sporangia find a new host, and the disease cycle starts again. However, the sporangium undergoes cleavage in harsh climatic conditions, forming a zoosporangium from which biflagellated spores (zoospores) are produced for long-distance dispersal (Kamoun et al., 2015). Sexual reproduction in *P. infestans* forms spores called oospores, which serve as future inoculum (Judelson & Blanco, 2005). The disease symptoms of the pathogen are not restricted to a specific host tissue. Infected plants exhibit dark blotches on leaf tissues (Figure 1.2B) and stems. Infected tubers develop dark patches and decay rapidly due to secondary infections (Kamoun et al., 2015). *P. infestans* produces numerous effector proteins that suppress host plant defenses. The first reported avirulence effector of *P. infestans* was AVR3a, which interacts with host resistance protein R3a (Armstrong et al., 2005). Comparison of AVR3a with avirulence effectors from other plant pathogenic oomycetes, such as *P. sojae* and *Hyaloperonospora arabidopsidis*, revealed that these pathogens shared conserved motifs RXLR (Arg-X-Leu-Arg) and EER (Glu-Glu-Arg) (Rehmany et al., 2005), which act as signals for translocation into host plants (Whisson et al., 2007). RXLR resides in mutation-prone genome regions, suggesting rapid genome evolution that enables fast adaptation. This genetic variability enables the pathogen to overcome plant defense strategies quickly and adapt to new environments (Coomber et al., 2024; Ivanov et al., 2021). The disease management of *P. infestans* has primarily been the use of fungicides, the breeding of resistant varieties, and the exploitation of RNA interference approaches (Coomber et al., 2024; Ivanov et al., 2021; Leesutthiphonchai et al., 2018). Due to this genetic variation of the pathogen, control strategies have been a concern for potato breeders. The annual cost of controlling the spread of the disease is estimated at billions of dollars due to crop losses and fungicide expenses (Ivanov et al., 2021; Leesutthiphonchai et al., 2018).

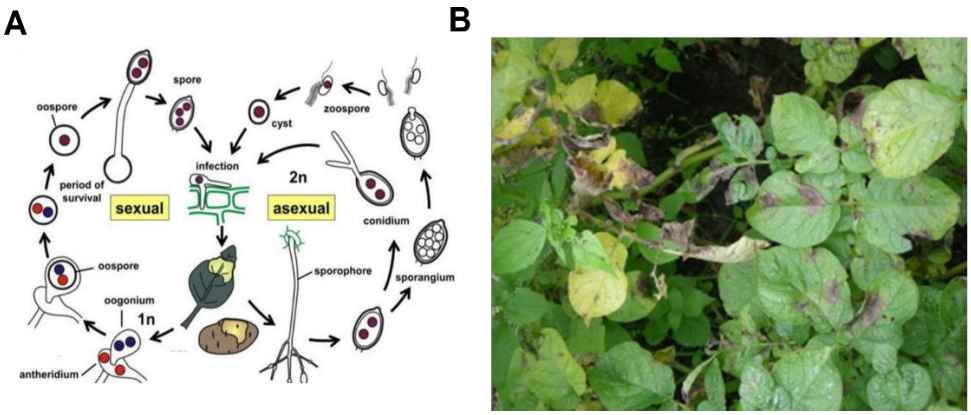

Figure 1.2: The potato pathogen *P. infestans*.

A. Infection cycle of *P. infestans*. **B**. Disease symptoms on the leaves of *an* infected potato plant (Kamoun et al., 2015).

1.3 Oomycetes: *Aphanomyces euteiches*

Among the pathogens of legumes, *A. euteiches* Drechs. (*Saprolegniaceae*), causing root rots of legumes are among the most detrimental pathogens in pea-growing areas in Europe, North America, New Zealand, and Japan (Pilet-Nayel *et al.,* 2009). *Aphanomyces,* a member of the oomycete class, is part of a diverse and extensive eukaryote group that includes water molds (Dick et al., 1999). The popularity of this pathogen has received much attention because of its enormous economic loss in pea production, with a yearly yield loss of 80% (Gaulin et al., 2007). To date, phytopathogenic species of *Aphanomyces* are known to be seedling or root pathogens of diverse crop species (Gaulin, 2007). Some well-documented phytopathogenic *Aphanomyces* include *A. iridis* and *A. cochliodes,* which are pathogens of iris and sugarbeet, respectively, while *A. euteiches* is known to affect several legume crops and is the most destructive soil-borne pathogen of legume plants such as pea and alfalfa (Gaulin et al., 2007). The initial disease symptoms of this pathogen are host roots becoming water-soaked. As the disease progresses, the hypocotyl darkens around the soil line, (Gaulin et al., 2007) followed by the decay of roots, reducing the function of the root system (Zitnick-Anderson et al., 2021). The lifecycle of *A. euteiches* consists of sexual and asexual stages, occurring either in the soil or in its host plant (Gaulin et al., 2007).

Disease cycles initiate after spores land on host plants. After establishing the infection site, coenocytic hyphae develop rapidly in the intercellular spaces of the host root tissue, which leads to the spread of the pathogen to the stem of the host plant (Scott, 1961; Wu et al., 2018). Within a few days of infection, the pathogen enters its sexual stage with the formation and fusion of haploid antheridia (male gametangia) and oogonia (female gametangia) (Figure 1.3), which accelerates the construction of a thick-walled oospore to ensure the long-term survival of the pathogen in the soil to serve as the primary source of inoculum for new infections (Hughes & Grau, 2007; Wu et al., 2018). Both sex gametes arise from the same hyphae, making *A. euteiches* a self-fertile-homothallic pathogen (Hughes & Grau, 2013). In the soil, oospores germinate in response to chemical signals from host roots, producing a germ tube that can grow as hyphae or develop into sporangia. Nuclei (2N), due to the fusion of the male and female gametangium, migrate through the sporangium and develop a cell wall to form primary spores (Hughes & Grau, 2013). Spherical primary spores gather at the apex of the sporangium and release biflagellate zoospores through a pore in the cell wall. These zoospores, equipped with two flagella, move through water-filled soil pores toward host roots. Upon reaching the rhizoplane, they lose their flagella and encyst and germinate. The resulting hyphae penetrate the root tissues to initiate colonization (Hughes & Grau, 2013). As the host tissue deteriorates, the hyphae differentiate into antheridia and oogonia, producing new oospores, and the entire cycle starts again (Hughes & Grau, 2013).

No known effective fungicides (Griffith et al., 1992) nor resistant cultivars are available to curb losses caused by *A. euteiches* (Gaulin et al., 2007). To prevent losses caused by *A. euteiches*, cultural or prophylactic methods such as crop rotation and bioassay methods to detect potential inoculum in the soil before sowing seem to be the only way to control the pathogen (Vandemark et al., 2000).

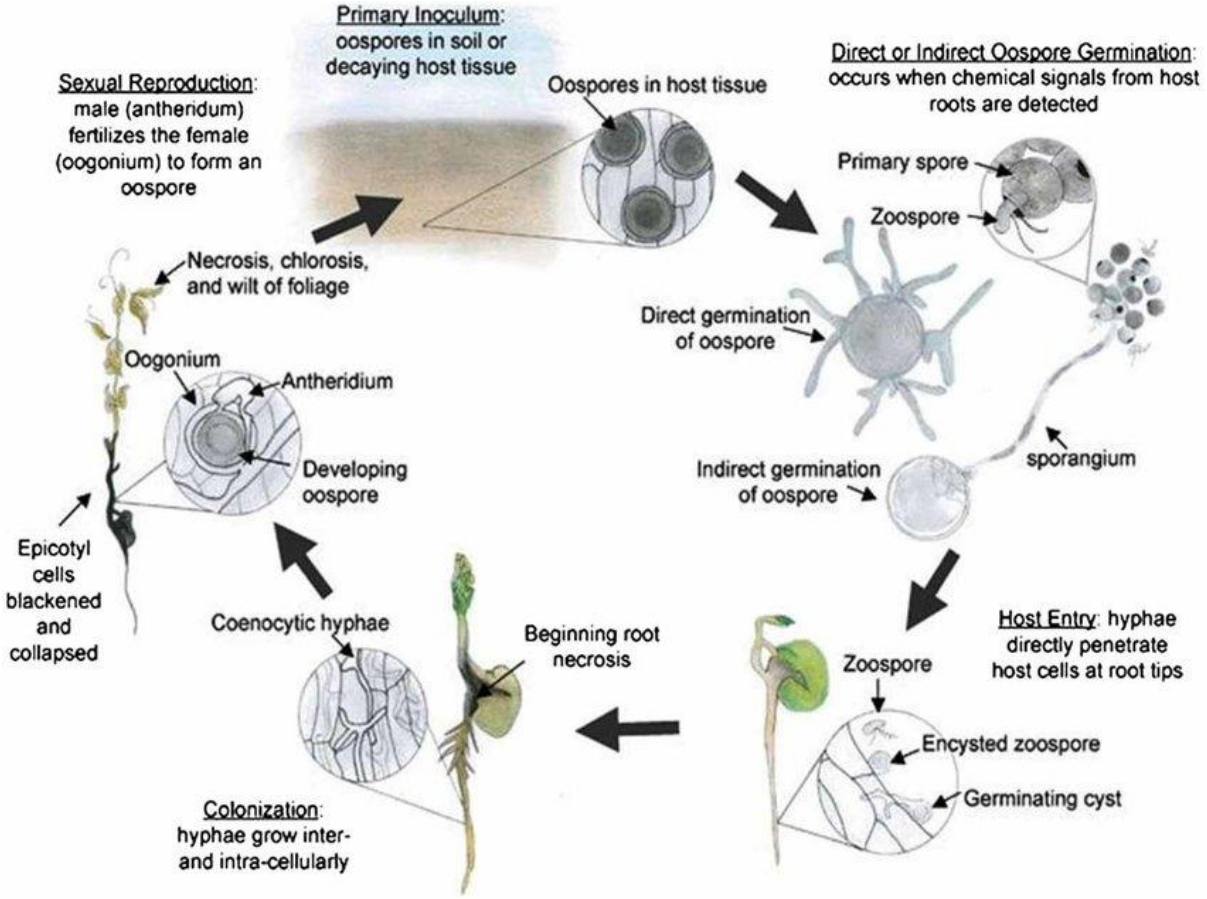

Figure 1.3 : Life cycle of *Aphanomyces euteiches* (Hughes & Grau, 2013).

1.4 Plant-Immunity

To a larger extent, plant adaptability and productivity are governed by their response to environmental cues. An environmental agent that reduces a plant's productivity below the maximal level for optimum growth may be considered stress (Kilian et al., 2012). Plants, though immobile, have evolved to cope with diverse environmental stresses by deploying specific mechanisms that allow them to detect specific changes in their environment (Choudhary & Meena, 2024; Kumar & Verma, 2018). Despite being sessile and lacking adaptive immune systems, similarly to animals, plants can surprisingly withstand threats posed by harsh environmental conditions and microbial pathogen infections solely by relying

on their innate immunity as a defense strategy (Dodds et al., 2024; Jones & Dangl, 2006; Zipfel, 2008). Unlike macrophages, with circulating cells specialized in recognizing external stimuli, in the plant's innate immunity, each plant cell can autonomously respond to a pathogen attack (Jones & Dangl, 2006). In addition, systemic signaling is triggered in response to microbial stimuli, preparing naïve plant tissues for an imminent attack (Kliebenstein, 2014). An invading microbe, however, must first overcome physical barriers like waxy cuticles and rigid cell walls of the plant to be pathogenic (Kliebenstein, 2014). Also, based on the microbial signatures perceived during the invasion, plants developed two interrelated innate immunity strategies to counterattack invading microbes. These strategies are pattern-recognition immunity (PTI) and effector-triggered immunity (ETI) (Jones & Dangl, 2006; Zipfel, 2008). PTI and ETI gene expression signatures are largely similar, suggesting that the responses are the same overall but vary in magnitude (Tao et al., 2003).

1.4.1 Pattern-triggered immunity (PTI)

PTI involves identifying signature patterns of microbes termed pathogen-associated molecular patterns (PAMPs) or DAMPs (damage-associated molecular patterns) through pattern-recognition receptors (PRR) on cell surfaces (Mengiste, 2012). Recognition of ‘non-self’ (PAMPs) or ‘self’ (DAMPs) by PRR triggers a danger alarm in the plant and activates PTI (Boller & Felix, 2009) (Figure 1.4). PTI can potentially fend off a wide array of microbes, regardless of the lifestyle, due to the conserved nature of PAMPs such as bacterial flagellin, fungal chitin, or cell wall-derived oligogalacturonides (OGs) (Zipfel, 2008). PRRs in plants are generally classified into two main types: they are receptor kinases (RKs), which have an ectodomain for ligand binding, a single-pass transmembrane domain, and an intracellular kinase domain, and receptor-like proteins (RLPs), which have a similar structure as RKs but lack the kinase domain (Mengiste, 2012; Zipfel, 2008). Due to the missing kinase domain, RLPs recruit one or more RKs to transduce ligand binding into intracellular signals (Zipfel, 2008). The first PRR that has been characterized is the leucine-rich repeats receptor kinase (LRR)-RK FLAGELLIN-SENSING 2 (FLS2), which recognizes flagellin via the direct binding of a conserved stretch of 22 amino acids, referred to as flg22 (Gómez-Gómez & Boller, 2000; Zipfel et al., 2004a). Flg22 binding to FLS2 leads to the immediate recruitment of the LRR-RK BRASSINOSTEROID INSENSITIVE 1–ASSOCIATED KINASE 1 (BAK1). This protein serves as a co-receptor for flg22 and is required for the activation of FLS2 and flg22-triggered immune signaling in plants (Chinchilla et al., 2007; Heese et al., 2007; Roux et al., 2011; Sun et al., 2013). Loss of function of BAK1 in *Arabidopsis* resulted in an increased susceptibility to detrimental pathogens such as *Pseudomonas syringae* and *Hyaloperonospora arabidopsidis* (Roux et al., 2011). In *Arabidopsis,* another well-studied LRR-RK is the ELONGATION

FACTOR-TU RECEPTOR (EFR), which perceives the bacterial elongation factor Tu (EF-Tu) (Zipfel, 2008). EFR specifically detects the conserved first 18 amino acids of EF-Tu, elf18, which is N-acetylated (Kunze et al., 2004; Zipfel et al., 2006). Interestingly, EFR perception of elf18 is limited to plants belonging to the Brassicaceae family (Boller & Felix, 2009). However, it was shown that overexpressing *EFR* in the Solanaceae plant family conferred responsiveness to elf18 in these plants and augmented the notion that interfamily transfer of PRR can be a helpful tool in engineering disease-resistant plants (Lacombe et al., 2010).

1.4.2 Effector-triggered immunity (ETI)

Microbes can still escape PTI by secreting virulence factors commonly called effector molecules (Jones & Dangl, 2006; Zipfel, 2008). Hence, ETI is an accelerated form of PTI response employed by plants to resist these escapees. This usually results in hypersensitive cell death of infected tissues to trap pathogens that have successfully bypassed PTI (Jones & Dangl, 2006). Effectors are secreted by invading pathogens to reprogram the plant's cellular environment towards infectious compatibility (Dodds et al., 2024; Jones & Dangl, 2006; Lopes Fischer et al., 2020). However, NB-LRR (Nucleotide Binding domain and Leucine-rich Repeat) receptors recognize these effectors and initiate a strong immune response, betraying the invading pathogen (Figure 1.4). (Jones & Dangl, 2006). Thereby, ETI solely depends on intracellular immune receptors, mainly nucleotide-binding leucine-rich repeat (NB-LRR) protein, to detect virulence effectors of invading pathogens (Dodds et al., 2024). Evolving new effectors by pathogens followed by their recognition by receptors is an evolutionary "arms race" where every adaptation in one counterpart, either plant or pathogen, drives a counter-adaptation in the other (Zipfel, 2008). This ongoing zigzag drives the diversity of effectors and plant resistance (R) proteins (Lopes Fischer et al., 2020). Structurally, NB-LRR proteins in plants resemble NOD-like receptors (NLRs) in mammals, which also play a role in innate immunity by detecting intracellular signals of infection (Dangl & Jones, 2001).

In plant pathogens, three distinct protein secretion systems enabling them to transfer effectors into host cells were identified. These include the type II secretion system (T2SS), the type III secretion system (T3SS), and the type IV secretion system (T4SS) (Abramovitch et al., 2006). The type III secretion system (T3SS) is widely studied among these three, which, like the bacterium flagellum, forms a pilus that injects effectors into its host cell to initiate enzymatic process that will facilitate its efficient colonization (Alfano & Collmer, 2004). Pathogens with biotrophic lifestyles rely on the T3SS, but some symbiotic bacteria also employ this secretion system to invade their hosts successfully (Abramovitch et al., 2006). Among pathogens, *P. syringae* pathovar (pv.) tomato (*Pst*) has been shown to have over 30 effectors (Chang et al.,

2005; Preston et al., 2005). In uninfected plants of *Arabidopsis,* RIN4 (RPM1 interacting protein 4), a negative regulator of plant immune responses, particularly those mediated by NB-LRR proteins RPM1 and RPS2 (Ribosomal protein 2), prevents premature activation of immune responses that could damage the host plant (Axtell & Staskawicz, 2003; Mackey et al., 2002, 2003). Two effectors of *P. syringae,* namely AvrRpt2 and AvrRpm1, have been shown to target RIN4, obstructing its immune response function by modulating its ability to regulate R genes However, modification of RIN4 by *P. syringae* effectors activates RPS2 and RPM1-dependent resistance, which in turn results in effector-triggered immunity (Abramovitch et al., 2006; Jones & Dangl, 2006a). In RIN4 mutant plants, it was shown that RPS2-dependent resistance was constitutively activated, contributing to the knowledge that the absence of RIN4 is a substantial indication to trigger a defense response (Abramovitch et al., 2006). Together, these findings make ETI a basis for exploiting many disease-resistance traits in breeding against biotrophic and hemibiotrophic pathogens (Mengiste, 2012).

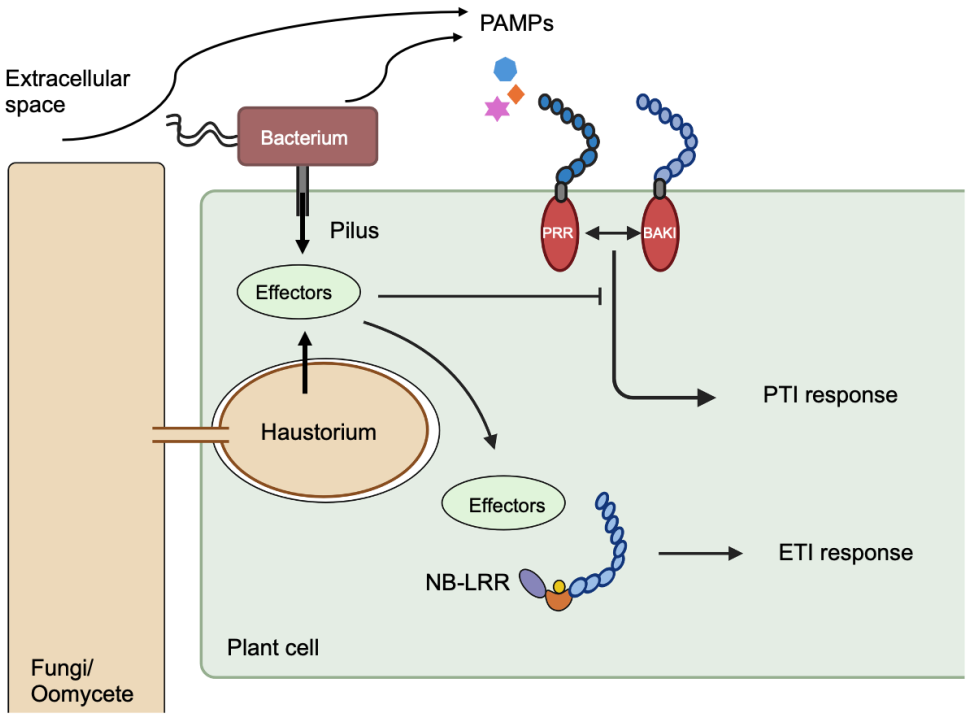

Figure 1.4: **The principles of plant immunity.**

Bacterial plant pathogens propagate specifically in the extracellular spaces of plant tissues. Most fungal and oomycete pathogens also extend their hyphae into this space, although many also form specialized feeding structures, known as haustoria, that penetrate host cell walls but not the plasma membrane. PAMPs released into the extracellular spaces, are recognized by cell surface pattern recognition receptors (PRRs) and elicit PAMP-triggered immunity (PTI). PRRs generally consist of an extracellular leucine-rich repeat (LRR) domain (mid-blue), and an intracellular kinase domain (red). Many PRRs interact with the related protein BRASSINOSTEROID INSENSITIVE 1-ASSOCIATED KINASE 1 (BAK1) to initiate the immune response. Bacterial pathogens deliver effector proteins into the host cell by a type-III secretion pilus, whereas fungi and oomycetes deliver effectors from haustoria or other intracellular structures by an unknown mechanism. These intracellular effectors often act to suppress PTI. However, many are recognized by intracellular nucleotide-binding (NB)-LRR receptors, which induce effector-triggered immunity (ETI).

1.5 *Medicago truncatula*: a model plant for legume immunity

Legumes play significant roles in agriculture due to their numerous environmental, economic, and nutritional benefits. These attributes make them the second most important plant species to humans after cereals (Graham & Vance, 2003), accounting for almost 27% of the world's crop production (Smýkal et al., 2020). Highlights of the benefits of legumes can be attributed to their ability to fix atmospheric nitrogen into the soil through symbiosis with rhizobia bacteria in their root nodules (Wang et al., 2018). This reduces the burden of using synthetic nitrogen

fertilizers, which are costly and environmentally damaging. In addition, legumes are integral to global food security since crops, such as soybeans and *Medicago sativa* (alfalfa), account for 56% of the global oilseed production (Wilson, 2008) and constitute a significant source of forage for animals, respectively (Fu et al., 2015). Legumes have contributed considerably to the study of plant biology, serving as the original models in Mendel's discovery of the law of inheritance (Mackay & Anholt, 2022).

The bottleneck, however, is that the genome size of some of the most economically important legume crops, *Glycine max* (2n = 20, ~ 1100 Mbp) and *Medicago sativa* (autotetraploid, 2n = 4x = 32, 800-1000 Mbp), makes it complex to work with them for the study of legume biology. To establish a genetic system for legume biology, the legume species *M. truncatula* was selected as a model system to study legume genomics and biology (Cook, 1999). This plant is an annual barrel clover that originates from the Mediterranean region (Küster, 2013) . Several ecotypes differing in their growth habits, reproduction, and interaction with microbes have been collected from this region (Cook, 1999). *M. truncatula* is self-fertile, has a small diploid genome (2n=16 , ~ 1100 Mbp), autogamous, and has a short regeneration time (Barker et al., 1990; He et al., 2009; Rose, 2008). With extensive genomic information available for all *M. truncatula* genes (Tang et al., 2014), *M. truncatula* has become a critical resource for understanding plant immunity due to its dual interaction ability with symbiotic microorganisms (Kelly et al., 2017; Peleg-Grossman et al., 2009) and pathogens (Martins et al., 2020). To explore the *M.truncatula* genome, two related but genetically distinct ecotypes, jemalong A17, released from Australian farmers, and R108 have been used as model systems (Garmier et al., 2017). The ecotype Jemalong A17, has served as the reference line for genomic approaches due to its transformability using agrobacteria-mediated methods (Barker et al., 1990). However, R108 has become the preferred ecotype for genetic studies requiring efficient transformation due to its high regeneration capacity, as A17 jemalong is described as highly recalcitrant to transformation (Garmier et al., 2017; Nandety et al., 2023; Wright & Wang, 2015). This promising nature of R108 made it a candidate for generating mutant lines at the

Noble research foundation (www.noble.org) where insertional mutagenesis are made in R108 using *Nicotiana tabacum Tnt1* retrotransposons (Tadege et al., 2008). In addition to R108, another *M. truncatula* line 2HA derived from the recalcitrant line A17 has also been shown to exhibit high somatic embryogenesis efficiency, making it a great candidate for plant regeneration and transformation (Kurdyukov et al., 2014; Song et al., 2013). Furthermore, *M. truncatula* is a remarkable plant model for generating chimeric plants harboring hairy roots via Agrobacterium-mediated hairy root transformation (Boisson-Dernier et al., 2001). This transformation results in rapid and efficient hairy root organogenesis and the subsequent development of vigorous composite plants consisting of a wild-type shoot and transgenic roots (Boisson-Dernier et al., 2001). The availability of the mutant population (Young et al., 2011) further facilitates the functional elucidation of important genes mediating several physiological functions in *M. truncatula*.

1.5.1 Plant pathogen interaction: *Medicago – Aphanomyces*

The interaction between *M. truncatula* and the oomycete *A. euteiches* has been an excellent area for studying plants' defense mechanisms against pathogens. In general, plants respond to oomycete infection by deploying a cascade of immune responses, including the production of reactive oxygen species (ROS), activating defense-related genes, and localized cell death of plant tissues to restrict the spread of invading oomycetes (Wang et al., 2019). Pathogenesis-related (PR) proteins are among the well-characterized proteins known to play a pivotal role in plant-oomycete interactions. It was reported that PR-1a exhibits antimicrobial properties against *P. infestans* (Niderman et al., 1995) *,* and the overexpression of this gene in tobacco increases resistance against the oomycete pathogens *P. parasitica* and *Peronospora tabacina* (Albert et al., 2015). PR-1a was also discovered to sequester sterols, which are known to be potent against sterol auxotrophs such as oomycetes (Gamir et al., 2017).

In the *M.truncatula – A. euteiches* pathosystem, a study by Djébali et al. (2009) revealed that *M. truncatula* ecotype A17 Jemalong exhibits partial resistance against *A. euteiches.* Through microscopic approaches, they demonstrated that, unlike the *M. truncatula* ecotype F83005.5 (susceptible line), the root stele of the A17 jemalong plants remained pathogen-free after *A. euteiches* infection, due to an observable increase in the pericycle region of the root, accompanied by lipid deposition and phenolic compound accumulation. Also, through a proteome analysis, it was shown that infection of *M. truncatula* by *A. euteiches* altered the abundance of several proteins in the plant, with a significant portion of the proteins belonging to the pathogenesis-related proteins, specifically PR10 (Colditz et al., 2004). Moreover, exposure of plants to biotic stress agents can lead to changes in specific secondary

metabolites, which in turn modulate the plant's response to invading pathogens, thereby enhancing immunity (Kogovšek et al., 2016; Seybold et al., 2020). For example, the *TERPENE SYNTHASE10* (*MtTPS10*) was reported to be highly induced in roots of seedlings of *M. truncatula* after *A. euteiches* infection, with a nearly 100-fold upregulation (Yadav et al., 2019). When a *M. truncatula* line carrying a tobacco retrotransposon *Tnt1* insertion in *MtTPS10* and therefore deficient in MtTPS10 (*tps10)* was infected with *A. euteiches*, a significant accumulation of oomycete biomass was recorded with an accompanying decrease in shoot and root biomass (Yadav et al., 2019), highlighting the significance of secondary metabolites, in particular terpenoids, in the defense of *M. truncatula* against *A. euteiches*.

1.6 Terpenoids

Secondary metabolites can be classified into three distinct chemical groups: phenols, nitrogen-containing compounds, and terpenes (Bennett & Wallsgrove, 1994). Among these, terpenes are the most abundant and diverse plant secondary metabolites, with over > 80,000 already reported (Christianson, 2017). Several terpenes have been well characterized as involved in plants' defense against biotic and abiotic stress factors (Bennett & Wallsgrove, 1994; Chen et al., 2004; Dudareva et al., 2004). In addition to this significant attribute of terpenes, most terpenes constitute a greater percentage of the bouquet of volatile organic compounds (VOC) emitted by plants during inter-organismal interactions because of their characteristic nature of volatilizing easily at ambient temperature (Boncan *et al.,* 2020). These volatile compounds act as signaling chemicals to attract pollinators and predators or to repel harmful herbivores (Chen et al., 2004). Several known volatile terpenes are involved in the aboveground mediation of plant-herbivore interactions upon mechanical injury caused by these herbivores (Bennett & Wallsgrove, 1994; Cascone et al., 2015; Nieuwenhuizen et al., 2009a). Also, in the rhizosphere, there have been reports of the accumulation of volatile monoterpenes and sesquiterpenes in the roots of plants (Bos *et al.,* 2002; Kovacevic *et al.,* 2002). These volatile terpenes equally exhibit antimicrobial properties or act as signaling compounds in the rhizosphere (Baetz & Martinoia, 2014; Chen et al., 2004). Internal or external factors highly regulate the biosynthesis and accumulation of these terpenoids in plants, and their release is often restricted to specific tissues or developmental stages. This mechanism enables the plant to fine-tune the deployment of these terpenoids for mediating environmental interactions (Karunanithi & Zerbe, 2019; Keeling & Bohlmann, 2006; Schmelz et al., 2014; Tholl, 2006).

The primary players in the biosynthesis of terpenoids are the C_5 isoprenoid precursors isopentenyl diphosphate (IPP) and dimethylallyl diphosphate (DMAPP) (Newman & Chappell, 1999). These precursors originate from two distinct plant pathways: the methylerythritol

phosphate (MEP) pathway in plastids and the mevalonic acid (MVA) pathway in the cytosol/peroxisomes (Bennett & Wallsgrove, 1994; Lichtenthaler, 1999; Sapir-Mir et al., 2008) (Figure 1.5). Downstream of these biosynthetic pathways is the formation of acyclic prenyl diphosphates of various chain lengths, such as GPP (C_{10}), FPP (C_{15}), and geranylgeranyl diphosphate GGPP (C_{20}) (Chen et al., 2004; Jia & Chen, 2016) serving as a substrate for a group of related enzymes called terpene synthases (TPSs) (Chen et al., 2011). Terpene synthase, a key player in the biosynthesis of terpenoids, controls the structural variety and the unique composition of terpenoids in plants. These TPSs, depending on the preferred prenyl diphosphates, can produce monoterpenes (C_{10}), sesquiterpenes (C_{15}), or diterpenes (C_{20}) through a series of cyclization and rearrangement of the backbone of these substrates (Chen et al., 2011; Tholl, 2006). Aside from TPS being the gatekeepers responsible for the production of structurally diverse terpenoids, another superfamily of heme oxygenases known as cytochrome P450s (CYPs) equally play a significant role in generating structurally diverse terpenoids with varying bioactivities (Bathe & Tissier, 2019; Guo et al., 2016; Karunanithi & Zerbe, 2019). In plants, cytochrome P450 monooxygenases (incorporating one oxygen atom) have received much recognition for their ability to modify terpenes into complex bioactive products. However, dioxygenases and dehydrogenases CYPs can also catalyze reactions such as epoxidation or hydroxylation and sometimes create novel carbon-carbon (C-C) linkages (Bathe & Tissier, 2019). These transformations are also necessary to generate volatile organic compounds and other bioactive metabolites. These enzymatic reactions are not just a biochemical process but a crucial step in producing several structurally diverse terpenoids that play significant roles in plants' defense, underscoring the importance of terpenes in plant biology (Zhou & Pichersky, 2020a). The protein structure of a TPS is characterized by two distinctive domains (Finn et al., 2016; Starks et al., 1997):The N-terminal domain (Pfam: PF01397) contains a motif responsible for the cyclization initiation during terpene synthesis, termed the RRX8W motif (“R” stands for Arginine, “W “for tryptophan, and “X” represents any amino acid); the C-terminal region (Pfam: PF03936) comprises two motifs, DDXXD (an aspartate-rich motif) coordinating metal ions crucial for enzyme activity and NSE/DTE motif involved in active site stabilization and ion coordination to allow efficient substrate binding (Rynkiewicz et al., 2001; Whittington et al., 2002). Although some terpenoids are common to most plants, the synthesis of others is governed by specific ecological conditions. For example, the diversity of terpenoid emissions from European corks was attributed to their geographical distribution in the Mediterranean zone (Loreto et al., 2009). In many cases, allelic variations of terpene synthases, such as the case of *TPS4* and *TPS5* in maize (Köllner et al., 2004) or *TPS02* and *TPS03* in Arabidopsis (Huang et al., 2010), can result in different quantitative volatile emissions. This chemical polymorphism allows plants to adapt to varying environmental conditions.

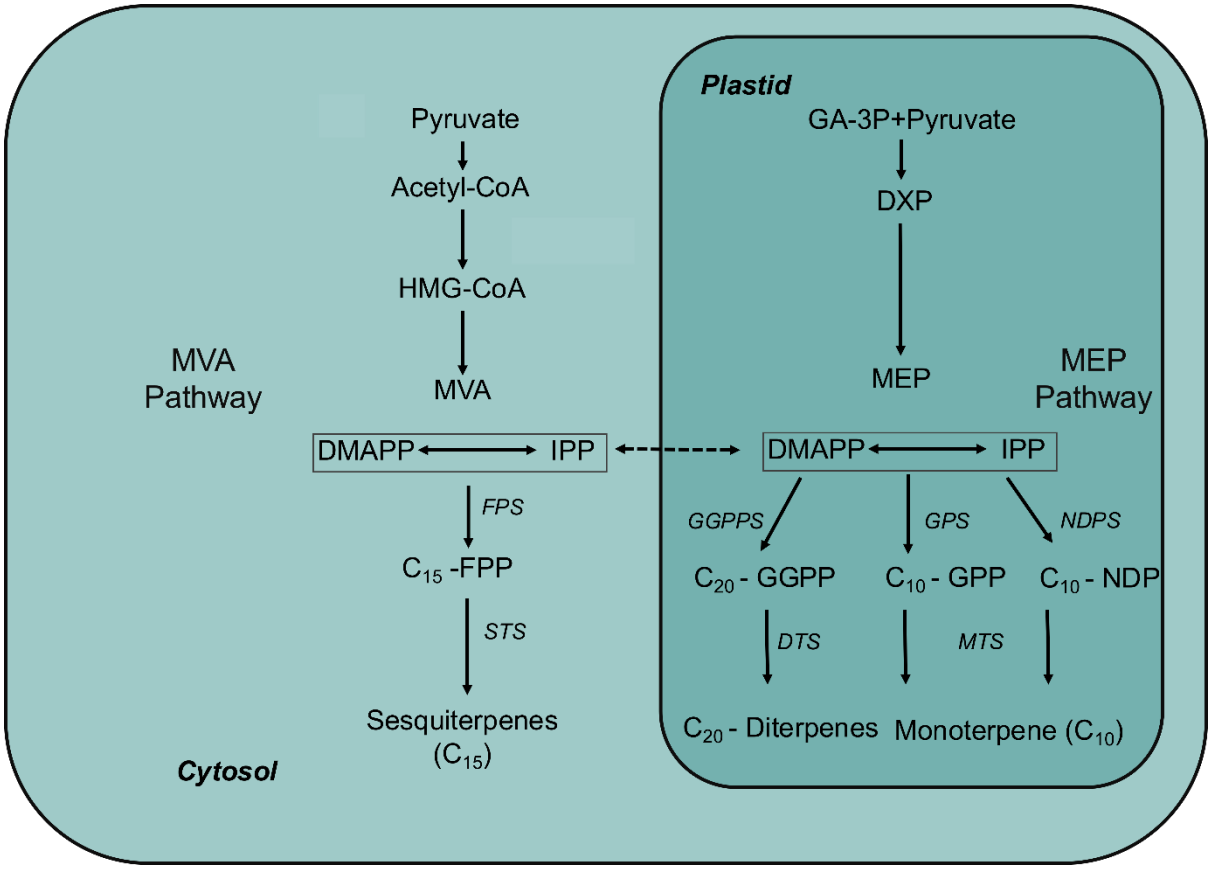

Figure 1.5: Schematic overview of terpenoid biosynthesis in plants.

The synthesis of terpenoids takes place in the cytosol through the mevalonate (MVA) pathway, in the plastid via the methyl-erythritol phosphate (MEP) pathway, but also (partly) in the mitochondria, ER, and/or peroxisomes (not depicted). Abbreviations: Acetyl-CoA, acetoacetyl-coenzyme A; HMG-CoA, 3-hydroxy-3-methylglutaryl-coenzyme A; MVA, mevalonate; DMAPP, dimethylallyl diphosphate; IPP, isopentenyl diphosphate; E, E-FPP, trans-farnesyl diphosphate; FPS, farnesyl diphosphate synthase; STS, sesquiterpene synthase; GA-3P, glyceraldehyde-3-phosphate; DXP, 1-deoxy-D-xylulose 5-phosphate; GGPP, geranylgeranyl diphosphate; GGPPS, geranylgeranyl diphosphate synthase; DTS, diterpene synthase; GPP, geranyl diphosphate; GPS, geranyl diphosphate synthase; NDP, neryl diphosphate; NDPS, neryl diphosphate synthase; MTS, monoterpene synthase.

1.6.1 The Medicago terpenome

Genome sequencing and annotation of the model plant *M. truncatula* have revealed a substantial number of putative terpene synthases (*MtTPS*) (Hendrickson et al., 2024; Parker et al., 2014). Parker et al. (2014) conducted a comprehensive analysis of the *M. truncatula* genome and identified 23 TPS homologs. These genes were found to cluster into five recognized phylogenetic subfamilies of the TPS superfamily, underscoring the diversity and evolutionary complexity of terpene biosynthesis in this species. Recently, several of the putative *MtTPS* genes have been characterized functionally, and strikingly, many of these *MtTPS*s have been reported to act as deterrents against pests and pathogens (Arimura et al.,

2007; Garms et al., 2010; Gomez et al., 2005; Leitner et al., 2005; Yadav et al., 2019). For instance, the *M. truncatula* terpene synthases *MtTPS1*, *MtTPS2*, *MtTPS3,* and *MtTPS4* were found to accumulate in leaves following mechanical damage or insect wounding, suggesting their role in an inducible defense response (Gomez et al., 2005). Furthermore, several terpene volatiles were emitted from *M. truncatula* after *Spodoptera littoralis* and *Tetranychus urticae* feeding (Leitner et al., 2005). At the below-ground level, *MtTPS10* has emerged as the only sesquiterpene synthase implicated in the defense against the oomycete *A. euteiches*, the causal agent of root rot disease in legumes (Yadav et al., 2019). The expression of *MtTPS10* is induced in infected roots, and its encoded sesquiterpene products are reported to deter *A. euteiches* growth (Yadav et al., 2019). These reports indicate that terpene synthases are a core part of the defense strategy in *M. truncatula*.

1.7 Thesis rationale and aims

Recent breakthroughs in legume biology have been game-changers in understanding the intricate networks and mechanisms that can be exploited to lessen or eradicate the detrimental effect *A. euteiches* has on legume production (Badis et al., 2015; Colditz et al., 2004; Hendrickson et al., 2024; Yadav et al., 2019). Among these is the work done by Yadav et al. (2019), where they demonstrated, using an Affymetrix MEDGene 1.1ST Array strip, that massive transcript reprogramming occurs in the plant within 2 hours post-inoculation of *M. truncatula* with *A. euteiches*. Among the genes showing significant up-regulation was a gene that encodes a putative sesquiterpene synthase, the *M. truncatula TERPENE SYNTHASE 10* (*MtTPS10)*. Induction of *MtTPS10* was shown to be oomycete-specific since significant induction of *MtTPS10* was only detectable in roots of *M. truncatula* infected with *A. euteiches* and *Phytophthora palmivora* (Yadav et al., 2019). Additionally, the heterologous expression of *MtTPS10* in yeast results in the production of antimicrobial sesquiterpenes, with himachalol as the major product. Interestingly, among the blend of volatiles from wild-type plants, the major product, himachalol, was absent. When the *M. truncatula* line carrying a tobacco retrotransposon *Tnt1* insertion in *MtTPS10*, *tps10,* was infected with *A. euteiches*, a significant accumulation of oomycete biomass was recorded with an accompanying decrease in shoot and root biomass. The work by Yadav et al. (2019) has provided an instructive example of the value of terpenoids in plant defense and, hopefully, will be a promising contribution to breeding programs that aim at reducing the agro-economic loss in legume production. However, their findings raised some questions that need to be answered. These include: (i) which specific PAMPs of *A. euteiches* induce the expression of *MtTPS10*? (ii) Do different *M. truncatula* ecotypes show natural variation in the expression of *MtTPS10*? (iii) What is the biological relevance of *MtTPSs*? Is the primary sesquiterpene alcohol produced by MtTPS10, himachalol, converted *in planta*? Therefore, this work aims to address these pending questions mechanistically and to decipher the importance of terpenoids in plant-pathogen interactions.

Thesis aims (see Figure 1.6)

I. To identify the specific molecules of *A. euteiches* inducing *MtTPS10* expression in roots of *M. truncatula*
II. To probe the natural variation of *MtTPS10* expression in different ecotypes of *M. truncatula*
III. To elucidate the biological relevance of *MtTPSs* in other agronomically important crops, such as potatoes
IV. To identify the specific enzymes converting himachalol *in planta*

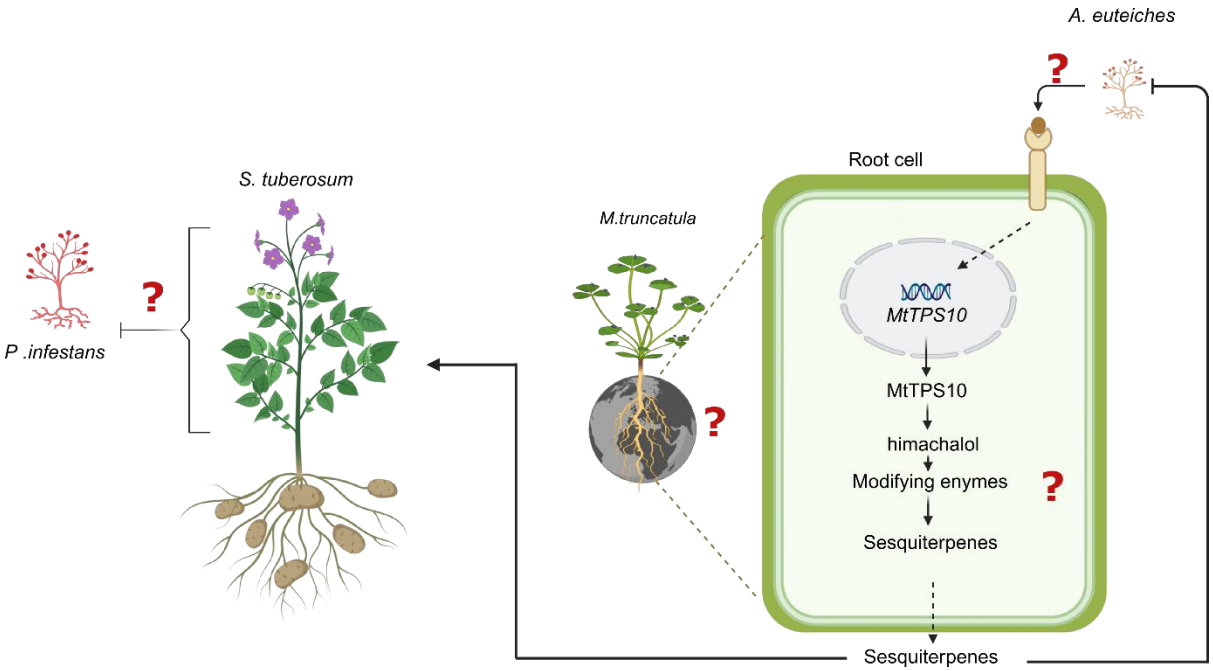

Figure 1.6: **Hypothetical illustration of thesis objectives**.

After inoculation of *M. truncatula* with *A. euteiches*, an oomycete-specific ligand (PAMP) may bind to a plant receptor, activating downstream signaling and leading to the expression of *MtTPS10*. *MtTPS10* catalyzes the formation of sesquiterpenes, which are then putatively modified by yet unknown enzymes. VOCs are released and act as defense compounds against *A. euteiches* but might also act against other oomycete pathogens affecting other plants.

2 Results

2.1 Identification of PAMPs inducing *MtTPS10* expression

Perception of microbial signatures by plants generally leads to the activation of defense-related genes in the attacked plant (Dodds et al., 2024; Zipfel et al., 2004). This phenomenon was further supported by the work of Yadav et al. (2019), who reported that the defense gene, *MtTPS10*, is a gene induced in the roots of *M. truncatula* as early as 2 hours post inoculation (hpi) after contact of the roots to living *A. euteiches* zoospores. Their work demonstrated that *MtTPS10* accumulation in *M. truncatula* roots was specifically induced by the oomycetes *A. euteiches* and *P. palmivora* and not by treatment of the roots with true fungi, symbionts, or abiotic stress factors. Consequently, they designated this gene as an oomycete-inducible gene (Yadav et al., 2019).This led us to hypothesize that specific molecules of oomycetes might be acting as PAMPs. To pinpoint the exact molecules responsible for the induction of *MtTPS10* expression in *M. truncatula* line A17 roots after *A. euteiches* infection, we generated root organ cultures (ROCs) expressing a GUS reporter gene under the control of a 2 kb promoter of *MtTPS10* according to Goossens et al. (2016). Positively transformed roots were treated with either zoospores or mycelium plugs of *A. euteiches*. Our results revealed that in addition to the detection of GUS activity in zoospore-treated roots, the mycelium-treated roots also accumulated the *MtTPS10* transcript, as visualized by the GUS staining (Figure 2.1). The effectiveness of the ROCs as a quick method for elicitor identification allowed us to narrow down which stages of the pathogen would be of interest for further experiments.

Figure 2.1: Expression patterns of the *MtTPS10* promoter-GUS fusion in the *M. truncatula* roots.

GUS staining of root organ cultures transformed with *pTPS10*::*GUS* and incubated with water, zoospores or mycelium for 2 h. Note the blue color of roots treated with zoospores and mycelium. Bars = 100 µm.

2.2 Elicitor M is a putative PAMP of oomycete *A. euteiches*

To augment our findings, different fractions of *A. euteiches* were tested for their ability to induce *MtTPS10*. Unfortunately, we could not perform this experiment with the ROCs because they lost the inducibility of GUS activity over time. Therefore, we tested the ability of *A. euteiches* fractions to induce *MtTPS10* using RT-qPCR. Roots of A17 were treated with three fractions from *A. euteiches*: mycelium plugs, zoospores, and elicitor M (water incubated for 24 h in the presence of a growing mycelium). In addition to this, other well-characterized PAMPs such as flg22, chitin, and Pep13 (Kaku et al., 2006; Nietzschmann et al., 2019; Zipfel et al., 2004) were also tested for their ability to induce *MtTPS10*. Roots treated with water were used as controls, and after 2 hpi, root samples were collected, and the *MtTPS10* transcript was determined. Our findings revealed that none of the PAMPs induced the expression of *MtTPS10* (Figure 2.2A). Although Pep13, a PAMP isolated from *P. infestans*, did not trigger the expression of *MtTPS10* in the roots of *M. truncatula*, treating the roots of *M. truncatula* with zoospores of *P. infestans* (kindly provided by Prof. Sabine Rosahl) resulted in the induction of *MtTPS10* (Figure 2.2B). This indicates that the expression specificity of *MtTPS10* extends to another oomycete, in this case, *P. infestans*. Regarding roots treated with *A. euteiches* fractions, we observed that mycelium-treated roots and even water collected from growing mycelium (elicitor M) induced transcript accumulation of *MtTPS10,* almost like zoospore-treated roots (Figure 2.2A). We also exposed *M. truncatula* leaves to elicitor M for 2 hours, and after this time, we extracted RNA from the treated leaves and determined the expression of *MtTPS10* from these leaf samples. Leaves treated with water were used as mock controls. Treating the leaves of *M. truncatula* with elicitor M for 2 hours resulted in higher levels of *MtTPS10* expression than mock-treated leaves (Figure 2.2C). Fractions exhibiting elicitor activity were used for further studies; in our case, because elicitor M had a higher inducibility comparable to zoospore induction, it was used for further analysis. So far, these results suggest that elicitor M might be a perfect candidate for identifying the microbial signatures involved in the induction of *MtTPS10* after *A. euteiches* infection.

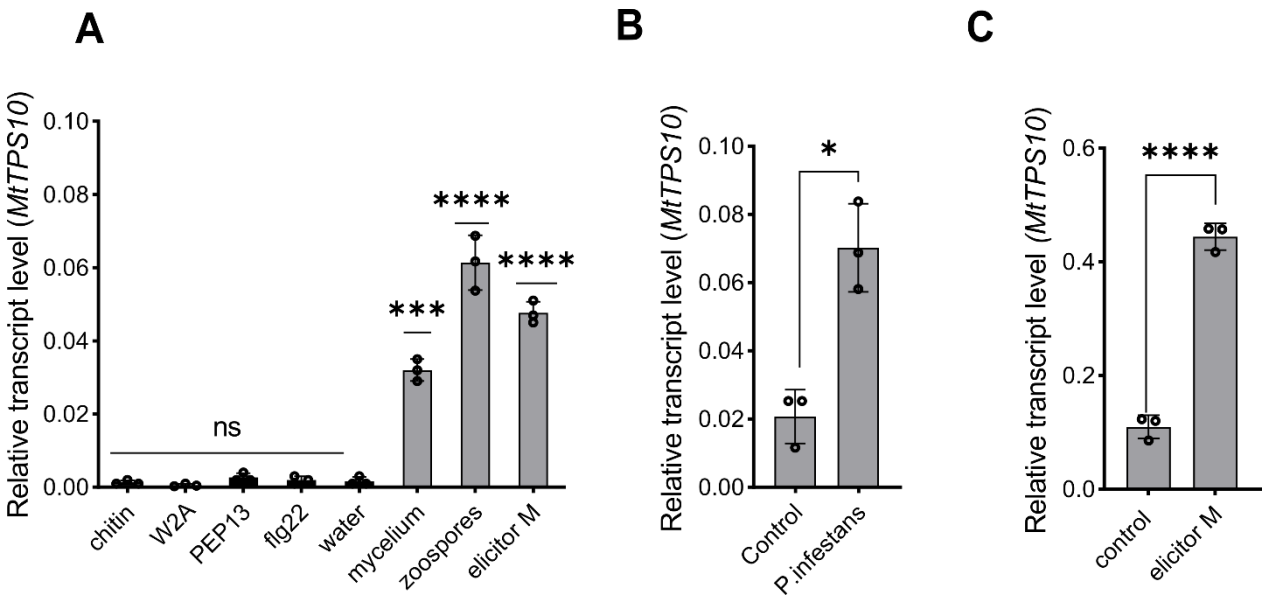

Figure 2.2: Elicitor M induces *MtTPS10* in *M. truncatula* roots and leaves.

A. *MtTPS10* transcript accumulation in *M. truncatula* roots treated with either well-characterized PAMPs or fractions of *A. euteiches.* **B**. *MtTPS10 transcript* accumulation in *M. truncatula* roots treated with *P. infestans.* ***C***. Relative *MtTPS10* transcript accumulation in *M. truncatula* leaves treated with mycelium water (elicitor M*).* In **A-C***,* expression levels of *MtTPS10* were measured in the root tissue of 7-day-old *M. truncatula* plants via RT-qPCR and were normalized to the housekeeping gene *MtActin2*. Statistical significance was determined by One-Way ANOVA followed by Tukey HSD ($p<0.05$). Bars represent mean +/- SD (n = 3), **P < 0.01, ***P < 0.001; ****P < 0.0001.

2.3 Transcriptomic data reveal a large overlap between zoospore-treated and elicitor M-treated roots

To definitively confirm that elicitor M does indeed possess the PAMPs that induce the expression of *MtTPS10,* the transcriptional differences or similarities between zoospore-treated and elicitor M-treated roots were determined. RNAseq analysis was performed from roots of 7-day-old seedlings of A17 Jemalong treated with either zoospore or elicitor M for 2 hours. Roots treated with autoclaved distilled water were used as a control. RNA integrity was analyzed for all samples, and RNA was sent to an external institution (www.novogene.com) for library preparation and sequencing. To investigate the differences or similarities between zoospore-treated roots and elicitor M-treated roots, a Venn diagram was generated from the differentially expressed genes (DEGs) in zoospore and elicitor M-treated roots using log2 (fold change) value ≥ 1 and a P-value of 0.05. 1105 and 1398 DEGs were specifically regulated in zoospore-treated roots and elicitor M, respectively, and 1610 DEGs were common to both zoospores and elicitor M-treated roots (Figure 2.3A). Pathway enrichment of the DEGs for both treatments remarkably showed some key pathways. Among many important upregulated pathways, the sesquiterpenoid and triterpenoid biosynthesis pathways, the Mitogen-Activated protein Kinases (MAPK) pathway, and the flavonoid biosynthesis pathways are among the key

pathways activated upon infection (Figure 2.3 B). These pathways are known to be activated in plants by pathogen recognition (Figure 2.3 B) (Geisler et al., 2013; Wang et al., 2020; Yadav et al., 2019; Zhang & Zhang, 2022).

Here, a strong similarity between the transcriptome of zoospores-treated roots and elicitor M-treated roots was evident in the expression heatmap, irrespective of the KEGG pathway (Figure 2.3C-D). Focusing on these highlighted pathways (Figure 2.3B), we chose 3 genes upregulated from either the MAPK or flavonoid pathway and performed RT-qPCR in an independent experiment. The results of the RT-qPCR correlated with the RNA-seq data. Indeed, gene expression of the selected genes significantly increased in both zoospore-treated roots and elicitor M-treated roots compared to the control samples (Figure 2.3E-F). It is worth mentioning that elicitor M was still active after boiling, pointing to non-proteinaceous components acting as putative PAMPs (Appendix, Figure 7.1). This result suggests that zoospores and elicitor M from *A. euteiches* trigger common transcriptional changes in *M. truncatula*. Now, to pinpoint which exact molecule is acting as a PAMP in elicitor M, a 4 L volume of elicitor M was produced; half of it was extracted with methanol, and the other half was concentrated by rotary evaporation and redissolved in deuterated water. Preliminary HPLC results showed no new compound compared to water incubated on only media (data not shown). Also, NMR results from the methanol extracts and the concentrated extracts showed no interesting data (data not shown). These later findings suggest that further analysis is needed to determine the exact molecules being recognized by *M. truncatula* during *A. euteiches* infection.

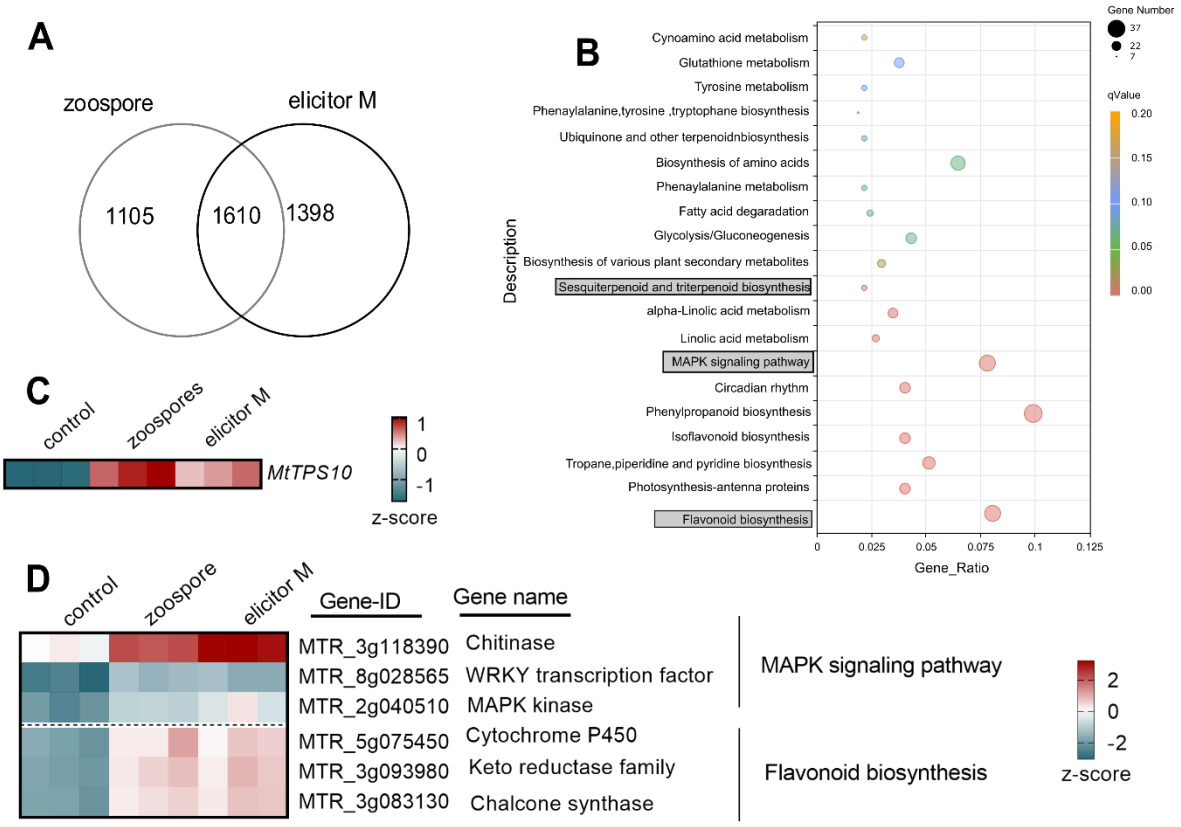
A
zoospore
elicitor M
1105
1610
1398
B
Cynoamino acid metabolism
Glutathione metabolism
Tyrosine metabolism
Phenaylalanine,tyrosine ,tryptophane biosynthesis
Ubiquinone and other terpenoidnbiosynthesis
Biosynthesis of amino acids
Phenaylalanine metabolism
Fatty acid degaradation
Glycolysis/Gluconeogenesis
Biosynthesis of various plant secondary metabolites
Sesquiterpenoid and triterpenoid biosynthesis
alpha-Linolic acid metabolism
Linolic acid metabolism
MAPK signaling pathway
Circadian rhythm
Phenylpropanoid biosynthesis
Isoflavonoid biosynthesis
Tropane,piperidine and pyridine biosynthesis
Photosynthesis-antenna proteins
Flavonoid biosynthesis
Description
Gene_Ratio
Gene Number
qValue
C
control
zoospores
elicitor M
MtTPS10
z-score
D
control
zoospore
elicitor M
Gene-ID
Gene name
MTR_3g118390 Chitinase
MTR_8g028565 WRKY transcription factor
MTR_2g040510 MAPK kinase
MTR_5g075450 Cytochrome P450
MTR_3g093980 Keto reductase family
MTR_3g083130 Chalcone synthase
MAPK signaling pathway
Flavonoid biosynthesis
z-score

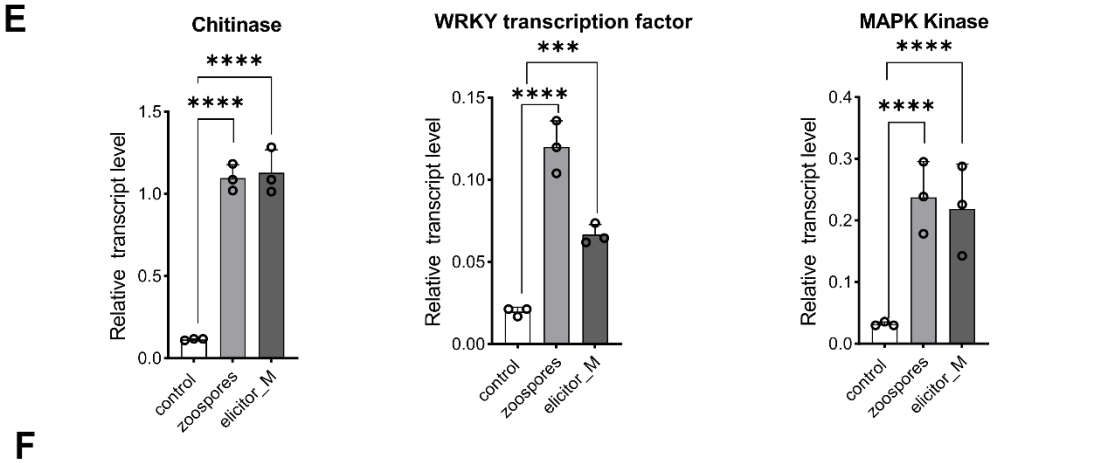
E
Chitinase
WRKY transcription factor
MAPK Kinase
Relative transcript level
control
zoospores
elicitor_M

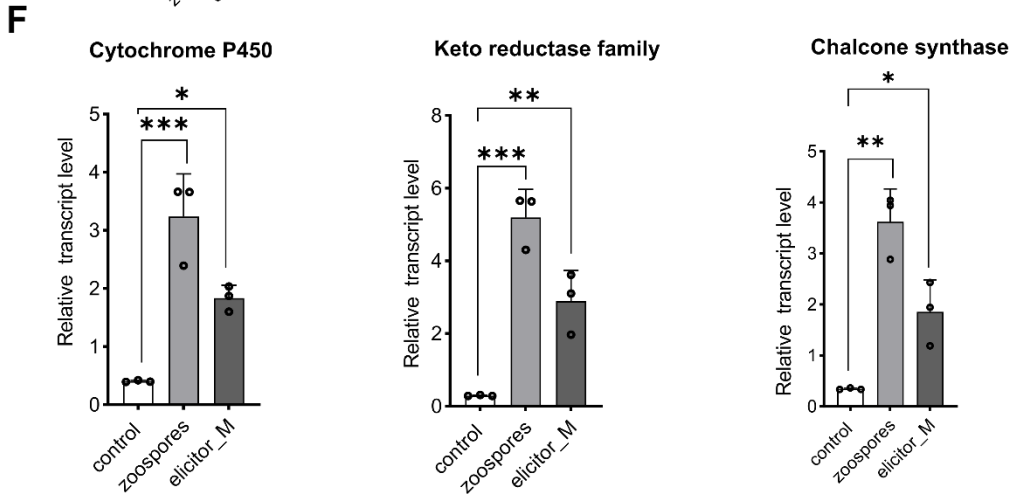
F
Cytochrome P450
Keto reductase family
Chalcone synthase
Relative transcript level
control
zoospores
elicitor_M

Figure 2.3: Roots of *M. truncatula* treated with zoospores or Elicitor M express the same defense genes.

A. Venn diagram showing the differences or similarities of the DEGs in zoospore and elicitor M-treated plants. **B**. Scatter plot of KEGG pathway enrichment analysis for upregulated DEGs for both zoospore and elicitor M-treated roots. The gene ratio is the number of genes of DEGs annotated in a particular pathway term to the total number of genes. The Q value is the corrected P-value, and it ranges from 0-1, with a lower Q value indicating greater intensity. The sizes of the circles indicate the number of genes in that pathway. The top 20 enriched pathway terms in the KEGG database are listed. Some particular genes within the highlighted pathways in gray were selected for validation. **C**. Expression profile of *MtTPS10* within the sesquiterpenoid and triterpenoid biosynthesis pathway. **D**. Expression profile of genes within the MAPK signaling pathway. For **C-D**. FPKM values of three independent biological replicates were transformed into a Z-score. In E-F, Expression levels of selected genes from the MAPK signaling pathway and flavonoid biosynthesis pathway, respectively. Expression levels of respective genes were measured in the root tissue of 7-day-old *M. truncatula* plants via RT-qPCR and were normalized to the housekeeping gene *MtActin2*. Statistical significance was determined by One-Way ANOVA followed by Tukey HSD ($p<0.05$). Bars represent mean +/- SD (n = 3), **P < 0.01, ***P < 0.001; ****P < 0.0001.

2.4 Probing the natural variation of *MtTPS10* in *M. truncatula* ecotypes

Now, previous work by Yadav et al. (2019) extensively characterized *MtTPS10* as an early-induced gene in the root of *M. truncatula* A17 lines 2 hpi with *A. euteiches* zoospores. Depending, however, on evolutionary history, individuals within the same plant population can accumulate or acquire genetic differences in their genomes. In the case of *M. truncatula,* it was reported that substantial variation exists in the susceptibility of *M. truncatula* to infections by *A. euteiches* (Bonhomme et al., 2014; Dreher et al., 2017). To better understand how evolutionary forces and natural selection have shaped the contribution of *MtTPS10* to different immunity levels in *M. truncatula*, we studied A17 as the reference ecotype along with five other additional ecotypes (L000163, L000213, L000368, L000542 and L000555) stemming from the Mediterranean regions (Table 2.1) (only the last three numbers were used in this thesis) and differing in their susceptibility to *A.euteiches* (Dreher et al., 2017).To analyze the expression levels of *MtTPS10,* we exposed the roots of 7-day-old seedlings of the selected natural accessions to *A. euteiches* zoospores for 2 hours. Roots treated with swamp water were used as control plants for all ecotypes. The ecotypes exhibited huge differences in *MtTPS10* transcript levels (Figure 2.4). Specifically, lines 213, A17, and 542 exhibited higher levels of *MtTPS10* than their respective mock-treated roots. In lines 368, 555, and 163, we did not observe a significant change in the *MtTPS10* transcript accumulation (Figure 2.4). Also, the CDS of *MtTPS10* from line 368 was not attainable because in infected roots of this line, the transcript of *MtTPS10* was not detectable (Appendix, Figure 7.3)

The sequence comparison of the CDSs (1.65 kb) encoding *MtTPS10* from all *MtTPS10*-expressing lines revealed no SNPs that could affect its activity, except in ecotype 555, which had a truncated protein compared to the other ecotypes due to loss of 140 amino acids from the C-terminal region (Appendix Figure 7.4).

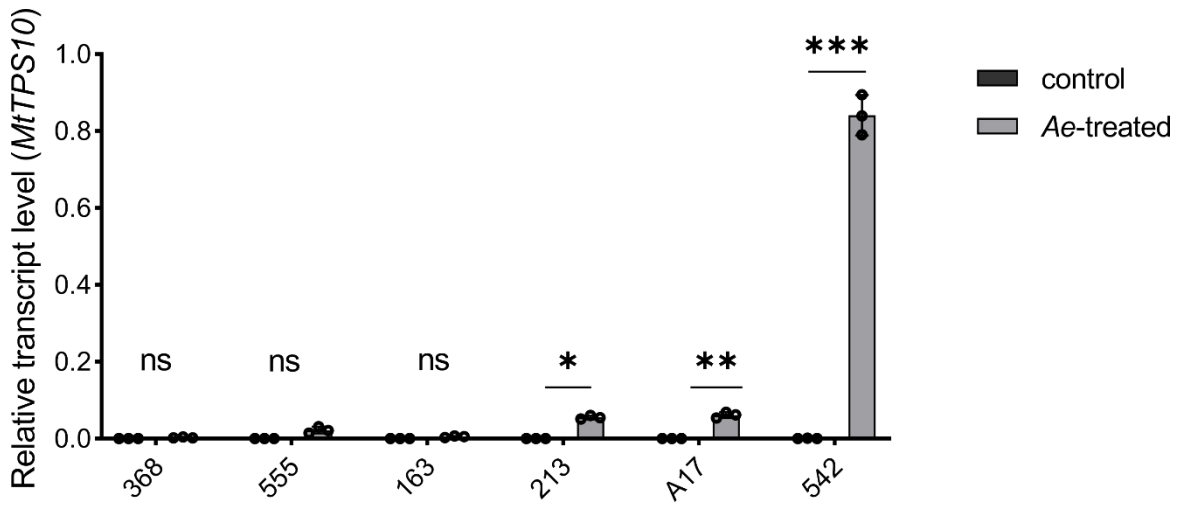

Figure 2.4: Expression levels of *MtTPS10* after *A. euteiches* infection in natural accessions of *M. truncatula*.

Expression levels were measured via RT-qPCR from the roots of 7-day-old *M. truncatula* plants treated with *A. euteiches* zoospores or water (control) and were normalized to the housekeeping gene *MtActin2*. Bars represent mean +/- SD (n = 3). Asterisks denote statistically significant differences among ecotypes as determined by the Student's t-test within each condition (** p<0.01, *** p<0.001, **** p<0.0001).

Table 2.1: Origin of selected *M. truncatula* ecotypes from the Mediterranean regions (Ronfort et al., 2006).

Ecotype Name	Country of origin	Latitude	Longitude
A17	Australia	ns	ns
163	Syria	35.017	-37.100
213	Morocco	33.083	6.667
368	Algeria	36.549	-3.183
542	Algeria	35.847	-4.951
555	Greece	38.122	-21.543

2.5 Terpene volatile emission from *M. truncatula* ecotypes

In addition to determining the expression of *MtTPS10* in all the previously mentioned ecotypes, the release of volatiles from the roots of these ecotypes was also analyzed to establish a correlation between susceptibility or expression and sesquiterpene emissions. To investigate this hypothesis, the ecotypes were grown in lecaton substrate for six weeks. Depending on the architecture of the roots, 2-3 Sorbstar® sticks, which have the property to adsorb emitted volatiles, were inserted in different regions of the root. The roots were either treated with zoospores or mock-treated with swamp water for 24 hours. The Sorbstar® sticks were collected, put in GC vials, and stored at -80 ºC for future measurements. The volatiles adsorbed on the Sorbstar® sticks were analyzed using the thermodesorption GC-MS (see

method), and the results were analyzed using the post-run analysis software (Thermo, Shimadzu). The identity of emitted volatiles was annotated by comparing the mass spectra and retention times with matches from the National Institute of Standards and Technology (NIST) database (http://chemdata.nist.gov). *tps10* mutant plants were included in this experiment as a negative control. We found that all 6 ecotypes emitted diverse blends of sesquiterpenoids, with some ecotypes exhibiting some similarities in their emitted volatiles (Appendix, Figure 7.5). As an example, volatiles emitted from the reference line A17 and the ecotype with no transcript of *MtTPS10*, 368, are shown (Figure 2.5).

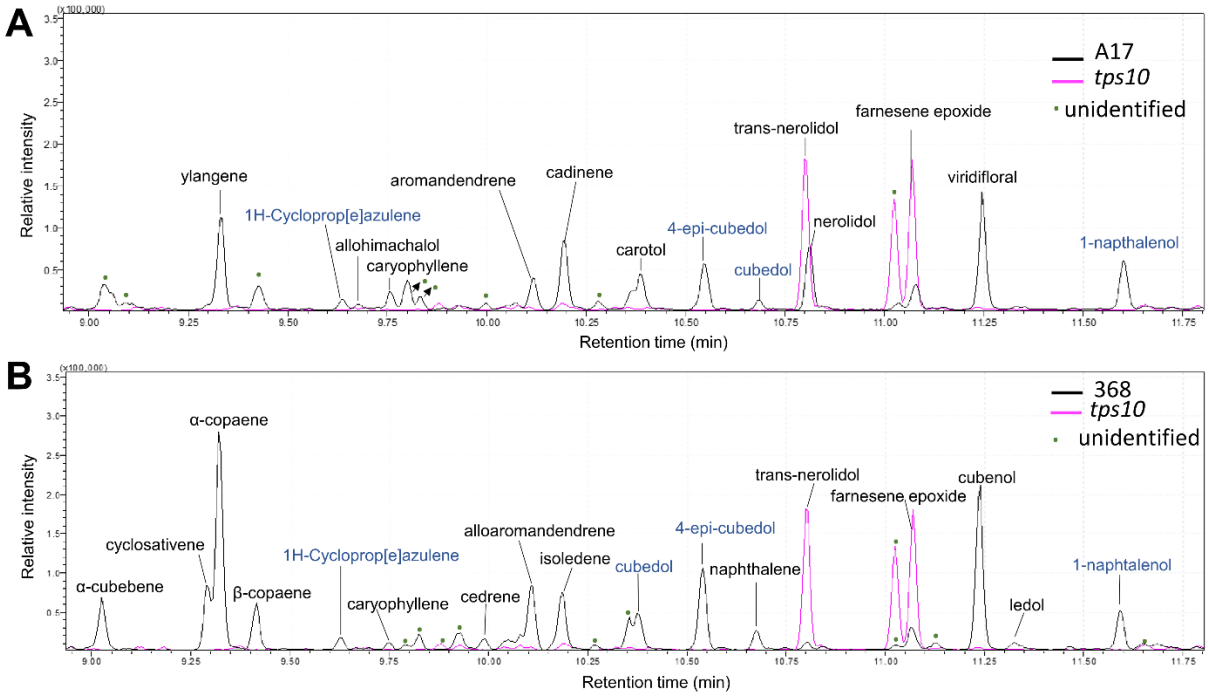

Figure 2.5: Sesquiterpene volatiles emitted from natural accessions of *M. truncatula* after *A. euteiches* infection.

GC-MS analysis targeted to identify sesquiterpenes emitted from infected plants of A17, 368, and *tps10* mutants. **A**. volatile emitted from A17. **B** volatiles emitted from 368. Pink peaks are volatiles measured from the *tps10* mutant. The chromatogram shows the relative intensity of extracted ion chromatogram (*m/z* 93,105,161 and 204). Green dots are unidentified products from the chromatogram.

2.6 Transcriptome-enabled discovery of sesquiterpenoid metabolic genes behind the blend of volatiles emitted from line 368

To identify the genes responsible for the sesquiterpene emission in line 368 after infection, we employed a comparative transcriptomic approach with roots of A17 and line 368. A17 served as the reference line. RNA was isolated from zoospore-treated seedlings and mock-treated samples with three replicates at 2 hours post-inoculation. The isolated RNA was sent to an

external organization for sequencing (www.novogene.com). Fragment per kilobase of transcript per million mapped reads (FPKM) was used to measure gene expression, and an absolute log2 (fold change) value ≥ 1 and P-value of 0.05 were set as the threshold for significant differential expression. DEGs were obtained by comparing gene expression levels between zoospore-treated roots versus mock-inoculated roots. To examine the impact of the treatments on the roots of A17 and 368, we conducted a principal component analysis to observe overall patterns and trends in the data after zoospore treatment. PCA of the DEGs from both lines showed that their DEGs substantially differed (Figure 2.6A). Importantly, zoospore-treated and mock-treated roots could be separated using two principal components. The first principal component (PC1), accounting for 58.68% of the variation in the data, separated the genotypes, and the second component (PC2) accounted for 24.65 % of the variation due to the treatments (Figure 2.6A). This resulted in a clear separation between the two lines with no outliers. The expression profile of the top 1,000 DEGs also clearly indicates that these two ecotypes respond differently to the zoospore treatments (Figure 2.6 B). Overall, a comparison between inoculated and mock-treated roots of both lines revealed a substantial number of DEGs. Volcano plot analysis showed that 9401 (2021 upregulated,1163 downregulated, and 6216 not significant) DEGs were differentially expressed in A17 2 hpi versus mock-treated roots, while 7790 (1901 up-regulated, 978 down-regulated, and 5716 not significant) DEGs were explicitly allocated to 368 2 hpi versus mock-treated roots (Figure 2.6C-D). Also, among the upregulated genes, we noticed that *MtTPS10* (Mtr_5g073200) was upregulated in A17 zoospore-treated roots, confirming the results of Yadav et al. (2019). *MtTPS6* (Mtr_2g089120) was also detected in A17 (Yadav et al., 2019) (Figure 2.6C) and 368 (Figure 2.6D). Interestingly, another uncharacterized terpene synthase gene annotated as *MtTPS25* (Mtr_4g048460) (Parker et al., 2014) located on chromosome 4 of *M. truncatula* was among the upregulated genes in both lines (Figure 2.6C-D).

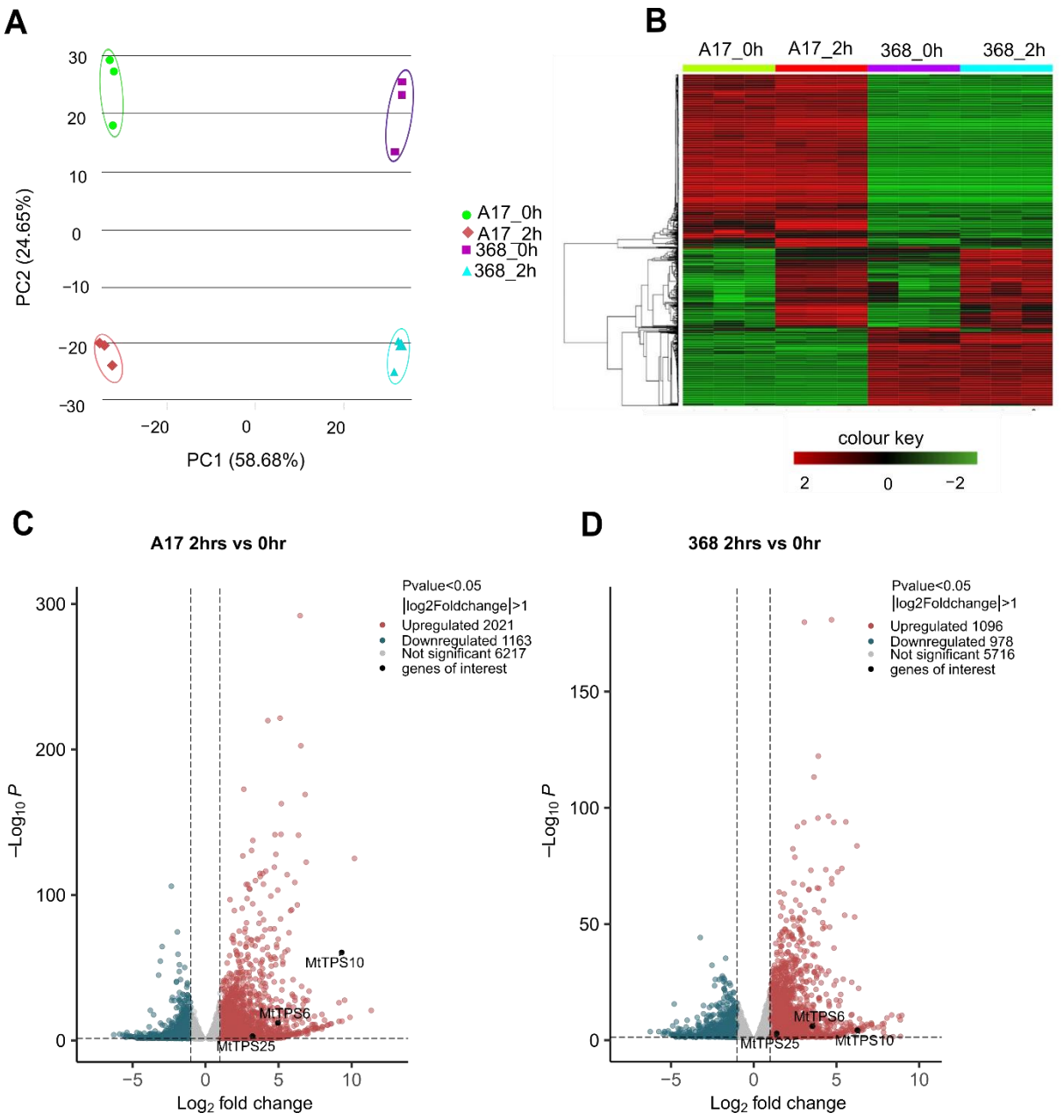

Figure 2.6: Ecotypes A17 and 368 behave differently upon zoospore treatment.

7-day seedlings from A17 and 368 were treated with zoospores, and RNA was extracted from these samples for RNAseq analysis. **A**. The PCA plot illustrates that ecotypes A17 and 368 can be distinctly differentiated both before and after zoospore treatment, with no outliers present. **B**. A heatmap of the top 1000 genes according to |log2FC|≥1 provides a global view of the differentially expressed genes (DEGs) in A17 and 368. **C-D**. A volcano diagram of the DEGs in A17 and 368 after 2 hours post-infection (hpi) versus mock treatment is shown. The X-axis represents the fold change in the difference after the log2 conversion, and the Y-axis represents the significant P-value after the log10 conversion. Red represents upregulated DEGs, blue represents downregulated DEGs, and gray represents DEGs that are not significant or below the threshold of |log2FC|≥1.

2.7 Expression profile of zoospore-induced *MtTPS*

Since our focus was to mine for sesquiterpenoid metabolic genes behind the bouquet of sesquiterpenoid volatiles produced from infected 368 roots, we filtered for the terpene synthases significantly upregulated upon zoospore infection in the volcano plots (Figure 2.6 C-D). Heatmap illustration of the FPKM values of the three biological replicates indicated that the *MtTPS10* transcript was exclusively expressed in roots of A17 2 hpi with zoospores and downregulated in line 368, confirming the results we observed earlier (Figure 2.4). On the other hand, *MtTPS25* was specific to line 368 and not A17 after the zoospore treatment (Figure 2.7A). Meanwhile, *MtTPS6* was expressed in the treated roots of both A17 and 368 compared to the control roots (Figure 2.7A). To validate the expression of *MtTPS10*, *MtTPS25*, and *MtTPS6* obtained from the transcriptomic data, relative transcript levels of *MtTPS10*, *MtTPS25*, and *MtTPS6* were determined in independent experiments. Roots of lines A17 and 368 were treated with either zoospores or swamp water, and 2 hpi RNA was extracted from root samples for the transcript determination of the *MtTPS*. The expression level of *MtTPS10* in line 368 remained statistically unchanged, whereas in reference line ecotype A17 the highest mRNA levels of *MtTPS10* were detected. This result was consistent with the findings of Yadav et al. (2019) and with our transcriptomic data (Figure 2.7A). In the case of *MtTPS25* expression, however, line A17 displayed lower *MtTPS25* accumulation in its roots after zoospores treatment with mRNA levels comparable to mock-treated roots (Figure 2.7B). In line 368, we noticed that the expression of *MtTPS25* was also significantly induced at 2 hpi with zoospores (Figure 2.7B). Accordingly, *MtTPS6* was induced significantly in roots of A17 and 368 after zoospore treatment (Figure 2.7B). These results complemented the findings from the transcriptomic data (Figure 2.7A), indicating that *MtTPS10* and *MtTPS25* were strongly induced at 2 hpi in lines A17 and 368, respectively, whereas this effect was significantly reduced in the mock-treated roots. These results confirmed that *MtTPS25* was not a false positive pick from the transcriptomic data.

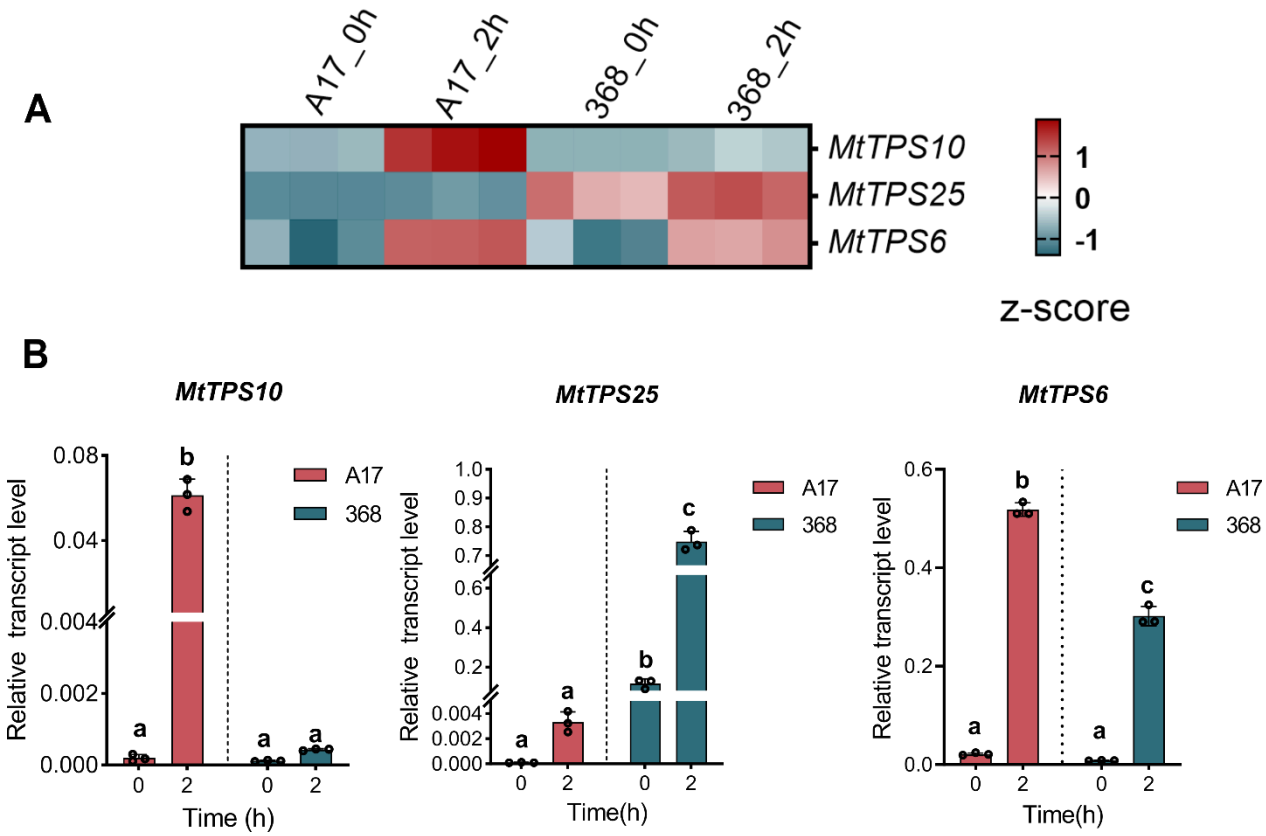

Figure 2.7: Validation of *M. truncatula* TPS:

Expression profile of *MtTPS*. **A**. RNA-seq data showing the expression pattern of *MtTPS* in the roots of *M. truncatula* after zoospore infection. RNA-seq data depict that *MtTPS10* is expressed only in infected roots of line A17, and *MtTPS6* is expressed in both A17 and 368 after infection. Meanwhile, *MtTPS25* is expressed exclusively in 368. **B**. RT-qPCR validation of *MtTPS* in A17 and 368, normalized to the housekeeping gene *MtActin2*. Statistically significant differences between 0 hpi and 2 hpi with *A. euteiches* were calculated using One-Way ANOVA followed by Tukey HSD ($p<0.05$), and differences are denoted by different letters.

2.8 Transient expression assay to understand *MtTPS10* and *MtTPS25* expression patterns driven by their accession-specific promoter sequence.

To understand the potential contribution of natural variation in the regulation of *MtTPS10* and *MtTPS25* in A17 and 368 respectively, we performed a series of promoter swapping experiments. Towards this, a 2.0 kb promoter sequence upstream of the start codon of the functionally active *MtTPS10* and *MtTPS25* from ecotypes A17 and 368 was cloned 5' to drive the β-glucuronidase (*GUS*) reporter gene. This led to the generation of transcriptional promoter::*GUS* reporter fusions designated as *pMtTPS10*^{A17}*::GUS*, *pMtTPS10*^{368}*::GUS, pMtTPS25*^{A17}*::GUS,* and *pMtTPS10*^{368}*::GUS* with superscripts indicating the ecotype-specific promoter. The promoter::*GUS* fusions were transiently transformed into roots of line A17 and

368 using hairy root transformation. The transformed roots were selected by DsRed fluorescence, and GUS readout was done on roots infected or uninfected with *A. euteiches* for 2 h by staining roots with X-gluc. Consistent with RT-qPCR (Figure 2.7B) data, we observed a differential, but significant *A. euteiches*-mediated induction of GUS activities driven through the set of *pMtTPS10::GUS* and *pMtTPS25::GUS* promoters in A17 and 368, respectively, compared to their respective basal levels (Figure 2.8A-H). Intriguingly, *pMtTPS10^{A17}::GUS* was sufficient to drive expression of *MtTPS10* in both A17 and 368 after *A. euteiches* infection (Figure 2.8A-B), even though *MtTPS10* was significantly expressed only in A17 (mid-root) (Figure 2.7B). The activity of *pMtTPS10^{A17}::GUS* in 368 was, however, not as strong as in A17 (Figure 2.8B). Another interesting observation regarding *pMtTPS10* was that there was promoter activity of *pMtTPS10^{368}*::*GUS* in A17 when infected with *A. euteiches* and not in its background, 368 (Figure 2.8C-D). Though basal levels showed some GUS activity (Figure 2.8C-D), it was rather an expected phenomenon when it comes to GUS staining (Yadav et al., 2019). To analyze the sequence similarities of *pMtTPS10* in both ecotypes, we sequenced the promoter region of *pMtTPS10^{A17}* and *pMtTPS10^{368}* and performed a multiple sequence alignment, which revealed that the promoter sequence of *pMtTPS10^{A17}* and *pMtTPS10^{368}* were almost identical except for the presence of some SNPS in *pMtTPS10^{368}* (Appendix, Figure 7.6A-B). We also subjected the promoter sequences of *MtTPS10* to computational predictions of potential binding sites for transcription factors. Our bioinformatics-aided analysis identified several conserved motifs in the promoter region of *MtTPS10* from both ecotypes. These included two MYB transcription motifs, MYC transcription motifs, ABRE2 (ABA-responsive element 2) motif, DLEC2 (Leucoagglutinating phytohemagglutinin), and three WRKY28 transcription motifs, suggesting that *pMtTPS10*^{A17} and *pMtTPS10*^{368} share a core promoter structure (Appendix, Figure 7.6A). However, the DLEC2 and one WRKY28 motif were absent in *pMtTPS10^{368}* (Appendix, Figure 7.6A-B). For the promoter region of *MtTPS25*, irrespective of where the promoter of *MtTPS25* was cloned from, we only observed strong GUS activities in *A. euteiches* treated roots of 368 (Fig. 2.8 D-H). Also, performing in-silico analysis on *pMtTPS25* produced some interesting sets of transcription factor motifs, including MYB transcription factor motifs, MYC transcription factor motifs, TGA-element sites, and GC-rich motifs (GC-box) (Appendix, Figure 7.7A-B). However, the promoter region of the two ecotypes, A17 and 368, exhibited sequence variation (Appendix, Figure 7.7A-B). Additionally, several SNPs were observed in A17, some of which overlapped with identified transcription binding sites (MYC sites) of the *MtTPS25* promoter region in this ecotype(Appendix, Figure 7.7A-B). This finding, in part, supports our GUS assay experiment (Figure 2.8E-H). Future experiments must focus on the interaction between these putative transcription factors and their respective

MtTPS target genes or involve experiments to identify any post-translational modifications that may have influenced either of these genes.

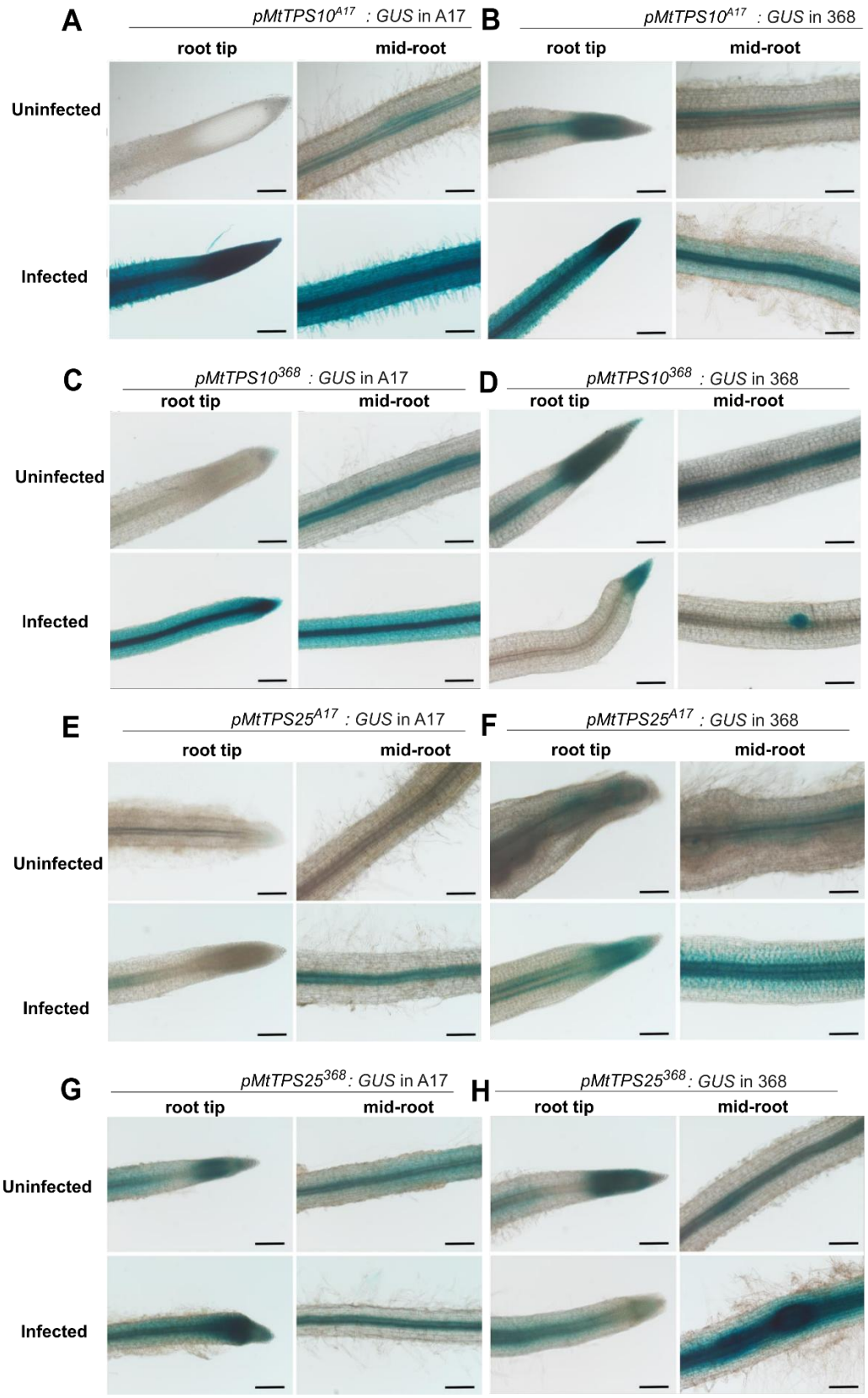

Figure 2.8: Transient GUS assay to determine basal and *A. euteiches*-induced activities of *MtTPS10* and *MtTPS25* promoters.

Visualization of GUS activity in *M. truncatula* ecotypes transiently expressing transcriptional promoter::GUS reporter fusions corresponding to *pMtTPS10A^{17}::GUS*, *pMtTPS10^{368}::GUS*, *pMtTPS25^{A17}::GUS*, *and pMtTPS10^{368}::GUS*. **A**. *pMtTPS10A^{17}* expression in A17 and 368 before and after *A. euteiches* infection. **B**. *pMtTPS10^{368}::GUS* expression in A17 and 368 before and after *A. euteiches* infection. **C**. *pMtTPS25^{A17}::GUS* expression in A17 and 368 before and after *A. euteiches* infection. **D**. *pMtTPS10^{368}::GUS* expression in A17 and 368 before and after *A. euteiches* infection. Scale bars = 200 µm. Roots from at least 3 seedlings were analyzed with similar results.

2.9 Molecular characterization of *MtTPS25*

To establish the relationship between *MtTPS25* and the other TPSs, we performed a phylogenetic analysis using the predicted protein sequence of the 22 *M. truncatula* TPSs previously assigned by Parker et al. (2014); these included *MtTPS25*. The phylogenetic analysis revealed that *M. truncatula* TPSs are distributed into four major clades with ten members in TPS-a, three in TPS-b, six in TPS-g, and three in TPS-e/f (Figure 2.9A). *MtTPS25* (highlighted blue) clusters in class TPS-a of the TPSs together with *MtTPS10* (highlighted red), which is a well-characterized oomycete-induced TPS (Yadav et al., 2019). Previous studies have shown that members of the TPS-a subfamily predominantly produce sesquiterpene volatiles in response to herbivory or pathogen attack (Arimura et al., 2007; Leitner et al., 2005; Yadav et al., 2019). In *S. lycopersicum,* the TPS-a family also produces sesquiterpenoids, whereas in *Arabidopsis,* the TPS-a subfamily produces both sesquiterpenoids and other terpenoids. (Zhou & Pichersky, 2020). Amino acid sequence alignment of all 22 *M. truncatula* TPS-encoding genes contained the characteristic sequence motifs of the TPS family DDXXD (Appendix, Figure 7.8). As depicted in Figure 2.9B, *MtTPS10* and *MtTPS25* share common motifs, including a second DDXXD motif, also known as the NSE/DTE motif (Christianson, 2006). DDXXD is involved in binding the substrate's diphosphate moiety by chelating the Mg^{2+} ion (Little & Croteau, 2002). While RXR motif is thought to act as a signaling mechanism that directs the diphosphate anion away from the reactive carbocation after ionization and is normally present upstream of the DDXXD. These observations guided our investigation to determine the functional landscape of *MtTPS25* through heterologous expression.

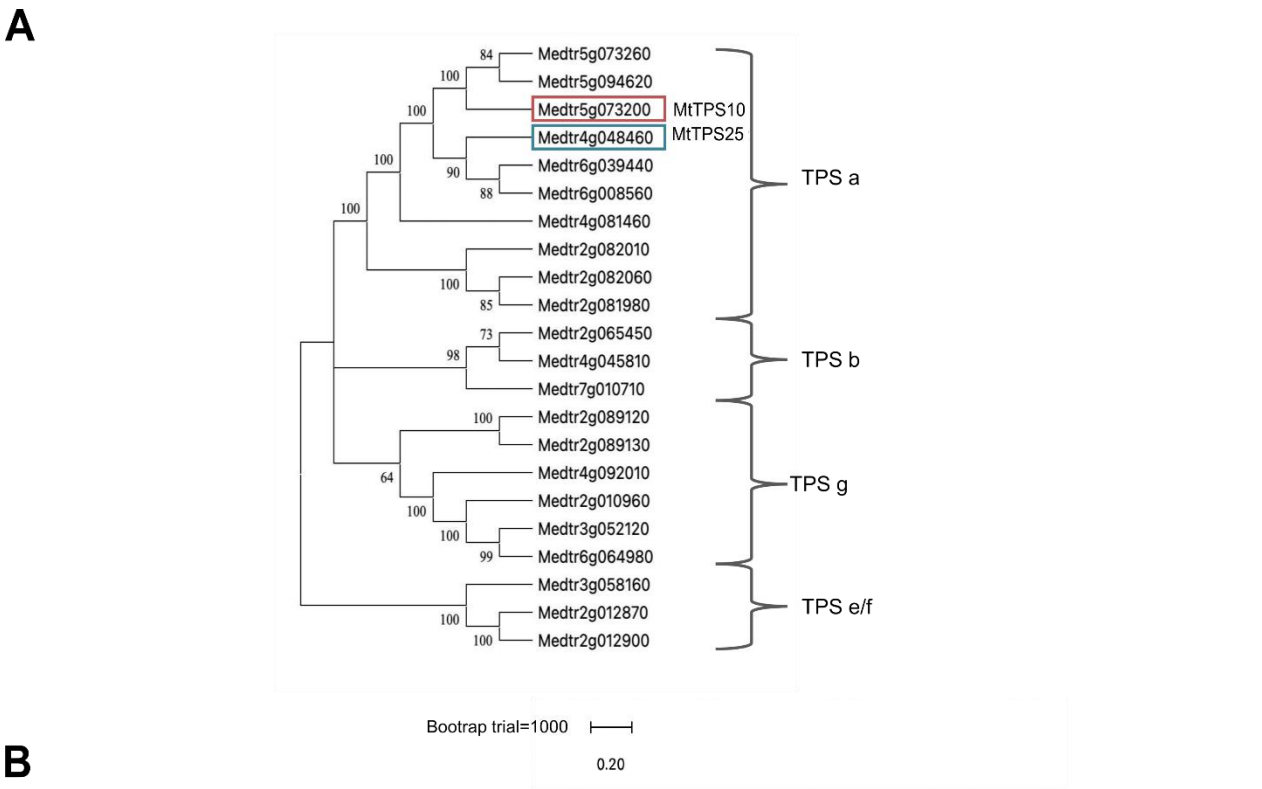

Figure 2.9: Phylogenetic tree of *M. truncatula* terpene synthases and the molecular nature of MtTPS25.

A. Neighbor-joining tree based on the degree of sequence similarity between *M. truncatula* TPSs. The maximum likelihood tree was inferred from MegaX with 1000 bootstrap replications. **B**. Global alignment between MtTPS25 and MtTPS10 protein sequences was performed using ClustalO. The red horizontal lines indicate the conserved regions RXR, DDXXD, and a second DDXXD, NSE/DTE.

2.10 Subcellular localization of MtTPS25 protein

Unlike most microbial organisms, plants utilize two distinct pathways for producing terpenoids: the acetyl-CoA-derived cytosolic mevalonate (MVA) pathway and the pyruvate-derived plastidial 2-C-methyl-D-erythritol-4-phosphate (MEP) pathway (Nagegowda, 2010). In general, MVA in the cytosol leads to the production of terpenoids such as sesquiterpenes, homoterpenes, and triterpenes, while synthesis of terpenes like monoterpenes, diterpenes, and tetraterpenes biosynthesis occur in the plastids (Karunanithi & Zerbe, 2019). Analysis of

putative targeting sequences using algorithms like TargetP (https://services.healthtech.dtu.dk/services/TargetP-2.0/) and ChloroP (https://services.healthtech.dtu.dk/services/ChloroP-1.1/) suggested that MtTPS25 has no transit peptide. To experimentally determine the subcellular localization of MtTPS25, the coding sequence of *MtTPS25* (without a stop codon) was fused to mCherry at the C terminus and inserted into the vector pICH75055 under the control of the cauliflower mosaic virus 35S promoter. This construct was transiently expressed in *Nicotiana benthamiana* protoplast, and the localization was studied using confocal microscopy. Consistent with the prediction made by TargetP and ChloroP, MtTPS25:mCherry was detected within the cytosol and the nucleus and was clearly not colocalized with chlorophyll (red autofluorescence) (Figure 2.10). This indicates that MtTPS25 is a cytosolic protein, whereas the observed nuclear localization is likely because of passive diffusion of the fluorescent protein through the nuclear pores, which is unsurprising for proteins of sizes > 60 kDa) (Timney et al., 2016; R. Wang & Brattain, 2007).

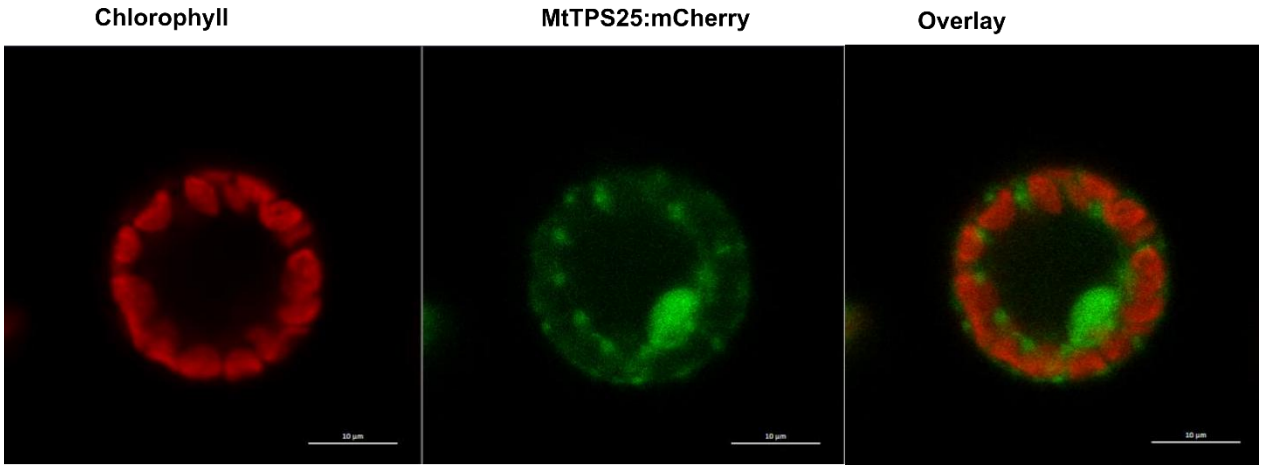

Figure 2.10: Subcellular localization of MtTPS25 protein in *N. benthamiana* protoplasts.

MtTPS25 fused C-terminally to mCherry were transiently expressed in *N. benthamiana* protoplasts, and the fluorescence images were taken using a confocal laser scanning microscope. MtTPS25:mCherry (shown in green) is visible in the cytosol and surrounds the red fluorescent chlorophyll occurring in the chloroplasts. The bars represent 10 µm.

2.11 Biochemical characterization of MtTPS25 in yeast

To assess the biochemical function of MtTPS25, the full-length CDS of *MtTPS25,* together with *farnesyl pyrophosphate synthase* (*FPPS*) and a truncated version of *HMG-CoA reductase (3-hydroxy-3-methyl-glutaryl-coenzyme A reductase*, *tHMGCR*) from *N. benthamiana* (kindly provided by Prof. Alain Tissier and Dr. Sylvestre Marillonnet, respectively) were cloned into yeast expression vector pAGT 564 and heterologously expressed in yeast (Invitrogen) under a galactose-inducing promoter using the Golden Gate system (Scheler et al., 2016). Cell

culture was extracted with n-hexane after galactose induction, and metabolites were analyzed using GC-MS analysis. MtTPS25 produced an assortment of 14 products, including sesquiterpene olefins and alcohol (Figure 2.11). MtTPS25 is a multiproduct synthase, with the most abundant product being α-copaene (**2**). Products were identified by comparing their mass spectra with those in the NIST database (ThermoScientific GC-MS). Many sesquiterpenes have been extensively studied, and their structures are well documented and deposited in relevant archives. Since α-copaene has been thoroughly studied to play a role in diverse plant-environment interactions (Magnani et al., 2025), it was relatively easy to compare the α-copaene derived from MtTPS25 yeast expression to an authentic standard (Appendix, Figure 7.9A-C). Results from the MtTPS25-derived α-copaene and the authentic standard showed similarities in their retention time (19.6 min) (Measurements were made on Agilent 8890) and fragmentation pattern (Appendix, Figure 7.9A-C), simplifying the structural determination process.

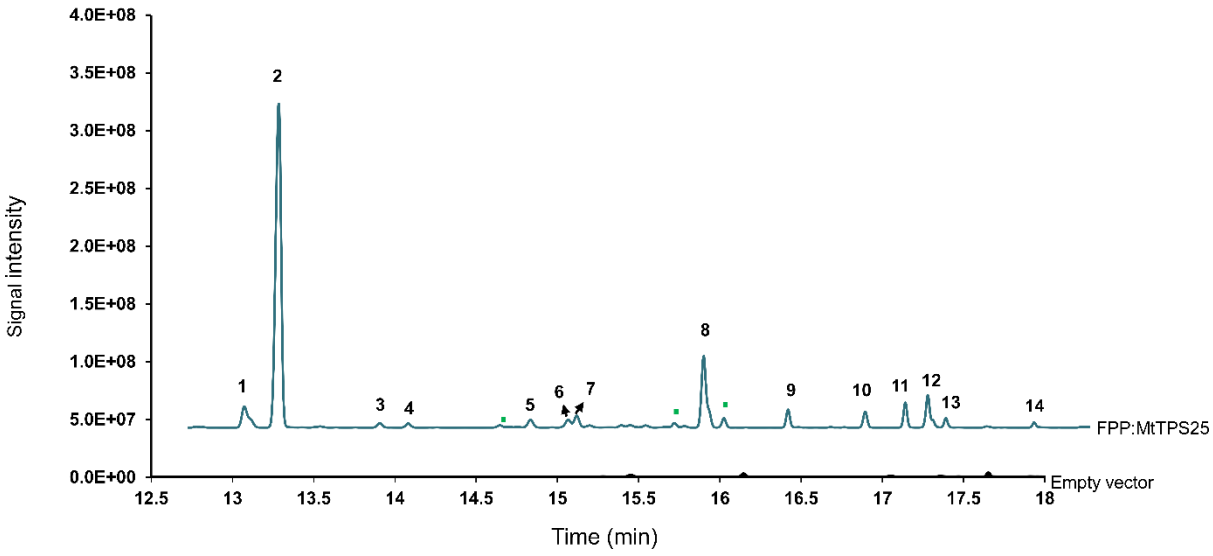

Figure 2.11: Product profile of MtTPS25 identified after heterologous expression in yeast.

Sesquiterpenes emitted from yeast cultures are presented as total extracted ion current (EIC, m/z 119,161 and 189). Sesquiterpenes were identified by comparing their mass spectra to those of the NIST library. EV is an empty vector (*FPP+tHMGCR*). Green dots represent unidentified putative terpenes. The number of each compound corresponds to the numbered peaks in the chromatogram. (1) cyclosativene, (2) α-copaene, (3) 1H-cyclopro(e)azule, (4) caryophyllene, (5) epi-β-caryophyllene, (6) cadina-1(10),4-diene (7) murolene (8) naphthalenol (9) trans-nerolidol, (10) ledol, (11) cubenol, (12) tau-muurolol, (13) epicubenol, (14) farnesol.

2.12 Biochemical characterization of *MtTPS25* in *E. coli*

Because no information is available about the biochemical properties of MtTPS25, we collaborated with Dr. Martin Dippe to investigate its substrate specificity. To this end, we performed in vitro assays using various terpene synthase substrates, including farnesyl diphosphate (FPP), geranyl diphosphate (GPP), and geranylgeranyl diphosphate (GGPP).

The recombinant protein was incubated with GPP, FPP, and GGPP. In the presence of FPP, MtTPS25 catalyzed the formation of α-copaene (Figure 2.12A). However, GPP and GGPP did not yield any new products, except for the internal standard, naphthalene, used in the measurement (Figure 2.12B-C).

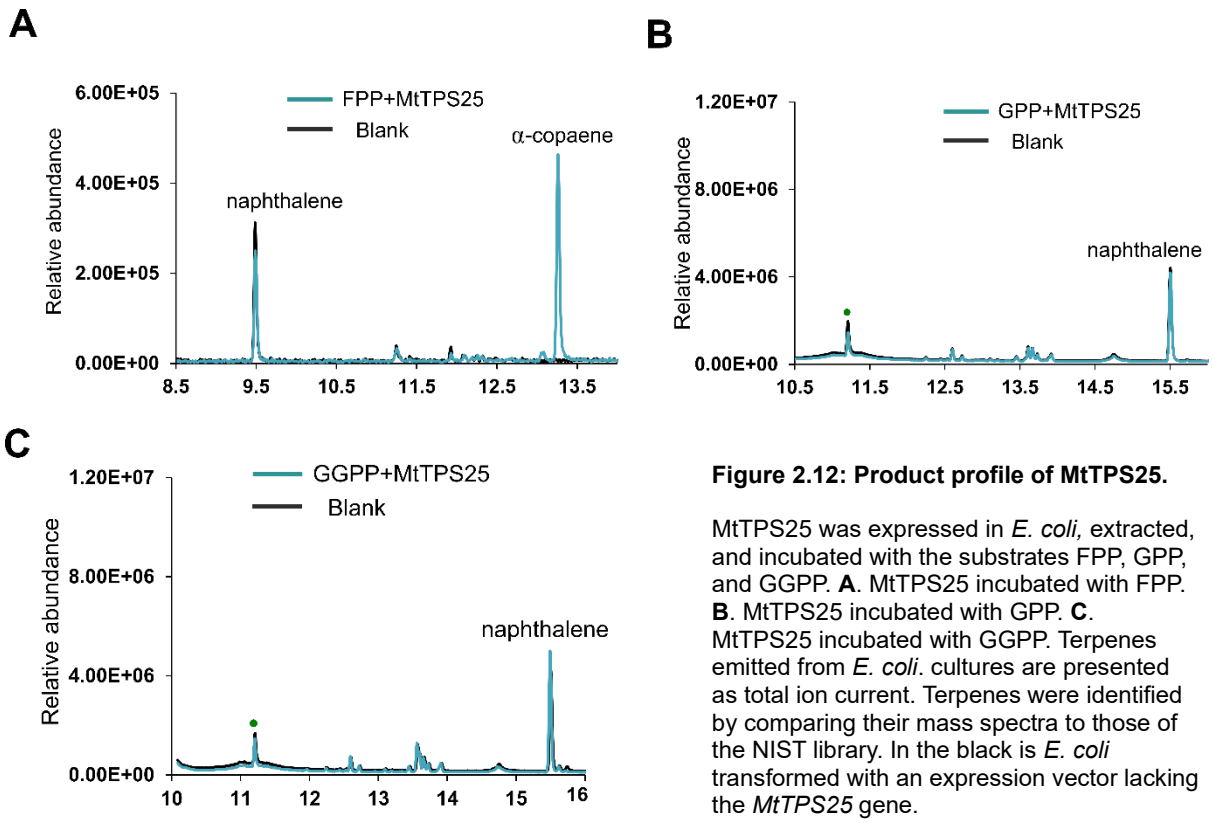

Figure 2.12: Product profile of MtTPS25.

MtTPS25 was expressed in *E. coli,* extracted, and incubated with the substrates FPP, GPP, and GGPP. **A**. MtTPS25 incubated with FPP. **B**. MtTPS25 incubated with GPP. **C**. MtTPS25 incubated with GGPP. Terpenes emitted from *E. coli*. cultures are presented as total ion current. Terpenes were identified by comparing their mass spectra to those of the NIST library. In the black is *E. coli* transformed with an expression vector lacking the *MtTPS25* gene.

2.13 Specificity of *MtTPS25* expression in *M. truncatula* after *A. euteiches* treatment

Plants' expression and accumulation of terpenoids are usually developmentally regulated and tissue-specific (Chen et al., 2003; Dudareva & Pichersky, 2000; Pichersky & Gershenzon, 2002). To determine the expression of *MtTPS25* in adult plants of line 368, roots of 6-week-old plants were inoculated with *A. euteiches* zoospores for two hours. Roots inoculated with swamp water served as a mock control. Our results showed that transcript levels of *MtTPS25* were increased in adult roots after *A. euteiches* infection compared to mock-treated roots (Figure 2.13A). Although *MtTPS25* expression was induced in adult roots, it accumulated more than double in roots of seedlings (Figure 2.13B). To investigate in which tissue *MtTPS25* was transcribed, roots and leaves of 1-week-old plants of line 368 were exposed to *A. euteiches* for two hours (2.13B). Expression of *MtTPS25* was very low in leaves inoculated with *A. euteiches* or mock-treated. However, *MtTPS25* was significantly induced in infected roots compared to the mock-treated roots (Figure 2.13B).

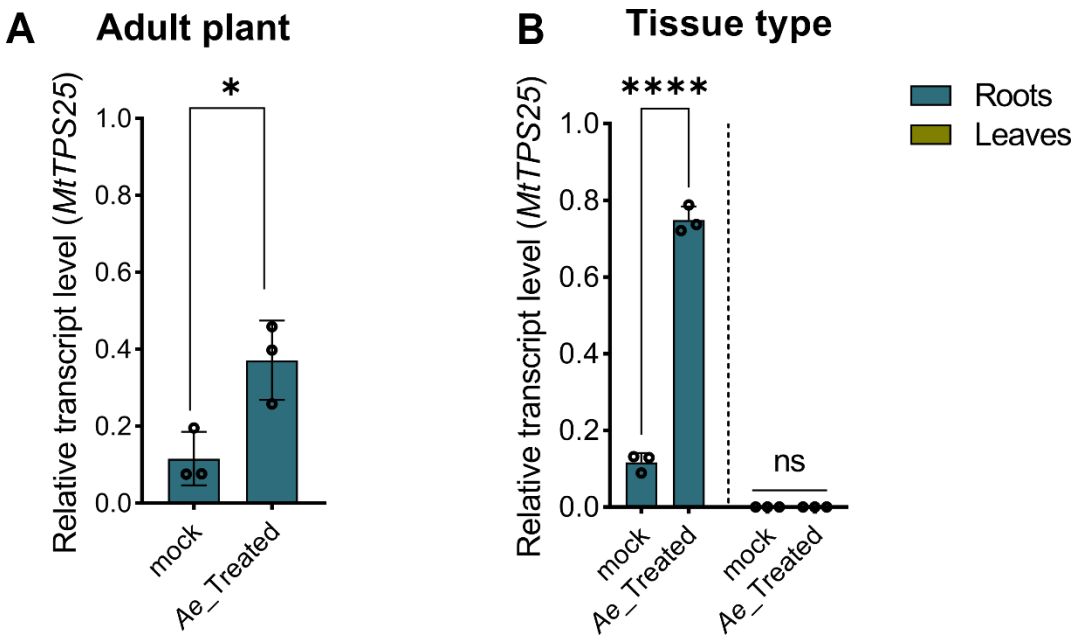

Figure 2.13: Transcript accumulation of *MtTPS25* after *A. euteiches* infection.

A. Transcript accumulation of *MtTPS25* in 6-week-old roots from line 368 at 2 hpi with *A. euteiches* (*Ae*) or swamp water. **B**. Leaves and roots of a one-week-old seedling from line 368 were treated with *A. euteiches*. *MtTPS25* transcript level was quantified using RT-qPCR and normalized against the housekeeping gene *MtActin2.* In A and B, bars represent mean +/- SD (n = 3), **P < 0.01, ***P < 0.001; ****P < 0.0001 according to Student's *t-test.*

2.14 Expression kinetics of *MtTPS25* in *M. truncatula* after *A. euteiches* treatment

To determine the expression kinetics of *MtTPS25*, transcript accumulation of *MtTPS25* was analyzed from roots of line 368 infected with *A. euteiches* at different time points ranging from early to late infection times. 1-week-old seedlings of line 368 were treated either with swamp water at 0h and with *A. euteiches* zoospores at 1h, 2h, 4h, and 24h, and the transcript levels were quantified at each time point using RT-qPCR. Interestingly, we observed that the expression of *MtTPS25* was significantly induced at 1 h post-infection (hpi), peaked at 2 hpi with zoospores treatment, and showed a modest decline in transcript levels at 4 and 24 hpi with zoospores (Figure 2.14).

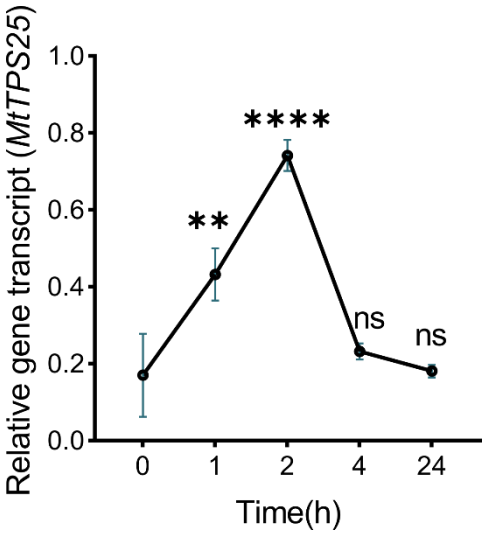

Figure 2.14: Expression kinetics of *MtTPS25* accumulation in 368 after *A. euteiches* infection.

One-week-old seedlings were either treated with *A. euteiches zoospores* or mock-treated with swamp water for the indicated time points, and data was analyzed using RT-qPCR and normalized against the housekeeping gene *MtActin2*. Bars represent standard error (SE) (n = 3), **P < 0.01, ****P < 0.0001 according to Student's *t-test.* ns = non significant.

2.15 Expression of *MtTPS25* in response to biotic and abiotic treatments

Until now, we have demonstrated that the transcript of *MtTPS25* accumulates in the roots of line 368 after infection by living zoospores of *A. euteiches*. To investigate whether *MtTPS25* is also induced by other stress factors besides the zoospores of *A. euteiches*, we subjected roots of line 368 to various stresses. For the biotic stress treatment, roots of one-week-old seedlings were inoculated with zoospores of *P. infestans* or with elicitor M of *A. euteiches*. As positive control, roots were treated with *A. euteiches*, whereas uninoculated plants (negative control) were treated with swamp water. RT-qPCR analysis of the roots showed that the *MtTPS25* transcript increased in roots treated for 2 hours with zoospores of both *A. euteiches* and *P. infestans*, as well as elicitor M, and not in swamp water-treated roots (Figure 2.15A). Like many plant-specialized metabolites, the production of terpenoids can be induced in response to elicitors such as methyl jasmonate (MeJA) (Hendrickson et al., 2024; Thimmappa et al., 2014). When the roots of one-week-old seedlings of line 368 were treated with 50 µM MeJA, we observed no apparent induction of *MtTPS25* compared to untreated roots. In addition, applying 100 mM NaCl directly to the roots of 1-week seedlings of line 368 showed no increase in the *MtTPS25* transcript compared to the mock-treated plants (Figure 2.15B).

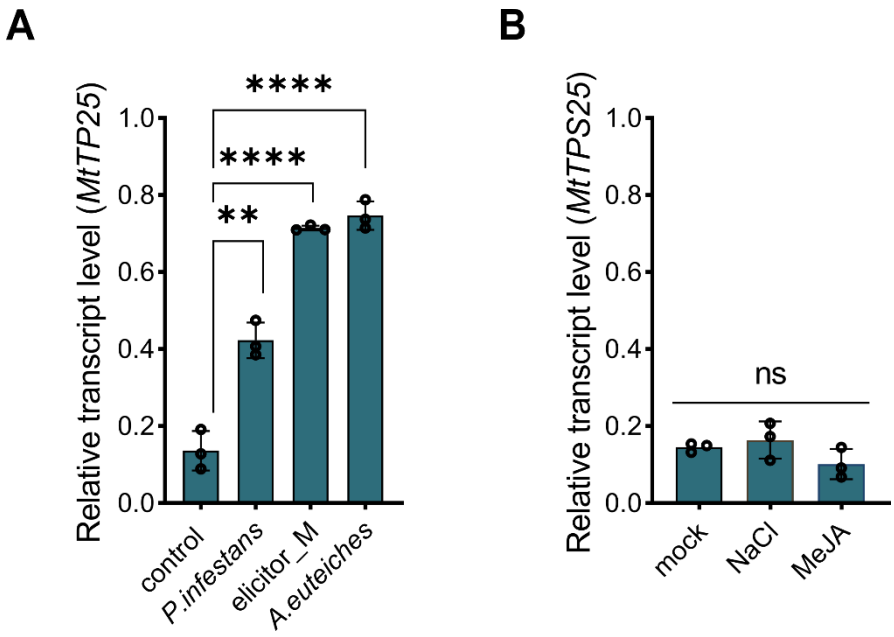

Figure 2.15: Transcript accumulation of *MtTPS25* in response to various biotic and abiotic treatments.

The transcript accumulation of *MtTPS25* was determined in seedlings of line 368 in response to biotic (**A**) and abiotic stress (**B**) agents. One-week-old seedlings were treated with *P. infestans*, elicitor M and *A. euteiches*, 100 mM NaCl, and 50 µM MeJA. *MtTPS25* transcript level was quantified using RT-qPCR and normalized against the housekeeping gene *MtActin2*. Bars represent mean +/- SD (n = 3). Statistical significance was determined by One-Way ANOVA followed by Tukey HSD (p<0.05). Bars represent mean +/- SD (n = 3), **P < 0.01, ***P < 0.001; ****P < 0.0001.

2.16 Functional Characterization of *MtTPS25*

Silencing of *MtTPS25* by RNAi in line 368

From the results obtained, we can hypothesize that *MtTPS25* is inducible solely by oomycetes. To establish whether *MtTPS25* plays a role in the defense of *M. truncatula* against the oomycete, we used a classical genetic approach of silencing *MtTPS25* in line 368 by RNA interference. A hairpin RNA construct targeting *MtTPS25* was designed using a 750 bp sense/antisense fragment of *MtTPS25* with anthocyanin produced within the root cap as the selection marker (Zhang et al., 2019) and was designated as *MtTPS25*_RNAi (Figure 2.16A). Roots of *M. truncatula* seedlings of line 368 were transformed with the *MtTPS25*_RNAi construct using hairy root transformation. Positively transformed roots had purple root tips due to the formation of anthocyanin in the root cap. Putative transgenic lines were validated by determining the expression of *MtTPS25* using RT-qPCR. 3-week-old plants of *MtTPS25*_RNAi, empty vector, and wild-type plants of line 368 were treated with zoospores of *A. euteiches* for two hours. *MtTPS25* transcript levels were significantly reduced in the roots of *MtTPS25*_RNAi plants compared to the empty vector and the wild-type plants (Figure 2.16B).

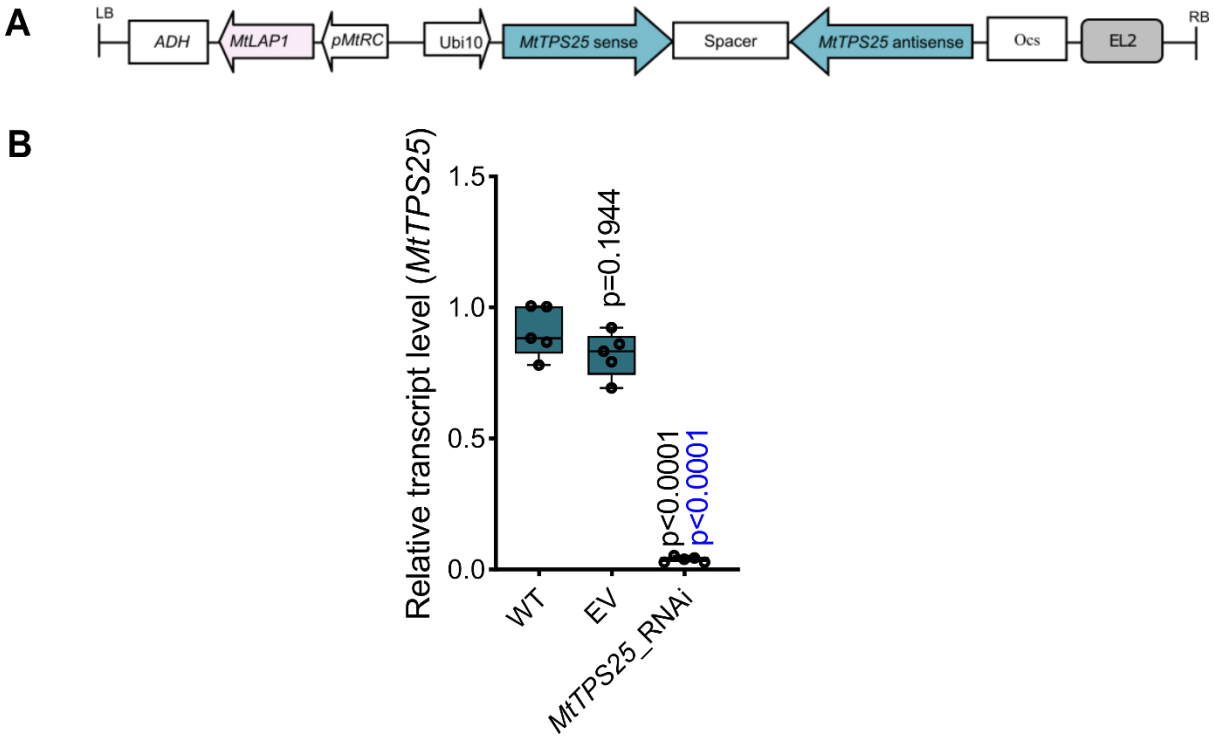

Figure 2.16: Silencing of *MtTPS25* by RNAi in 368 leads to a decrease in *MtTPS25* transcript in 368.

A. Schematic representation of *MtTPS25*_RNAi constructs showing the Ubi10 promoter-driven sense and anti-sense fragments interposed with a spacer**. B**. Transcript accumulation in *MtTPS25* in transgenic roots. *MtTPS25* transcript level was quantified using RT-qPCR and normalized against the housekeeping gene *MtActin2*. P values were determined by a two-way analysis of variance (ANOVA) and Tukey's multiple comparisons test. P values are relative to WT (black) and EV (blue).

2.17 Effect of RNAi silencing of *MtTPS25* on sesquiterpene production in line 368

Root terpenoids are known to mediate below-ground interactions and protect plants against root pathogens (Huang & Osbourn, 2019). Thus, we hypothesized that the terpene volatiles of *MtTPS25* might affect the microbial communities in the rhizosphere and specifically act in defense against *A euteiches*. Therefore, to investigate the potential role of *MtTPS25* volatiles against *A. euteiches*, we set a static headspace experiment to collect the volatile organic compounds (VOCs) from wild-type and *MtTPS25*_RNAi plants of line 368. Volatiles were sampled for 24 and after volatile collection, PDMS tubings were placed in GC vials, and roots were detached from whole plants and stored at -80 ºC. VOC analysis was done using GC-MS, and data was analyzed by comparing the chromatograms of line 368 wildtype plants and *MtTPS25*_RNAi plants. The identity of emitted volatiles was confirmed by comparing the mass spectra and retention times with matches from the NIST database (http://chemdata.nist.gov). Overall, a comparison of volatiles from *MtTPS25*_RNAi with wild-type plants of line 368 provided clear evidence that *MtTPS25* suppression leads to a dramatic decline of sesquiterpenoids in *MtTPS25*_RNAi roots. α-Copaene, the major sesquiterpene from the

heterologous expression in yeast (Figure 2.11) and emitted by wild-type roots (Figure 2.5B), was also not detectable in the *MtTPS25*_RNAi roots (Figure 2.17). The total emitted VOCs from the *MtTPS25*_RNAi roots were strongly decreased, with longifolene being the only abundant sesquiterpenoid detected.

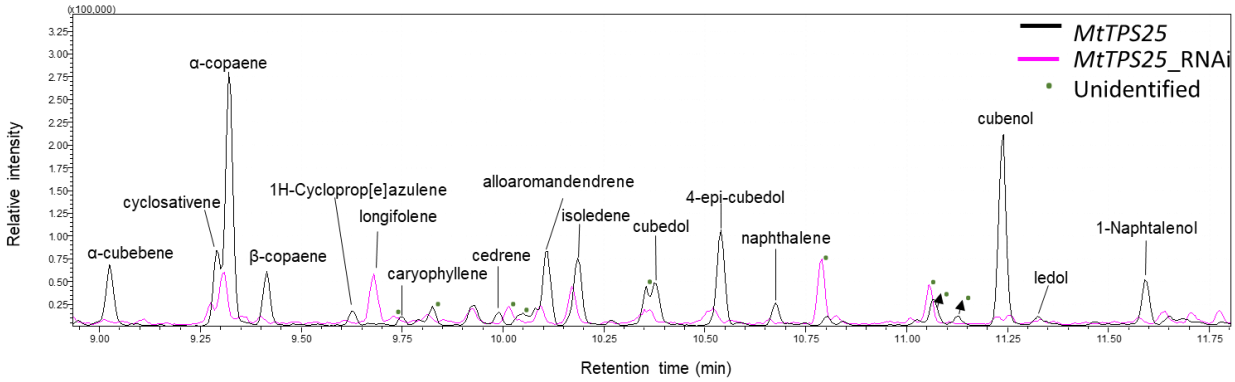

Figure 2.17: Suppression of sesquiterpenes in *MtTPS25*_RNAi.

GC-MS chromatograms of volatiles collected from infected plants of the natural accession 368 and the *MtTPS25*_RNAi.The chromatogram shows the relative intensity of the extracted ion chromatogram (m/z 93,105,161, and 204). Green dots show unidentified compounds.

2.18 Effect of RNAi-silencing of *MtTPS25* on resistance against *A. euteiches*

To examine the potential role of MtTPS25-produced sesquiterpenoids in the interaction of *M. truncatula* line 368 with *A. euteiches*, we determined the accumulation of *A. euteiches* in infected roots of this line in comparison to *MtTPS25*_RNAi. Here, 2-week-old plants were inoculated with *A. euteiches* zoospores, and after 4 weeks of infection, the amount of *A. euteiches* 5.8s rRNA was determined using RT-qPCR. In parallel, the transcript levels of *MtTPS25* were also quantified in these roots. As expected, the transcript levels of *MtTPS25* significantly declined in the *MtTPS25*_RNAi roots compared to the wild type and the empty vector (Figure 2.18A). A general overview of the oomycete biomass accumulation in the wild-type roots and the *MtTPS25*_RNAi roots gave an indication that there was a massive decline of the oomycete biomass in the wild-type plants, and this was significantly lower than the oomycete biomass accumulated by *MtTPS25*_RNAi roots (Figure 2.18B). So far, the result implies that *MtTPS25* might contribute at least partially to 368 resistance against *A. euteiches*. To examine the possible antimicrobial role of α-copaene, the major product of MtTPS25, plugs of mycelium from an actively growing colony of the *A. euteiches* were placed on cornmeal agar. Different concentrations of α-copaene (commercially purchased) were dissolved in n-hexane and applied to a filter paper disc placed equidistant from the mycelium plug. The

places were incubated at room temperature for 10 days, and after this period, the mycelium growth was monitored. From this antimicrobial assay, we observed no inhibition of mycelium growth of α-copaene concentrations ranging from 20 µM to 300 µM (data not shown). This could imply that the reduced amount of *A. euteiches* biomass in line 368 reported by Dreher et al. (2017) or in this work (Figure 2.18B) could be a collective action of the bouquet of volatiles emitted during infection and not just by α-copaene. Higher concentrations could also be included in future experiments.

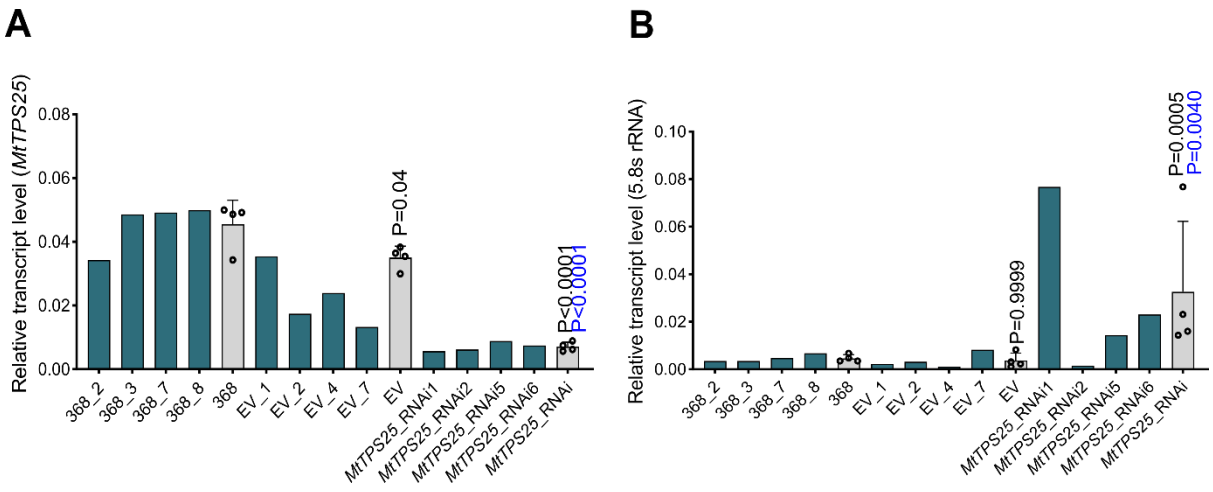

Figure 2.18:***MtTPS25* is required for oomycete resistance in line 368**.

A. *MtTPS25* transcripts were significantly reduced in *MtTPS25*_RNAi lines compared to wild type and empty vector (EV). *MtTPS25* transcript level was quantified using RT-qPCR and normalized against the housekeeping gene *MtActin*. **B**. *A. euteiches* 5.8s rRNA. The transcript accumulation was normalized against *MtActin*. P values were determined by a one analysis of variance (ANOVA) and Tukey's multiple comparisons test. P values are relative to WT (black) and EV (blue).

2.19 Bioengineering *MtTPS10* and *MtTPS25* in potato to enhance resistance against *P. infestans*

2.19.1 Constitutive expression of *MtTPS10* and *MtTPS25* in potato

Attempts to engineer plants to emit terpenoids constitutively have resulted in a series of promising experiments demonstrating improvement in plant fitness and repellency to herbivores (Aharoni et al., 2005; Robert et al., 2013). Of specific interest in this current study is improving potato resistance to the economically important pathogen *P. infestans*. This interest stemmed from the fact that *MtTPS10* and *MtTPS25* are specifically induced in the roots of *M. truncatula* upon contact with *A. euteiches* and *Phytophthora* species such as *P. palmivora* (Yadav et al., 2019) and *P. infestans* (Figure 2.2B and Figure 2.15A). The products of MtTPS10 exhibited antimicrobial properties against *A. euteiches* (Yadav et al., 2019).

Therefore, we speculated that both enzymes might help protect other plants that are infected by oomycetes.

To assess the constitutive emission of MtTPS10 and MtTPS25 products, the coding region of either *MtTPS10* or *MtTPS25* was cloned under the control of the *35S* promoter (see method). Potato plants were transformed using *Agrobacterium tumefaciens*-mediated leaf disk transformation. The expression levels of the terpene synthases were detected in the leaves of transgenic potato plants by RT-qPCR. From our data, no transcript of *MtTPS10* and *MtTPS25* was detected in wild-type plants and empty vector-transformed plants (Figure 2.19 A, B). The total number of transgenic plants is shown in the appendix (Figure 7.10A-B). Our results revealed that the transformed plants did not suffer from any developmental costs and were phenotypically similar to wild-type plants or empty vector plants under standard growth conditions (Figure 2.19C). Four transformed lines obtained from independent transgenic calli and expressing almost similar levels of the respective terpene synthases were selected for further analysis (Figure 2.19A-B).

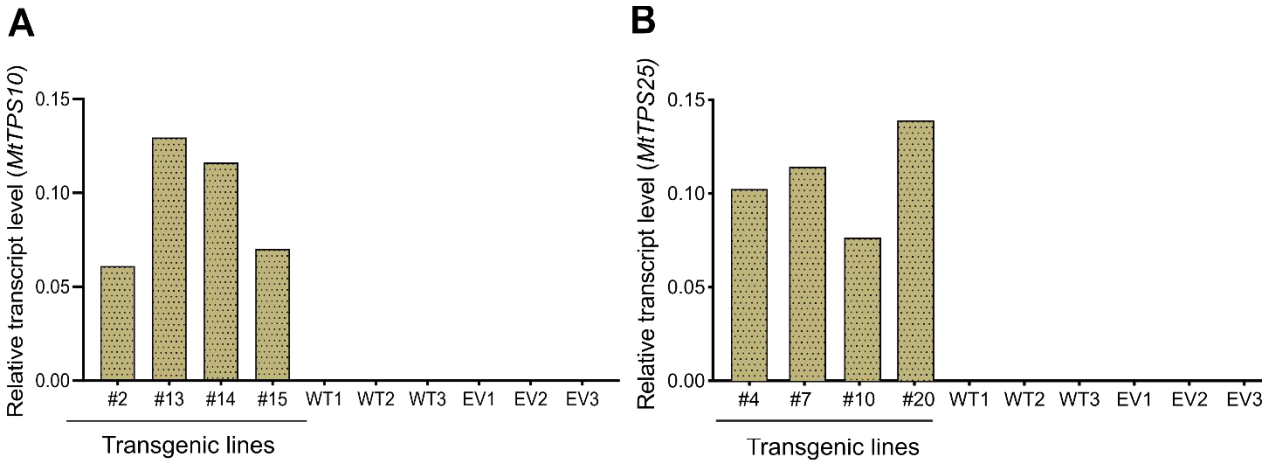

Figure 2.19: Overexpressing *MtTPSs* in potatoes results in no developmental tradeoffs.

A-B. Transcript levels of *MtTPS10* and *MtTPS25* were significantly enhanced in transgenic lines compared to wildtype (WT) and empty vector (EV). X-axis numbers represent selected transgenic lines selected for further experiments. *MtTPS* transcript level was quantified using RT-qPCR and normalized against the housekeeping gene *EF1α*.**C**. Pictures of the wild-type plants, empty vector, and transgenic plants overexpressing *MtTPS*. Scale bars = 6.5 cm.

2.19.2 Constitutive emission of sesquiterpenes may increase potato resistance to *P. infestans*

The importance of terpenoids for effective pest and pathogen control in plants has been demonstrated in various instances throughout the plant kingdom (Kappers et al., 2005; Liu et al., 2024; Magnani et al., 2025; Pichersky & Gershenzon, 2002). The current study is specifically interested in the effect of terpene synthases from *M. truncatula* on potato resistance against *P infestans*. When the leaves of the susceptible potato cultivar Desirée are inoculated with *P infestans*, a compatible interaction occurs characterized by the development of leaf lesions and significant oomycete growth within 3 days (Eschen-Lippold et al., 2007).
To assess the resistance of *P. infestans* in transformed and non-transformed potato plants, an infection assay was conducted by inoculating potato leaves with $1x10^5$ zoospores of *P. infestans*. The biomass of the pathogen in each plant was determined via RT-qPCR. Our results revealed that transgenic plants expressing *MtTPS10* accumulated a lower amount of *P. infestans* biomass relative to the wild-type and empty vector plants, there was even a negative correlation between *MtTPS10* expression and biomass accumulation of *P. infestans* (Figures 2.19A and 2.20A). However, in the case of the potato lines overexpressing *MtTPS25*, one line of the transgenic plant (7) exhibited a significant increase in *P. infestans* biomass compared to the wildtype, while the remaining lines showed no difference in oomycete accumulation compared to Wild-type plants (Figure 2.20B). In parallel, leaves were harvested from transgenic and control plants (wild type and empty vector) and subjected to sesquiterpene analysis (GC-MS). Our results show that the introduction of *M. truncatula*-derived terpene synthases*, MtTPS10* and *MtTPS25,* into the genome of potatoes results in the formation of quite a few sesquiterpenes. In transgenic lines expressing *MtTPS10*, there was only one sesquiterpene alcohol annotated as shyobunol (8) (Figure 2.20C) detected in the chromatogram. Meanwhile, the wild type and empty vector plants released the same sets of sesquiterpenoids, namely (1) caryophyllene, (2) cis-farnesene, (3) cubebol, and (7) germacrene D-4-ol. This indicated that the potato cultivar used in this experiment inherently possesses the ability to produce sesquiterpenes. In the case of the transgenic lines expressing *MtTPS25*, a substantial amount of sesquiterpenoids were produced compared to the wild type and the empty vector control. These products included (4 and 5) β-copaene and (6) 7-epi-cis-sesquisabinene hydrate (Figure 2.20D). Overall, it was evident from our results that the wild-

type and empty vector plants shared some metabolites with the transgenic lines. However, the intensity of these compounds was somewhat higher in the transgenic lines compared to the wild-type and empty vector plants. These results show that transgenic approaches could be promising tools for boosting secondary metabolite production in plants.

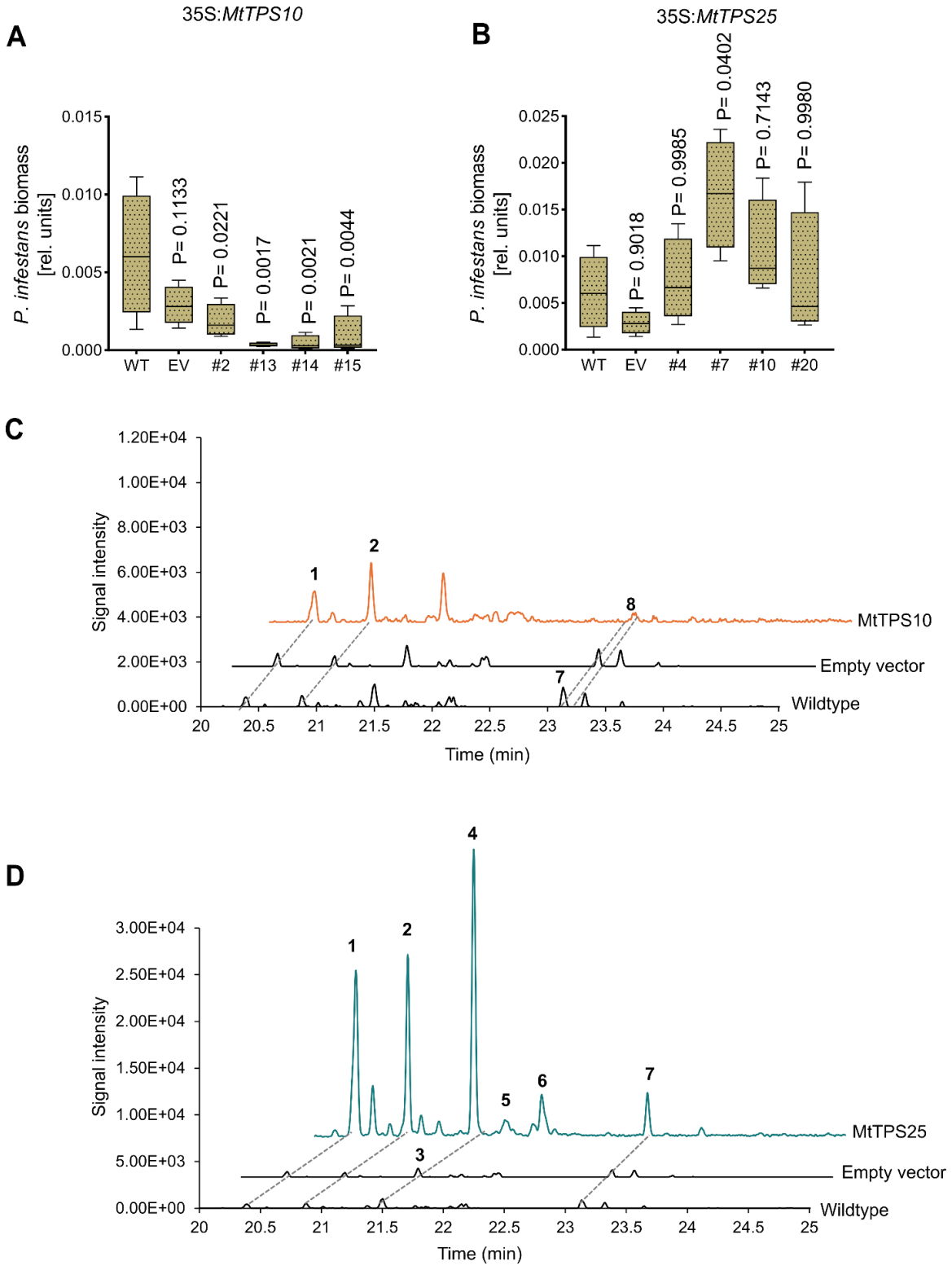

Figure 2.20: Emission of MtTPS may increase the fitness of potato against *P. infestans*

A-B Growth of *P. infestans* on transgenic plants. Leaves of wild-type (wt) and transgenic plants carrying the empty vector (EV) or 35S::*MtTPS* were infected with $1x10^5$ *P. infestans* zoospores/ml. Pathogen biomass was determined 3 days after infection by RT-qPCR with DNA isolated from infected leaves using *P. infestans*-specific primers. P values are relative to wt, and the exact P-values are indicated on each bar. **C-D**. Sesquiterpenes emitted from potato leaves are presented as total extracted ion current (EIC, m/z 93,105,161,204,222). Sesquiterpenes were identified by comparing their mass spectra to those of the NIST library. The number of each compound corresponds to the numbered peaks in the chromatogram. (1) caryophyllene, (2) cis-β-farnesene, (3) cubebol, (4 and 5) β-copaene, (6) 7-epi-cis-sesquisabinene hydrate, (7) germacrene D-4-ol and (8) shyobunol. Peaks with no assigned numbers were unknown products.

2.20 Identification of enzymes converting MtTPS10 products in *M. truncatula* roots

Our data clearly indicates that line 368 serves as a naturally occurring mutant of *MtTPS10* (Figure 2.7). Additionally, background knowledge on MtTPS10 shows that heterologous expression of *MtTPS10* in yeast produces several bouquets of metabolites, primarily composed of sesquiterpenes (15-carbon compounds); however, the major compound, himachalol, detected in yeast was absent from the volatiles released by infected roots. With this information, we hypothesized that the absence of himachalol from the volatiles of infected roots might be due to its conversion *in planta*. Therefore, the transcriptomic data obtained from A17 and 368 (using 368 as *Mttps10*) (Figure 2.6) were employed to identify candidate enzymes that may be converting himachalol. *MtTPS10* was used as bait to retrieve tightly coregulated genes. A thorough analysis of our transcriptomic data showed *CYP71D61*, *CYP71D62,* and *MtTPS10* emerging as the most tightly co-expressed genes with correlation coefficients r=0.98 and 0.99, respectively (Figure 2.21A).

The expression patterns of CYP*71D61* and *CYP71D62* (Figure 2.21A) also hint that they might be acting on MtTPS10 products. The genomic organization of *CYP71D61*, *CYP71D62,* and *MtTPS10* further supported this finding in that *CYP71D61* and *CYP71D62* are genes on chromosome 5 of the *M. truncatula* genome, just as *MtTPS10* and are only separated from each other by 1.9 kb nucleotide sequences and from *MtTPS10* by 10 kb nucleotide sequences (Figure 2.21B). The two cytochrome enzymes are transcribed in the same direction as *MtTPS10* (Figure 2.21B), hinting that these three genes might form the core of a larger metabolic cluster (Nützmann & Osbourn, 2014). *CYP71D61* and *CYP71D62* were selected, and their expression was validated by RT-qPCR. After infection of roots with *A.* euteiches, these genes showed a significant induction like that of *MtTPS10* in A17 and a reduced expression in line 368 (Figure 2 .21C-D).

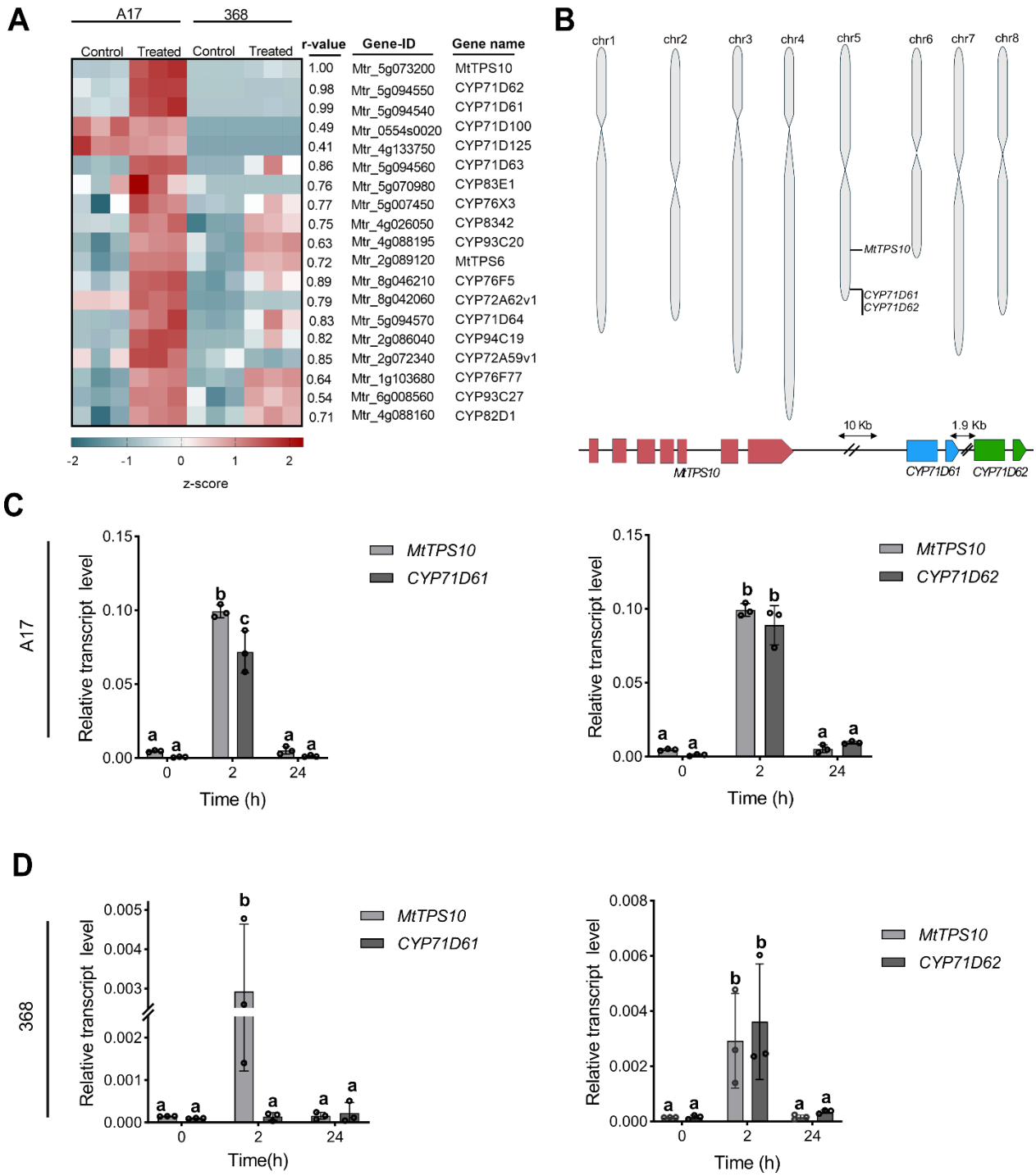

Figure 2.21: *CYP71D61* and *CYP71D62* are co-expressed and physically clustered on chromosome 5 with *MtTPS10*.

A. Heatmap of 19 genes showing the highest coregulation with *MtTPS10*. The FPKM of three biological replicates was transformed into z-scores. Medtr5g094550 (*CYP71D62*) and Medtr5g094540 (*CYP71D61*) were selected for further analysis. **B.** Map of the two CYPs, *CYP71D61* and CYP71D62, together with *MtTPS10* gene cluster on chromosome 5 (top) and representation of the genes and genomic distances between each gene (bottom). Chr1-8 represents chromosomes 1-8 of the M. truncatula genome. MtTPS10 is red-filled, and *CYP71D61* and CYP71D62 are blue and green-filled, respectively. **C**. Validation of co-expression of *CYP71D61* and *CYP71D62* with Mt*TPS10*

by RT-qPCR in the reference ecotype **A17**. **D**. Validation of co-expression of *CYP71D61* and *CYP71D62* with *MtTPS10* by RT-qPCR in ecotype 368 (acting as a *MtTPS10* mutant line). Gene expression was normalized against the housekeeping gene *MtActin2*. Letters represent statistically significant differences using one-way ANOVA and Tukey's post-hoc test. Bars, Mean ± SEM (n=3).

2.21 CYP71D62 reduces himachalol emission in yeast

MtTPS10 was previously reported to generate a complex blend of more than fourteen sesquiterpenes, including himachalol as the major component when the gene was expressed in yeast. To test the hypothesis of a functional link between the two cytochrome-P450s and *Mt*TPS10, we tested the activity of CYP71D61 and CYP71D62 on MtTPS10 products in yeast, a more suitable host for expressing P450 enzymes because of its eukaryotic properties. The full coding sequences of *MtTPS10*, *CYP71D61*, and *CYP71D62* were individually expressed in yeast after creating appropriate constructs using the Golden Gate system (Scheler et al., 2016) and extracted using n-hexane. Yeast cultures expressing *MtTPS10* featured the expected mixture of sesquiterpene hydrocarbon and alcohol, with himachalol as the major sesquiterpene alcohol (Figure 2.22A-B). Yeast cultures collected from yeast expressing *MtTPS10* and *CYP71D61* revealed no additional compounds but showed a similar product profile as *MtTPS10* alone. However, the yeast culture expressing *MtTPS10* and *CYP71D62* revealed 4 additional products, likely resulting from CYP71D62-dependent oxidation of MtTPS10 products. The new products **5/8**,**6/7** were annotated as 1R,7S, E)-7-isopropyl-4,10-dimethylenecyclodec-5-enol and longifolenaldehyde, respectively, according to the NIST library. Due to the different retention times of these compounds, it makes it difficult to conclude that products **5** and **8** or **6** and **7** are the same compound. Thus, structure elucidation of these compounds is envisioned for future experiments. The neighboring gene Mtr_5g094560 (*CYP71D63)* with the correlation coefficient of 0.86 was also analyzed for its catalytic activity on MtTPS10 products (Figure. 2.21A). The heterologous expression of *CYP71D63* in yeast and *MtTPS10* did not reduce himachalol but yielded a new product,(**9**) 7, epi-cis-sesquisabinene hydrate (Figure 2.22D). Future work can include LC-MS measurement to help make conclusive decisions.

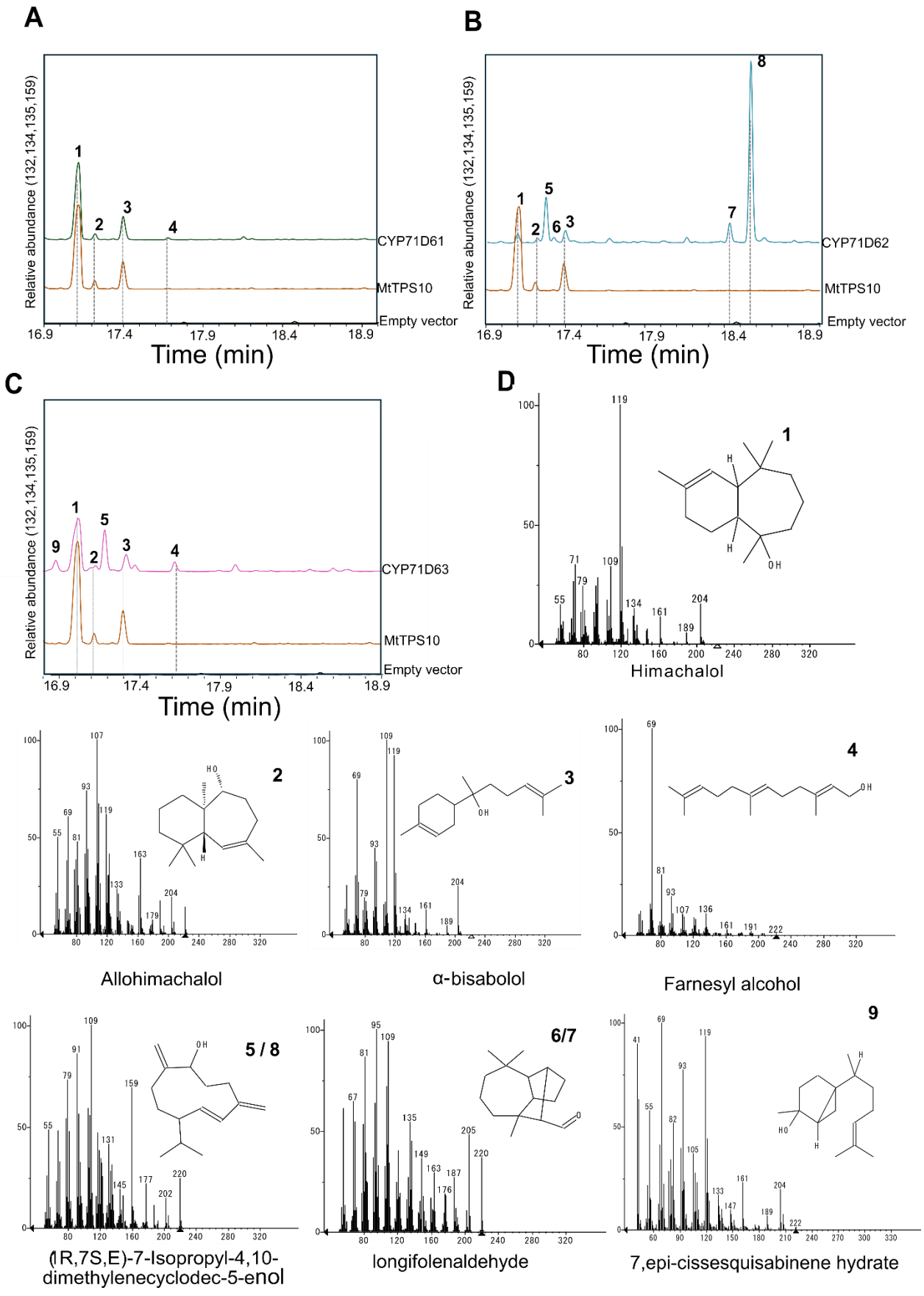

Figure 2.22: CYP71D62 oxidizes major MtTPS10 products in yeast.

A. GC-MS chromatograms of cultures of yeast expressing the gene combination of MtTPS10 and CYP71D61. **B**. GC-MS chromatograms of cultures of yeast expressing the gene combination of MtTPS10 and CYP71D62. Chromatograms show the sum of extracted ions (m/z 132+134+135+159). **C**. MS/MS spectra of products 1-8. Products were (1) himachalol, (2) allohimachlol, (3) α-bisabolol, (4) farnesyl alcohol, (5/8) (1R,7S, E)-7-Isopropyl-4,10-dimethylencyclodec-5-enol, and (6/7) longifolenaldehyde, and(9) 7, epi-cis-sesquisabinene hydrate according to the NIST database.

2.22 Functional characterization of *CYP71D62*

Now that *CYP71D62* had been proven to be a potential candidate modifying himachalol *in vivo,* the next approach was to study the impact of *CYP71D62* loss-of-function in himachalol metabolism. For this, we searched for *Tnt1* in the Samuel Nobel foundation database, which houses a large collection of *M. truncatula* insertions. The genomic sequence of *CYP71D62* was blasted against either *Tnt1* high-confidence FSTs (flanking sequence tags) or low-confidence FSTs in the Noble Foundation web database. One insertion line, NF19103, showed 100 % similarity to *CYP71D62.* The seeds of this insertion line were ordered and genotyped. From the genotyping results, a plant with a homozygous *Tnt1* insertion in the gene of interest was obtained (PLANT #1) (Figure 2.23B). Seeds of this plant have been stored for future experiments.

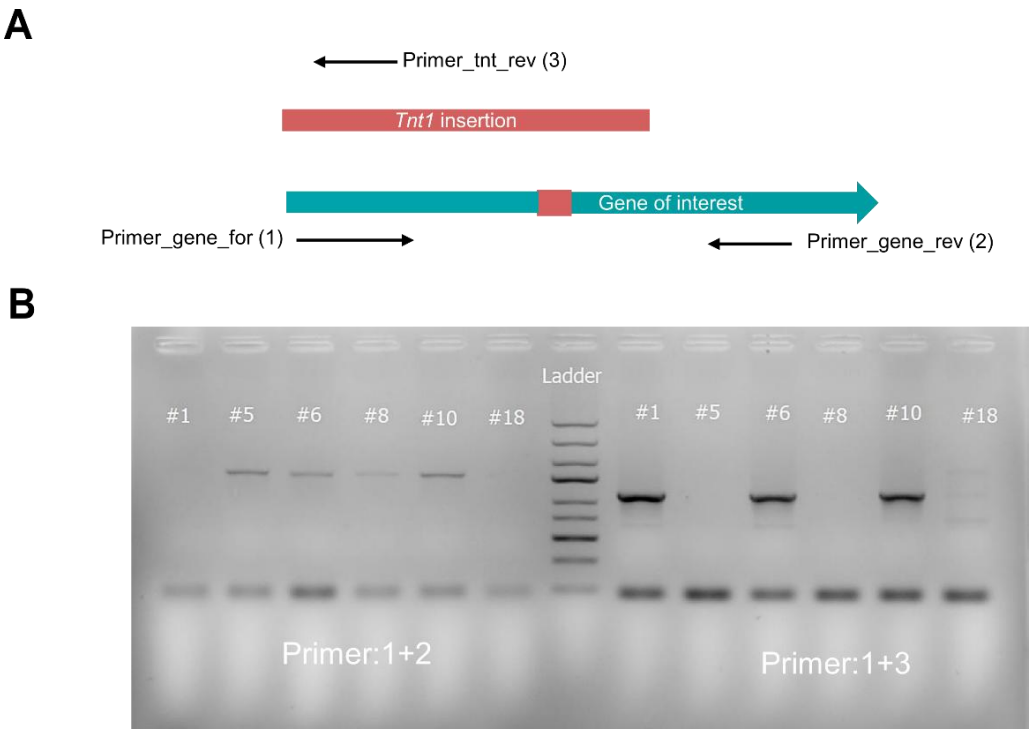

Figure 2.23: Genotyping of *Tnt1* insertion lines.

A. A scheme of primer design of *Tnt1* insertion lines. To test the presence of the wt allele, primers of the gene of interest depicted as primers 1 and 2 were used to test the presence of the *Tnt1* insertion; the forward primer of the gene of interest (1) was combined with a reverse primer located on the *Tnt1* sequence (3). **B**. Example of a PCR analysis of 6 different plants with the two primer combinations for the wt allele and the *Tnt1* insertion, showing a heterozygous insertion in plants # 6 and #10 and a homozygous insertion in plant #1. No insertion was detected in plants #5,#10, and #18.

3 DISCUSSION

Aside from primary metabolites needed by plants for growth and development, plants have also evolved to produce a vast array of specialized metabolites, likely as an adaptation to different environmental niches (Chae et al., 2014). One key factor that influences a plant's fitness and survival in the environment is its ability to fine-tune the deployment of secondary metabolites during stress. Sesquiterpenoids are plant-specialized metabolites that function in plant defense and have antimicrobial activities (Degenhardt et al., 2009; Lin et al., 2017; Rasmann et al., 2005; Schnee et al., 2006; Yadav et al., 2019). They are the largest and most structurally diverse family of plant-natural products (Holopainen & Gershenzon, 2010). The model plant *M. truncatula* has been reported to harbor 32 *TPS*s (Hendrickson et al., 2024) with 22 assigned numbers by Parker et al. (2014). Several of these *MtTPSs* have been implicated in defense against pests and pathogens (Arimura et al., 2007; Boland & Garms, 2010; Garms et al., 2010; Yadav et al., 2019). Among these is *MtTPS10,* a stress response gene playing a pivotal role as an early defense gene against oomycete infection (Yadav et al., 2019). This study aimed to dissect the gene-metabolite relationship in the *M. truncatula* terpenome after infection by *A. euteiches*.

3.1 Elicitor M induces defense genes and *MtTPS10* expression in *M. truncatula*

Many plants respond to a microbial attack by accumulating transcripts of defense-related genes. The products of which impede the pathogen's colonization and degree of infection (Jones et al., 2024; Jones & Dangl, 2006). Molecules of microbial origin that trigger the transcription of defense-related genes are termed elicitors (Nars et al., 2013). The *M. truncatula-A. euteiches* interaction is known to result in the induction of the defense gene, *MtTPS10* (Yadav et al., 2019), a gene rapidly induced after pathogenic oomycete infection (Yadav et al., 2019, Figure 2.3C). *MtTPS10* transcript levels were neither induced by contact with beneficial fungi (*R. irregularis*) nor by pathogenic fungi (*C. trifolii*), nor by abiotic stresses such as NaCl, wounding, or MeJA treatment (Yadav et al, 2019). So far, the sole induction of *MtTPS10* has been attributed to three pathogenic oomycetes *(A. euteiches, P. palmivora*, and *P. infestans*). To prove whether PAMPs from *A. euteiches* function as elicitors, we showed here using the GUS reporter system and RT-qPCR that, aside from zoospores, even mycelium and water incubated in the presence of a growing mycelium (elicitor M) induced the expression of *MtTPS10* after contact with roots (Figure 2.2A). Our experiments also revealed that elicitor M triggers similar defense responses as zoospores (Figure 2.3), giving strong evidence of the similarity in the mode of action of these two developmental stages of the pathogen. The elicitor

activity observed at the various developmental stages of *A. euteiches* may stem from unique components of the oomycete cell wall or from other oomycete-specific molecules. In most eukaryotic pathogens, however, PAMPs are typically derived from cell wall components (Camborde, 2020). Reported examples include Pep-13, a conserved amino acid sequence within the cell wall glycoprotein (GP42) of *P. sojae* (Brunner et al., 2002); a carbohydrate-binding Module Family 1 (CMB1) found in the cell wall of *P. parasitica* (Gaulin et al., 2006); and NPP1, an ectonucleotide phosphodiesterase from *Phytophthora* species (Fellbrich et al., 2002), all of which are known to trigger immune responses in plants.

It has long been established that the oomycete cell walls are primarily composed of cellulose and β-(1,3;1,6)-glucans (Bartnicki-Garcia, 1968). However, a more recent finding by Nars et al. (2013) revealed the presence of an additional heteroglycan branch containing β-(1,3;1,4)-glucans. Interestingly, these glucans are structurally similar to those found in the members of the Poaceae family and certain fungal pathogens such as *Aspergillus fumigatus* and *Rhynchosporium secalis* (Nars et al., 2013), suggesting a potentially broader biological relevance of these cell wall structures. The β-(1,3;1,4)-glucans structure identified in *A. euteiches* contains *N*-acetyl glucosamine (GlcNAc) residues, a feature that sets it apart from similar glucans found in plants and fungi (Mélida et al., 2013; Nars et al., 2013). This unique structural composition may influence how the plant immune system perceives these glucans and could potentially contribute to the elicitor activity of *A. euteiches*. Given that cell wall polymers are well established as signatures capable of triggering plant immune responses (Gust et al., 2012; Oldroyd, 2013), we sought to investigate the elicitor potential of a commercially sourced GlcNAc in *M. truncatula* roots. This was based on the hypothesis that GlcNAc may be the key component in elicitor M, inducing *MtTPS10* expression in *M. truncatula.* By testing this hypothesis, our data showed no induction of *MtTPS10* by GlcNAc at a concentration of 100 $\mu g.ml^{-1}$ (Appendix, Figure 7.2), which is the conventionally used concentration for determining elicitor activity (Aziz et al., 2007; Mithöfer et al., 2001). This suggested that GlcNAc alone does not account for the elicitor activity observed in elicitor M. This finding was particularly interesting in relation to previous reports that identified GlcNAc as a significant component of *A. euteiches* cell wall fraction capable of inducing defense-related genes in *M. truncatula* (Nars et al., 2013). However, given that *Phytophthora* species that equally induce *MtTPS10* (Figure 2.2B) lack GlcNAc residues in their cell wall (Mélida et al., 2013) (Figure 3.1), it becomes even more conclusive that GlcNAc is not a contributing factor to the elicitor activity of elicitor M. This strongly suggests that the PAMPs inducing *MtTPS10* are possibly shared among different oomycetes. A definitive understanding of elicitor M's function necessitates precise identification of the molecules or compounds present in elicitor M. This represents a significant challenge, given the complexity of cell wall-derived

components (Nars et al., 2013). Nonetheless, Nars et al. (2013) demonstrated a promising approach by employing the enzymatic digestion of *A. euteiches* cell wall, followed by mass spectrometry analysis. Through this effort, they were able to characterize specific motifs within the *A. euteiches* cell wall and link them to biological activity in *M. truncatula*, offering a fundamental step toward unravelling the molecular identity of elicitor M.

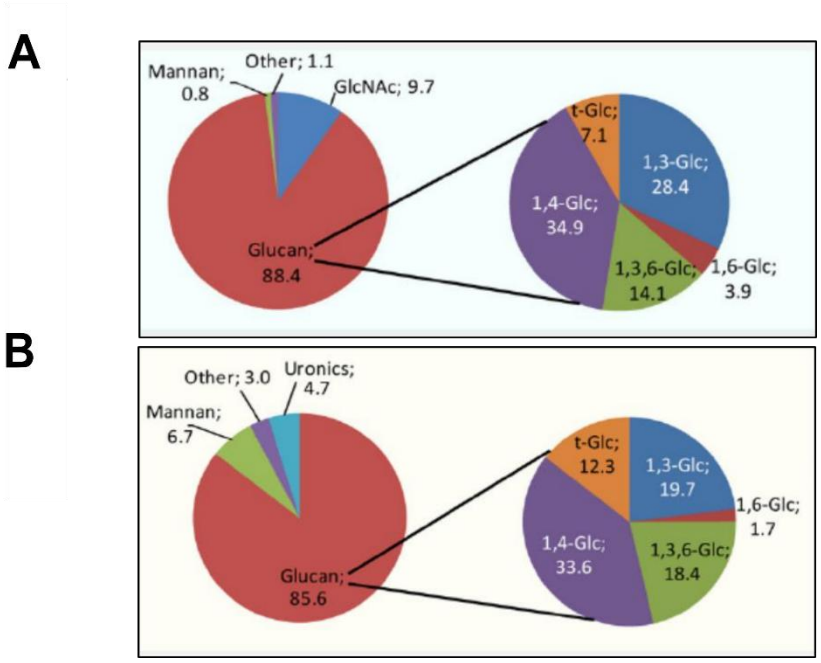

Figure 3.1:The typical carbohydrate composition of cell walls from two oomycetes.

A. *A. euteiches* and **B** *P. infestans* (modified after Mélida et al., 2013).

Our future research could also aim to further employ the use of orthogonal analytical technologies (e.g. GC/MS) or preparative approaches (preparative LC coupled to elemental analysis or NMR analysis) to shed light on this currently unknown molecule in elicitor M. These approaches then could serve as a blueprint to determine which cell wall component of oomycetes trigger the induction of defense genes in *M. truncatula*. In addition, mutant plants defective in PAMP recognition, such as those carrying a mutation in lysin-motif receptor-like kinases (e.g., *Mtlyk9*) and displaying increased susceptibility to *A. euteiches* (Gibelin-Viala et al., 2019), offer a valuable tool for assessing the role of specific PAMPs in immune activation. These mutants can potentially be utilized to test their capability to accumulate *MtTPS10* transcripts upon the treatment of isolated PAMPs of *A. euteiches*. *MtLYK9* and the *Lotus japonicus* orthologue *LjLYS6* have been implicated to mediate disease resistance in legume species, since it was demonstrated that mutant plants of these receptors exhibited lower responses to chitin and increased susceptibility to *Botrytis cinerea* (Bozsoki et al., 2017; Mélida et al., 2013). Also in *Pisum sativum*, *LYK9 RNAi*-lines were shown to be more

susceptible to *Fusarium culmorum* (Leppyanen et al., 2018), again depicting the significance of these receptors in plant immunity and how they can be utilized to better understand the connection between plant immunity and the microbial features that trigger these immune responses.

Previous studies indicated that *MtTPS10* is expressed solely in the roots of *M. truncatula* and its expression was not detectable in shoots (Yadav et al., 2019). However, our findings revealed for the first time the expression of *MtTPS10* in leaves of *M. truncatula* after elicitor M treatment (Figure 2.2C) Here, we hypothesize that the molecules in elicitor M were able to diffuse efficiently into the leaves of the plant without hindrance from the physical barriers of the leaf compared to the zoospore's counterpart. Zoospores on the surface of the leaf may encounter resistance to encyst or stick to the leaf surface, probably due to the waxy surface of the leaves. Additionally, the short 2 hpi time is probably not sufficient for infection of the leaves by zoospores, and it is worthwhile to note that *A. euteiches* is a specialized root pathogen (Hossain et al., 2024; Wu et al., 2018), therefore, it is not adapted to infection of leaf tissue. Based on this, we can further speculate that the receptor responsible for mediating defense responses in *M. truncatula* roots may also be expressed in the leaves. The ability of elicitor M to induce *MtTPS10* in leaves of *M. truncatula* suggests that the pattern recognition receptor (PRR) of *A. euteiches* PAMPs is not limited to roots and may be functional in aerial parts of the plant as well. In *M. truncatula*, there have been reports on a couple of LysM-RLK that play critical roles in *M. truncatula*-microbe interaction. Notably, *MtLYK9* is known to play a dual role in plant immunity and in establishing AM symbiosis (Mélida et al., 2013). Again, beyond symbiosis, *M. truncatula* Nod Factor Perception (*MtNFP*) contributes to immunity by modulating defense responses against pathogens, including *A. euteiches* (Rey et al., 2013). It is worthwhile to state that some of these receptors mediating pathogenic responses in *M. truncatula* may have broad expression patterns that may not be developmentally controlled or restricted to specific tissues of the plant. Supporting this idea, *LjLys6*, the orthologue of *MtLKY9*, has been reported to maintain consistent expression levels in all the tissues of the plant (Lohmann et al., 2010), indicating that similar receptor expression could exist in *M. truncatula*. This would explain the responsiveness of foliar tissues to elicitor M. Given this insight, further investigation of putative receptor complexes involved in the perception of elicitor M would be a valuable next step. This could provide an additional understanding of how *M. truncatula* orchestrates immune responses across tissues.

In our case, a receptor study would also be an interesting field to explore which specific receptor or receptor complexes are involved in the elicitor M-induced *MtTPS10* expression in roots and leaves of *M. truncatula*.

Collectively, our work paves the way for further identification of *A. euteiches* PAMPs responsible for the accumulation of *MtTPS10* transcript in *M. truncatula*. In addition, we unequivocally show for the first time that a still unknown component of *A. euteiches* mycelium can equally induce the same gene responses as its zoospores. Furthermore, we have also provided evidence of the expression of *MtTPS10* in leaves of *M. truncatula,* which was initially reported to be exclusively expressed in roots. Taken together, our work opens perspectives to a better understanding of the microbial signatures of *A. euteiches* that may act as PAMPs.

3.2 Two *MtTPSs* are responsible for resistance against *A. euteiches* in *M. truncatula*

While intraspecific variation in stress-responsive terpene synthases and their associated products has been broadly studied in aboveground interactions (Booth et al., 2020; Huang et al., 2010; Köllner et al., 2004; Xu et al., 2020), similar investigations in belowground systems remain scarce. In *M. truncatula*, despite reports describing the significance of *M. truncatula*-derived terpene synthases in biotic interactions, many of these were associated with aboveground herbivory defense (Gomez et al., 2005; Hendrickson et al., 2024), with little to no understanding of how these genes function across different *M. truncatula* accessions. To our knowledge, *MtTPS10* is the only reported terpene synthase in *M. truncatula* implicated in defense against the root pathogen *A. euteiches* (Yadav et al., 2019). In this study, by exploring the influence of *MtTPS10* on the immunity of A17 Jemalong along with five other ecotypes of *M. truncatula*, we show that there are indeed huge differences in transcript levels of *MtTPS10* in these ecotypes (Figure 2.4). Additionally, most ecotypes emitted blends of sesquiterpenoids (Figure 2.5 and appendix, Figure 7.5), the majority of which have been identified in volatile mixtures induced by other biotic stress in legumes (Kigathi et al., 2019; Leitner et al., 2010; Yadav et al., 2019) or the exogenous application of plant defense elicitors such as MeJA and salicylic acid (SA) in legumes (Hendrickson et al., 2024). There was a conserved overlap in the composition of volatiles induced by *A. euteiches* infection and herbivory (Boland & Garms, 2010), suggesting the emission of conserved volatile blends across different stress conditions in *M. truncatula*. In Arabidopsis, *P. syringae* and the fungal elicitor alamethicin were found to trigger the emission of blends of volatiles closely resembling those induced by herbivory (Attaran et al., 2008; Herde et al., 2008). These observations indicate that conserved volatile blends across different stress conditions explain an evolutionarily optimized strategy to mount defense arsenals in plant species. Among the ecotypes investigated, no apparent correlation could be found between geographical distribution and volatile profiles, except in ecotypes 542 and 368, which shared some common sesquiterpenes, such as α-copaene and several minor

compounds (Appendix, Figure 7.5C). Notably, these two ecotypes originated from the same country, Algeria (Table 2.1).

Interestingly, the expression of *MtTPS10* in these ecotypes was found to be negatively correlated with their susceptibility to *A. euteiches* (Dreher et al., 2017). While the plant immune response is a complex process involving numerous signaling pathways (Afrin et al., 2020), our data revealed a consistent association between *MtTPS10* expression and reduced *A. euteiches* biomass. This observation supports the hypothesis that a functional link exists between *MtTPS10* expression and enhanced resistance, highlighting its potential role as an important component of the root immune response in *M. truncatula*. Our assumption was proven correct for all ecotypes except ecotype 368, which stood out as the *MtTPS10* transcript was completely absent in this ecotype, and we were unable to amplify the CDS by PCR (Appendix, Figure 7.3). This is despite it being previously reported to be among the *M. truncatula* ecotypes exhibiting resistance to *A. euteiches* (Dreher et al., 2017). These unexpected results led us to hypothesize that ecotype 368 employs an alternative, *MtTPS10*-independent defense mechanism. Furthermore, volatile emissions of 368 consisted primarily of sesquiterpenoids Figure 2.5B), suggesting a different sesquiterpene synthase could be the driving factor behind the blends of sesquiterpene volatiles seen in infected roots of 368 (Figure 2.5B) and potentially be responsible for the observed resistance to *A. euteiches* in this ecotype, as previously reported by Dreher et al. (2017). We therefore focused our investigation on 368 to better understand the underlying mechanisms contributing to its *MtTPS10*-independent resistance.

Three lines of evidence supported these observations. First, our transcriptomic analysis confirmed that *MtTPS10* expression is restricted to A17 and is not significantly induced in 368 following *A. euteiches* infection (Figure 2.7). In contrast, a previously uncharacterized sesquiterpene synthase, *MtTPS25*, emerged as the predominantly upregulated terpene synthase upon infection in 368 but not in A17 (Figure 2.7A). This contrasting expression pattern suggested that *MtTPS25*, rather than *MtTPS10*, may be the key contributor to sesquiterpene biosynthesis and *A. euteiches* resistance in 368. These results underscore the presence of ecotype-specific biochemical diversity in the *M. truncatula-A. euteiches* interaction, suggesting that different ecotypes may activate distinct pathways during pathogen infection. Pioneering studies have shown that differences in gene expression between accessions are attributable to variation in trans-regulatory elements (Afrin et al., 2020; Huang et al., 2010; Nasim et al., 2025). Consistent with this finding, we hypothesize that the lack of expression of *MtTPS10* in 368 may be due to important regulatory elements present or absent in 368. We confirmed this by using *GUS* reporter constructs driven by either $pMtTPS10^{A17}$ or $pMtTPS10^{368}$ and expressed in A17 or 368. While the $pMtTPS10^{A17}$ can drive expression in

A17 and 368 (Figure 2.8A-B), the intensity in 368 was relatively low compared to the activity of *pMtTPS10*^{A17} in its background (Figure 2.8B).Also, while *pMtTPS10*^{368} drives expression in A17 (Figure 2.8C), though at a lower intensity compared to *pMtTPS10*^{A17} in A17, it fails to do so in its native background (Figure 2.8C), implying that ecotype-specific cis-elements and trans-regulatory elements likely play a role in controlling *MtTPS10* expression in 368. Notably, our bioinformatics-aided analysis of the promoter of *MtTPS10* from both ecotypes showed that *pMtTPS10*^{368} lacks specific transcription binding sites for WRKY28 (TTTGTGACTATT) and DLEC2 (GTCACGTCAGCG), which were found to be present in *pMtTPS10*^{A17} and found at the -1560 and -965 upstream of the transcription start site (Appendix, Figure 7.6). These differences in transcription factor binding sites could likely be the reason for the reduced activity of *pMtTPS10*^{368} in A17 and 368. However, the inability of *pMtTPS10*^{368} to function in its background also suggests an ecotype-specific regulation of *MtTPS10* expression in 368. Focusing on the combination of cis-element loss in *pMtTPS10*^{368} and the probable ecotype-specific trans-regulation in future work can provide a compelling explanation for the absence of the *MtTPS10* transcript in 368. In Arabidopsis, the lack of transcript of a flower regulator gene, *FLOWERING LOCUS M* (*FLM),* in the Arabidopsis accession Ellershausen (El-0) was attributed to polymorphism within the gene's first intron, which disrupted essential regulatory elements in that region (Nasim et al., 2025). Notably, replacing this intron with the corresponding sequence from Col-0 completely recovered the expression of *FLM* in El-0 (Nasim et al., 2025). This observation highlights that beyond cis-elements, other ecotype-specific genomic elements, such as intronic or distal genomic sequences, can significantly influence gene expression. Future experiments can explore additional genomic regions that may contribute to the regulation of *MtTPS10*. Similarly, in the case of *MtTPS25*, irrespective of where the promoter was cloned from, we only observed strong GUS activities in *A. euteiches* treated roots of 368 (Figure 2.8E-H). These results suggest that the promoter of *MtTPS25* is only active in 368 perhaps due to the presence of regulatory factors enhancing the expression of *MtTPS25*. This indicates that A17 perhaps lacks the necessary transcriptional machinery required for *MtTPS25* expression. Again, in the case of *MtTPS25,* sequence comparison between *pMtTPS25*^{A17} and *pMtTPS25*^{368} revealed notable differences, including SNPs and deletions in *pMtTPS25*^{A17} (Appendix, Figure 7.7A). Approximately 60 bp deletion in the *pMtTPS25*^{A17} resulted in a loss of MYC transcription factor binding site (CATTTG) (Appendix, Figure 7.7B), suggesting that the loss of this transcription element could have likely resulted in diminished expression of *MtTPS25* in A17 (Figure 2.8G). However, the fact that *pMtTPS25*^{368} could not drive the expression of GUS in A17 (Figure 2.8) again suggests the possibility of ecotype-specific trans-factors influencing *MtTPS25* expression in A17, again hinting at the need for further studies at the genomic level.

Our finding aligns with several studies that have documented ecotype-specific expression of defense-related genes, highlighting how this phenomenon contributes to natural variation in disease resistance among plant populations (Huang et al., 2010; Köllner et al., 2004; Zhou et al., 2017). A comparable case of ecotype-specific terpene synthase utilization has been documented in Arabidopsis, where the expression of two related genes, *TPS02* and *TPS03*, varied among the ecotypes Col-0 and Wassilewskija (W) in response to coronatine treatment and *Plutella xylostella* feeding (Huang et al., 2010). While both genes encode enzymes with (E)-β-ocimene and (E, E)-α-farnesene activity, only *TPS03* was expressed in Col-0 leaves due to the partial deletion of *TPS02*, whereas in the W ecotype, only *TPS02* was expressed in this accession (Huang et al., 2010). Interestingly, similar observations have been made in other plant species. In maize, the herbivory-inducible volatile emission in two inbred lines, B73 and Delprim, was shown to be controlled by two distinct terpene synthases, *TPS4* and *TPS5*, respectively (Köllner et al., 2004).

Second, although terpene composition frequently varies among and within plant species, linking these differences to specific genes is challenging due to the complexity of metabolic networks and gene regulation (Köllner et al., 2004). Here, we showed that *MtTPS25* contributes to the emission of sesquiterpenes in 368. The volatile profile of 368's oomycete-infected roots revealed a blend of 15 sesquiterpenoids, with α-copaene as the major constituent (Figure 2.5B). Notably, silencing *MtTPS25* in 368 completely abolished α-copaene emission along with the other minor sesquiterpenoids (Figure 2.17), confirming MtTPS25 as the key enzyme responsible for this metabolic output. Furthermore, heterologous expression of *MtTPS25* in yeast resulted in the production of α-copaene and several of the minor compounds also observed *in planta* (Figure 2.11), providing additional evidence that MtTPS25 is indeed the enzyme determining the observed sesquiterpene profile (Figure 2.5B). With the difficulty involved in establishing a gene-metabolite relationship, a limited number of studies have successfully identified genes that directly underlie specific metabolic traits. Regarding belowground terpenoids, two closely linked genes, *At3g25820* and *At3g25830*, were identified as the terpene synthases responsible for the formation of the monoterpene 1,8-cineole in Arabidopsis (Chen et al., 2004). In *N. attenuata*, several attempts using both forward and reverse genetic approaches led to the conclusion that the herbivory-inducible volatile (*E*)-a-bergamotene was controlled solely by the terpene synthase NaTPS38 (Zhou et al., 2017). Similarly, in maize, a diterpene synthase ZmKSL4 was identified as the primary enzyme responsible for the release of the defense metabolites dolabralexins, as CRISPR-Cas9-derived loss-of-function *ZMksl4* mutants resulted in plants deficient in dolabralexins (Murphy et al., 2023). An interesting phenomenon was reported in Arabidopsis and kiwi, where the entire complex mixture of sesquiterpenes emitted from the flowers was found to be associated

with two genes: *At5g23960* and *At5g44630* in the case of Arabidopsis (Tholl et al., 2005), and *AdAFS1* and *AdGDS1* in kiwi (Nieuwenhuizen et al., 2009).

Third, silencing of *MtTPS25* in 368 resulted in a higher accumulation of *A. euteiches* biomass in these roots compared to plants transformed with the empty vector control. Although some variation in *A. euteiches* colonization was observed among *MtTPS25*_RNAi roots, the overall trend consistently indicated enhanced susceptibility relative to wild-type plants (Figure 2.18). Interestingly, the exogenous application of α-copaene, the major product of MtTPS25, did not exhibit antimicrobial activity against *A. euteiches*, suggesting that α-copaene may not be the sole contributor to the defense phenotype highlighted by Dreher et al. (2017). Notably, the antimicrobial effect of MtTPS10 products was reported to be a result of the combined effects of the full sesquiterpene blend, rather than the major constituent himachalol (Yadav et al., 2019). This raises the possibility that, like MtTPS10, the cocktail of MtTPS25 products may be required for effective defense against *A. euteiches*. In addition, the significance of metabolite mixtures in plant defense has gained increasing recognition, as evidence suggests that compound blends, rather than individual compounds, often contribute more effectively to pest and pathogen deterrence (Gershenzon & Dudareva, 2007). For instance, the metabolite combination of the steroidal glycoalkaloid α-solanine and α-chaconine from potato had enhanced antifungal properties against *Ascobolus crenulatus*, *Alternaria brassicicola*, *Phoma medicaginis,,* and *Rhizoctonia solani* compared to the individual activity of each compound (Fewell & Roddick, 1993). It was hypothesized that mixtures of compounds with differing physical properties may facilitate deployment or longer persistence of defenses (Gershenzon & Dudareva, 2007). A supporting example of such synergism has been reported in conifer resin, where a mixture of a monoterpene and diterpene, both possessing anti-herbivory activity, acted in concert (Phillips & Croteau, 1999). The low molecular weight monoterpene was believed to have acted as a solvent, enhancing the delivery of the high molecular weight diterpene to the site of attack (Phillips & Croteau, 1999). Based on these examples, it will be worthwhile to check the mixture of MtTPS25-derived compounds on *A. euteiches* to test their combined effect on the oomycete.

3.3 *MtTPS25* shares properties similar to other terpene synthases.

The massive diversity of terpene natural products is attributable to the remarkable catalytic versatility of terpene synthases that enables them to transform prenyl diphosphate into a wide range of primary terpene skeletons, often followed by the generation of multiple products from a single substrate (Chen et al., 2011; Tholl, 2006). Almost half the characterized mono and sesquiterpene synthases are classified as multiproduct synthases (Christianson, 2017;

Lesburg et al., 1997). This reflects nature's tendency to use existing resources to maximize chemical diversity through the least expensive routes (Brock et al., 2013; Yamada et al., 2015). The most diverse class of terpenoids isolated from plants, fungi, bacteria, and marine invertebrates consists of sesquiterpenes (Stevens, 1992). To date, the δ-selinene synthase with 52 products and γ-humulene synthase with 34 products from *Abies grandis* hold the current record for the biosynthesis of multiple sesquiterpenes from FPP (Steele et al., 1998). In *M. truncatula,* some notable multiproduct sesquiterpene synthases are MTPS5*,* which produces 27 distinct sesquiterpenes in response to herbivory attack (Arimura et al., 2007; Garms et al., 2010), MtTPS7 and MtTPS8 have also been characterized as multiproduct terpene synthases forming 2 or up to 20 compounds, respectively, when recombinantly expressed in *E. coli* (Hendrickson et al., 2024). Among root-derived terpene synthases, MtTPS10 produces 17 sesquiterpenoids following *A. euteiches* infection with himachalol as the main product (Yadav et al., 2019). Our work now adds MTPS25 as a root-derived multiproduct sesquiterpene synthase of *M. truncatula*, producing 14 sesquiterpenes, with α-copaene being the major product when heterologously expressed in yeast together with FPP (Figure 2.11). Interestingly, the volatile profiles of MtTPS7 include two sesquiterpene olefins, α-copaene, and cyclosativene (Hendrickson et al., 2024), which are also present among the sesquiterpenes produced by MtTPS25 (Figure 2.11). However, MtTPS7 exhibits 44.2 % sequence similarity to MtTPS25 *(*Appendix, Figure 7.11*)*. It can be hypothesized that *M. truncatula* ecotypes harboring genes encoding MtTPS7 and MtTPS25 may have evolved to produce similar products due to shared challenges in their respective environments.

Our data clearly show that MtTPS25 clusters with MtTPS10 in the TPS-a class of the TPSs (Figure 2.9A). Additionally, previous studies indicate that members of the TPS-a subfamily predominantly produce sesquiterpene volatiles in response to herbivory or pathogen attack (Arimura et al., 2007; Leitner et al., 2005; Yadav et al., 2019). In *S. lycopersicum,* the TPS-a family also produces sesquiterpenoids, whereas in *Arabidopsis,* the TPS-a subfamily produces both sesquiterpenoids and other terpenoids. (Zhou & Pichersky, 2020).The deduced amino acid sequence of MtTPS25 contains conserved regions that are highly conserved among members of the same gene class. One of these includes the most distinct conserved region, the aspartate-rich DDxxD motif at the C-terminal of the gene (Figure 2.9B), which is involved in coordinating divalent metal ions that are important for enzyme activity (Christianson, 2006). MtTPS25 also contains a second aspartate-rich motif, DDIVSSEFE, termed the NSE/DTE motif (Christianson, 2006). This motif, together with the DDxxD, forms an active site entrance for the coordination of divalent ions necessary for substrate binding and catalysis (Christianson, 2006). The first DDxxD motif has been proven to be an essential determinant in product formation (Little & Croteau, 2002). The importance of this motif was

demonstrated for γ-humulene synthase, a multiproduct sesquiterpene synthase from *Abies grandis* (Steele et al., 1998). It was shown that substituting the first aspartate in the DDxxD motif of γ-humulene synthase led to a reduction in enzymatic activity (Little & Croteau, 2002), confirming that these motifs are essential for accurate substrate catalytic functions (Driller et al., 2018; Schrepfer et al., 2016). Also, like other sesquiterpene synthases, MtTPS25 lacks the N-terminal signal peptide for plastid targeting (Figure 2.9B), suggesting that MtTPS25 is resident in the cytoplasm (Figure 2.10) and functions as a sesquiterpene synthase *in vivo*. Supporting this, the recombinant MtTPS25 exhibited no detectable activity when assayed with either GPP or GGPP (Figure 2.12B-C), indicating strict substrate specificity. Also, when expressed in yeast or *E. coli*, MtTPS25 consistently converted FPP to α-copaene (Figure 2.11 and Figure 2.12A). These results confirmed MtTPS25 as a functional sesquiterpene synthase and showed that its catalytic activity is maintained across heterologous systems. This is not an unprecedented scenario, because sesquiterpene synthases are deemed situated in the cytosol where FPP is present in a higher abundance (Dudareva et al., 2004, 2006). However, it is important to note that despite the compartmental separation between the MVA and MEP pathways, metabolic cross-talk between the two pathways is a typical phenomenon that can occur in plants (Karunanithi & Zerbe, 2019).

3.4 The transcript levels of *MtTPS25* are root-specific and regulated by oomycete infection.

By RT-qPCR (Figure 2.13B), we demonstrated that the expression of *MtTPS25* is specific to the roots of line 368 following infection by *A. euteiches* zoospores, showing no detectable expression in leaves of infected plants. Similarly, *MtTPS10* transcripts were detected in the roots of A17 Jemalong but not in the leaves after *A. euteiches* infection (Yadav et al., 2019). Yadav et al. (2019) further suggested that the root-specific expression of *MtTPS10* is associated with its role as a defense gene against the root pathogen *A. euteiches,* a conclusion that may also apply to *MtTPS25*. Because terpene synthases function as gatekeepers for terpene biosynthesis (Degenhardt & Gershenzon, 2000; Karunanithi & Zerbe, 2019), their transcript accumulation in plants is usually sequestered in specific tissues and their release is regulated by specific internal or external factors (Karunanithi & Zerbe, 2019), a process that allows plants to fine-tune the deployment of terpenoids for various environmental interactions (Keeling & Bohlmann, 2006; Schmelz et al., 2014). For instance, in *Arabidopsis*, a *GUS* reporter gene fused to the promoter of *At5g23960*, a gene encoding a caryophyllene synthase, showed that the highest expression of the gene occurred in open flowers, with some activity in sepals and no expression in petals (Tholl et al., 2005). In *A. thaliana* again, Chen et al. (2003) showed that the expression of the monoterpene synthase gene *At3g25810* is mainly restricted to open flowers.

The expression profiles of these terpene synthases in the flowers of *A. thaliana* suggested that volatile terpenoids of these terpene synthases could play a dual role in attracting pollinators and fending off detrimental pests, while simultaneously deterring pathogens from the exposed floral tissue (Tholl, 2006). These observations again show that the tissue-specific regulation of terpenoids is a critical evolutionary strategy to optimize resource allocation in plants.

The regulation of most terpenoids has been attributed to external factors such as herbivory (Degenhardt & Gershenzon, 2000; Huang et al., 2010; Magnani et al., 2025), pathogen attack (Liu et al., 2024; Yadav et al., 2019) or by the application of plant hormones (Hendrickson et al., 2024). Maize plants attacked by the herbivore release a blend of terpenoids that attract natural enemies of the herbivores (Degen et al., 2004). The cereal pathogens *Bipolaris sorokiniana* and *Fusarium graminearum* induce the release of the diterpenoid hordedanes in barley plants (Liu et al., 2024). A regulation of another diterpenoid can be observed in the case of Sitka spruce, where the levels of diterpene synthase and diterpene acids in the bark and xylem of the plant increased with the application of the phytohormone MeJA (Miller et al., 2005). In our study, we also observed that phytopathogenic oomycetes seem to be solely responsible for inducing the expression of *MtTPS25*. A conclusion was made based on the observations that transcript levels of *MtTPS25* increased by 5-fold and 3-fold after infection by *A. euteiches* and *P. infestans*, respectively, compared to basal levels in roots and not by salt stress or the topical application of the oxylipin MeJA (Figure 2.15A-B). These observations suggest that specific cell wall components or elicitors derived from oomycetes may be acting as PAMPs, eliciting the expression of *MtTPS25*. It is interesting to note that the application of elicitor M to the roots of line 368 also resulted in *MtTPS25* expression (Figure 2.15A), suggesting that both *MtTPS*s are induced by the same PAMPs from *A. euteiches*. Furthermore, the expression of *MtTPS25* is time-regulated, peaking at 2 hpi and diminishing over time (Figure 2.14). This characteristic makes *MtTPS25* an early defense gene that may lead to a quick production of sesquiterpenes as antimicrobial compounds to inhibit oomycete growth. In *Petunia hybrida* flowers, it was also reported that the accumulation of the sesquiterpene β-cadinene from the terpene synthases *PhTPS3* and *PhTPS4* was time-regulated, with the highest accumulation detected 2 days post-anthesis, hence protecting reproductive organs of Petunia against microbes (Boachon, Lynch, et al., 2019). Until now, only *MtTPS10* has been recognized as a root-specific terpene synthase. This study has added *MtTPS25* to the list of root-specific terpene synthases in *M. truncatula*.

3.5 Genetic engineering of terpenoid metabolism increases defense against *P. infestans* in potato

Across the continent, potatoes have become a high-value crop after wheat and rice, serving as a staple crop for over 1.3 billion people (Stokstad, 2019). The crop's increasing popularity now demands efforts to adapt it to varying environmental changes and boost its fitness against pests and pathogens. The complex biology of the potato plant poses significant challenges in the breeding process. Also, commercial varieties are tetraploids (2n = 4x = 48), requiring breeders to evaluate several thousand seedlings because of phenotype dilution, and this can span over a long period of time (more than 10 years) to identify a single plant with the ideal combination of traits (Jansky et al., 2016; Stokstad, 2019; Watanabe, 2015). As a crop that is propagated clonally, potato is constantly exposed to pests and pathogens that are transmitted from one growing season to the next, leading to progressive collapse in yield (Gebhardt & Valkonen, 2001). This systemic accumulation of diseases adds another layer of complexity to the breeding program aimed at obtaining a potato variety fit for the environment. Although significant efforts are continuously being made to enhance the crop's fitness, this crop remains persistently threatened by an array of pathogens that diminish its yield and quality (Regina, 2021). Among these are potato virus Y (Quenouille et al., 2013), *Ralstonia solanacearum* (Charkowski et al., 2020), and the "potato killer" *P. infestans* (Kamoun et al., 2015; Yoshida et al., 2013). Late blight, caused by *P. infestans,* continues to be the most destructive pathogen threatening potatoes and global food security, necessitating the use of expensive chemicals for management (Fry et al., 2015; Ristaino et al., 2020). The destructive nature of *P. infestans* is largely driven by the rapid evolutionary adaptation of the pathogen's effectors, which results in resistance breakdown in the potato late blight pathosystem (Leesutthiphonchai et al., 2018; Win et al., 2007). Given the pathogen's ability to escape resistance breeding, plant engineering has emerged as a promising tool for developing resistant potato varieties (Bi et al., 2024; Kieu et al., 2021). Jumping on this approach, we aimed to investigate the potential role of *MtTPS10* and *MtTPS25* in enhancing resistance against *P. infestans*.

To achieve this, we generated transgenic potato lines (Désirée) with constitutive expression of *MtTPS10* or *MtTPS25*. Based on the observations that *MtTPS10* and *MtTPS25* mediate resistance against the oomycete *A. euteiches* (Yadav et al., 2019, this thesis), we aimed to assess the feasibility of utilizing *MtTPS10* and *MtTPS25* to enhance potato resistance against *P. infestans*. Our results showed that the effort to overexpress *MtTPS* in potato was successful, with almost all the transgenic lines expressing high levels of *MtTPS* (Figure 2.19A-B). Although genetic engineering of target plants to express agronomically important genes is an attractive strategy for improving desired traits, as the introduced trait can be inherited across generations, there may still be some undesired physiological and ecological impacts

on the modified plants (Huang & Osbourn, 2019). Targeting of a nerolidol synthase implicated to have a role in plant-herbivore interactions for expression in the mitochondria of *A. thaliana* (as opposed to the classical sesquiterpene cytosolic sesquiterpene biosynthetic compartment), led to a slight retardation of the growth of basal rosette in transgenic plants (Kappers et al., 2005). Robert et al. (2013) also showed in their work that overexpressing an oregano terpene synthase in maize reduced the growth and yield of maize in lab and field trials. Interestingly, in our case, we observed no growth trade-offs in our transgenic plants that may outweigh the potential benefits of our *MtTPS* since the transgenic lines exhibited a phenotypic resemblance to the wildtype (Figure 2.19C). However, we must mention that the physiological cost of the transgenic potato plant was measured only in above-ground tissues (Figure. 2.19C). For future experiments, it may be important to include the below-ground effects on these transgenic plants, especially regarding tuber yield, size, and shape.

The *MtTPS10*-overexpressing plants exhibited enhanced resistance to *P. infestans* (Figure 2.20A). Furthermore, GC-MS analysis revealed that while both wild-type and transgenic plants displayed similar metabolites, the transgenic lines demonstrated an increased metabolic composition (Figure 2.20C). Notably, the *MtTPS10*-overexpressing plants specifically accumulated shyobunol (8) (Figure 2.20C), suggesting a potential role for this metabolite. From these observations, we hypothesize that in the case of *MtTPS10* overexpression in potato plants, shyobunol (Figure. 2.20C) contributes to the enhanced resistance seen in these plants. This is also reflected in *M. truncatula*, where plants expressing *MtTPS10* showed higher resistance to *A. euteiches* compared to mutant plants lacking the gene transcript. Even the products of MtTPS10 exhibited antimicrobial effects against *A. euteiches* (Yadav et al., 2019). This finding aligns with previous studies in *Arabidopsis*, where a chloroplast-targeted overexpression of strawberry linalool/nerolidol synthase (*FaNES1*) repelled the aphid *Myzus persicae* in dual-choice assays (Aharoni et al., 2003). Interestingly, a similar approach with potatoes resulted in increased linalool levels, which attracted predatory mites, influencing trophic interactions (Lücker et al., 2006). These phenomena highlight the significance of terpenoid emission in plant-environment interactions. A crucial next step in validating this hypothesis would be to perform LC-MS analyses to investigate whether additional sesquiterpenes are emitted in the *MtTPS10*-overexpressing plants. Identifying other volatile or non-volatile terpenoid compounds will help elucidate whether the protective effect in *MtTPS10* overexpressing plants against *P. infestans* arises from a single or broader metabolic shift in terpene biosynthesis. Additionally, we can postulate that the observation in the *MtTPS10* overexpressing lines may have resulted from an unknown signaling or regulatory function of *MtTPS10.* Probably beyond its role in sesquiterpene biosynthesis, *MtTPS10* could influence plant defense responses by altering the immune signaling network or inducing stress-responsive genes.

A preliminary experiment conducted to explore the signaling role of *MtTPS10* showed that the application of himachalol, the major product of MtTPS10, to the roots of *M. truncatula* induced *MtTPS10* expression (Appendix, Figure 7.12). This observation suggests that MtTPS10 products may have the capacity to activate stress response genes, potentially through a positive feedback loop that amplifies defense. Notably, in lima beans, exposing uninfected leaves to β-ocimene induced the expression of defense genes, such as pathogenesis-related (PR) genes PR-2, PR-3, and the phenylalanine ammonia-lyase gene (PAL), after 24 hours of exposure (Arimura et al., 2000). Interestingly, applying jasmonate to the lima bean leaves activated similar genes with the same expression pattern (Arimura et al., 2000), indicating that terpenoids can modulate plant stress responses either by directly interacting with plant defense pathways or by influencing hormonal crosstalk. With this, it would be interesting to investigate the transcriptional reprogramming in *MtTPS1*0-overexpressing lines to gain deeper insights into the potential regulatory functions of this gene. It is also noteworthy that the major product of MtTPS10, himachalol, from yeast, along with other previously established MtTPS10-derived compounds, were absent from the volatile profile of transgenic potato (Figure. 2.20C). Similarly, in *M. truncatula*, himachalol was absent from the blend of volatiles emitted from *A. euteiches* infected roots (Yadav et al., 2019). This observation suggests potential conversion of metabolites by certain endogenous enzymes. For *M. truncatula*, further studies (in this thesis) identified putative cytochrome P450s that may act on himachalol (Figure. 2.21). For the transgenic potato plants, we can hypothesize that a similar class of enzyme associated with himachalol conversion in *M. truncatula* could also be responsible for the absence of MtTPS10-derived volatiles in potato. A review by Degenhardt et al. (2003) explicitly emphasized that not all efforts to manipulate terpene production lead to complete complementation of metabolites. In carnation (*Dianthus caryophyllus*), the constitutive expression of linalool synthase from *Clarkia breweri* led to the accumulation of oxidized derivatives of linalool instead of linalool in the petals of the transformed plants (Lavy et al., 2002). All these data suggest the presence of endogenous metabolic modification(s). An excellent example that points to the fact that species-specific enzymatic activity can influence the fate of foreign genes was nicely seen in the work of Kappers et al. (2005). When strawberry-derived (3S)-(E) nerolidol synthase was overexpressed in *Arabidopsis*, elevated levels of nerolidol were detected. However, this was accompanied by the formation of a homoterpene, 4,8-Dimethylnona-1,3,7-triene ((E)-DMNT), which was not naturally present in *Arabidopsis*. The authors suggested that this unexpected product likely resulted from a side chain cleavage by an unknown *Arabidopsis* cytochrome P450 (Kappers et al., 2005). Future experiments can consider feeding MtTPS10-derived metabolites to wild-type potato plants to confirm the occurrence of any modification(s).

Unfortunately, our attempt to enhance *P. infestans* resistance through *MtTPS25*-overexpression in potato was unsuccessful (Figure. 2.20B). Although *MtTPS25* has been implicated in defense against *A. euteiches* in 368 (Figure.2.18), its overexpression in potato resulted in the opposite effect, with transgenic plants accumulating more *P. infestans* biomass than wild-type plants (Figure. 2.20B). Here, the increased emission of β-copaene and 7-epi-cis-sesquisabinene hydrate (Figure. 2.20D) evidently did not contribute to the defense of potato against *P. infestans*. These observations point to the fact that despite efforts to manipulate plant immunity, the overall outcome can be unpredictable. A similar example is the constitutive expression of the sesquiterpene synthase, (E)-β-caryophyllene from oregano in maize, which was initially shown to enhance root protection by attracting entomopathogenic nematodes (Degenhardt et al., 2009). However, later studies revealed that overexpressing this gene again in maize led to an increase in herbivore damage on transgenic leaves and negatively impacted seed germination, plant growth, and yield (Robert et al., 2013). The unexpected increase in disease severity following the overexpression of *MtTPS25* in potato aligns with previous findings demonstrating that plant manipulation is complex with unpredictable outcomes (Gruner et al., 2020; Kieu et al., 2021; Kim & Hwang, 2012). The loss of function of a susceptibility (S) gene, *Mildew resistance locus O* (*MLO*), has conferred resistance to powdery mildew (Kusch & Panstruga, 2017), but also to *P. palmivora* in barley and *Xanthomonas campestris pv. vesicatoria (Xcv)* in pepper (Kim & Hwang, 2012). However, the loss of function of a potato *MLO* gene (*StMLO*) did not enhance resistance to *P. infestans*, as the transgenic plants exhibited similar susceptibility to that of wild-type plants, despite the previously reported benefits of *MLO* disruption. Thus, the usefulness of plant engineering can be host-dependent. In *MtTPS25* overexpressing plants, we observed that α-copaene, which was identified as the primary product among the yeast-derived products of MtTPS25 (Figure. 2.5B and Figure 2.11), was absent. Instead, β-copaene emerged as the dominant product in these transgenic plants (Figure.2.20D). Interestingly, β-copaene was also detected to be among the terpenoids released from infected roots of 368, confirming that MtTPS25 is probably capable of producing these two compounds *in vivo*, and the cellular environment in potato probably influenced the formation of β-copaene instead of α-copaene. To the best of our knowledge, no special role has been associated with β-copaene, unlike α-copaene, which has been found to play pivotal roles in plant defense against biotic stress agents (Magnani et al., 2025). Also, the absence of the yeast-derived volatiles in the MtTPS25 overexpressing plants could be associated with a probable conversion of these volatiles to non-volatile forms, a situation that has been already discussed for overexpression of *MtTPS10*. In Petunia and tomato plants engineered to overexpress S-linalool synthase from *Clarkia breweri*, it was found that linalool accumulated in non-volatile, glycosylated forms and hydroxylated forms, respectively, due to the action of endogenous enzymes of these plants (Lewinsohn et al.,

2001; Lücker et al., 2001). This observation again highlights the complexity associated with engineering plants for terpenoid production. A crucial step in future experiments is to perform LC-MS analysis to investigate the probable conjugation of products in these transgenic potato plants.

We also noticed that the overexpression of *MtTPS10* and *MtTPS25* in potato resulted in increased production of (**1**) caryophyllene, (**2**) cis-farnesene, (**3**) cubebol, and (**7**) germacrene D-4-ol in the potato (Figure.2.20C-D). This finding can be attributed to the overload of precursors like *FPP* synthase within the potato cells, potentially driving enhanced flux through the MVA pathway. A comparable effect was noted in *Artemisia annua*, where the overexpression of cotton *FPP* synthase resulted in a two-to-threefold increase in artemisinin (Chen et al., 2000). This outcome further supports the idea that manipulating upstream steps in terpene biosynthesis can substantially enhance metabolite production.

So far, our study has revealed that plant genetic manipulation remains a promising strategy for disease control, despite the unpredictability and challenges that may arise. However, it is essential to evaluate potential side effects during the manipulation process thoroughly (Robert et al., 2013). Certain avenues to explore in future experiments could include the use of tissue-specific promoters, which will ensure targeted release of terpenoids in desired tissues (Huang & Osbourn, 2019).

3.6 *CYP71D62* activity on himachalol results in the formation of new sesquiterpenoids

Himachalol has been reported to be the major product of MtTPS10 when heterologously expressed in yeast and *N. benthamiana* (Yadav et al., 2019). However, following *A. euteiches* treatment, himachalol was not detected among the emitted blends of sesquiterpenes (Yadav et al., 2019). This observation hints at the possible modification of himachalol by endogenous enzymes. Here we report that a single gene, *CYP71D62*, plays an essential role in himachalol metabolism in *M. truncatula* by reducing himachalol emission and probably facilitating the production of oxidized derivatives of himachalol.

Our co-expression analysis using *MtTPS10* as bait showed that *CYP71D61* and *CYP71D62* were the most tightly regulated with *MtTPS10* (correlation coefficient r = 0.99 and 0.98, respectively) (Figure 2.21A), with the highest levels of expression detected 2 hpi with *A. euteiches* (Figure 2.21C-D). This temporal and transcriptional co-regulation provided the first hint that *CYP71D61* and *CYP71D62* are involved in the downstream modification of MtTPS10-derived products. Interestingly, the CYP71 clade has been extensively studied (Alagna et al., 2023; Carelli et al., 2011; Muchlinski et al., 2021), and subfamilies within this clade, such as

CYP71D, have been identified as genes involved in isoprenoid metabolism, particularly for monoterpenes and sesquiterpenes (Hamberger & Bak, 2013). Certain members of the CYP71D subfamily, such as *SmCYP71D373* and *SmCYP71D375* from the Chinese herb *Salvia miltiorrhiza* (Lamiaceae), have been reported to be responsible for decorating the anti-cancer diterpenoid of this herb, tanshinone (Lee et al., 2010), with a furan ring, distinguishing these diterpenoids from other Lamiaceae diterpenoids (Ma et al., 2021). Additionally, in *N. tabacum*, the phytoalexin sesquiterpene, capsidiol, is formed through the action of *NtCYP71D20*, which catalyzes the conversion of 5-epi-aristolochene and 1-deoxycapsidiol to capsidiol (Ralston et al., 2001). Again, these observations highlight that the CYP71D subfamily acts in tandem with terpene synthases to tailor terpene metabolism.

Using heterologous expression in yeast, we provided clear data that *CYP71D62* might be the major player reducing himachalol also *in planta* into (**5/8)** (1R,7S, E)-7-Isopropyl-4,10-dimethylenecyclodec-5-enol and (**6/7**) longifolenaldehyde (Figure 2.22B). The other tested enzymes, CYP71D61 and CYP71D63, did not show a clear activity towards himachalol (Figure.2 22A and C). A similar incident was reported in *N. attenuata,* where three cytochrome P450 monooxygenases (NaCYP716A419, NaCYP716C87, and NaCYP716E107) out of ten characterized cytochrome P450 monooxygenases were identified as key enzymes modifying the ecologically important triterpenoid β-amyrin (Yang et al., 2024). NaCYP716A419 catalyzed a consecutive 3-step oxidation at the C28 position of β-amyrin, yielding the corresponding alcohol, aldehyde, and carboxylic acid, while NaCYP716C87 and NaCYP716E107 hydroxylated the C2α and C6β positions, respectively. The remaining seven candidates showed no activity towards β-amyrin, alone or in combination with NaCYP716A419, NaCYP716C87, and NaCYP716E107 (Yang et al., 2024). Given that certain cytochrome P450 enzymes exhibit strict substrate specificity, often requiring a prior modification of the primary substrate with specific functional groups (Yang et al., 2024), we cannot rule out the possibility that CYP71D61, CYP71D63, and even the other cytochrome P450 enzymes (Figure.2.21A.) may be involved in himachalol modification. For instance, in *M. truncatula*, two cytochrome P450 enzymes, MtCYP72A61v2 and MtCYP72A68v2, exhibited C-22β and C-23 oxidation activity, respectively, toward the β-amyrin derivatives, 24-hydroxy-β-amyrin and ursolic acid, instead of directly acting on β-amyrin (Fukushima et al., 2013). Also, GuCYP72A154 from *Glycyrrhiza uralensis* has been identified as a C30 oxidase that catalyzes a 3-step oxidation of 11-oxo-β-amyrin to produce glycyrrhizin, rather than acting directly on the β-amyrin scaffold (Seki et al., 2011). From these results, we can not exclude the possibility of CYP71D61 and CYP71D63 exhibiting catalytic activity toward himachalol. It is, however, worthwhile to mention that though CYP71D63 did not exhibit significant catalytic activity towards himachalol, its co-expression in yeast together with *MtTPS10* led to the production of a new compound, (**9**) 7,

epi-cis-sesquisabinene hydrate (Figure 2.22C). This observation suggests that CYP71D63 may act on an alternative MtTPS10-derived product or minor products, pointing out an important characteristic of cytochrome P450 enzymes, as being agents of terpene diversification (Bathe & Tissier, 2019; Frey et al., 2024). This characteristic ability of cytochrome P450 enzymes to generate diverse products by using terpene scaffolds can be an interesting avenue to explore in *M. truncatula* to investigate the possibility of generating libraries of metabolites that may confer medicinal or antimicrobial properties. To get a broader spectrum of the extent to which CYP71D61, CYP71D62, and CYP71D63 act on himachalol or on other MtTPS10-derived products, an LC-MS measurement coupled with NMR will be required for future work, as used in several experiments to detect additional enzyme products and to elucidate compound structures, respectively (Bathe & Tissier, 2019; Boachon, et al., 2019; Boachon et al., 2015; Frey et al., 2024; Liu et al., 2024).

It is noteworthy to mention that recent genetic and biochemical studies have revealed another aspect of secondary metabolism, that is, the physical clustering of genes in the genome for specialized metabolic pathways (Nützmann & Osbourn, 2014). Functional gene clusters are typically described as groups of at least three non-homologous biosynthetic genes that are physically adjacent in the genome and collaboratively contribute to a distinct chemical pathway (Nützmann et al., 2016; Nützmann & Osbourn, 2014). We show here that even a minimal composition of two physically clustered and coregulated genes, *MtTPS10* and *CYP71D62*, might constitute an efficient functional unit capable of producing a whole range of compounds (Figure 2.22B). Despite its simplicity, this gene pair aligns with the criteria for metabolic gene clusters (Nützmann et al., 2016; Nützmann & Osbourn, 2014), as it includes the initial committed step of the pathway, a terpene synthase generating the core scaffold, and a cytochrome P450 for downstream structural modification. Similarly, “a two-unit” gene cluster was described in Arabidopsis, where a cytochrome P450 enzyme, CYP706A3, was reported to be solely responsible for converting Arabidopsis sesquiterpene products of AtTPS11 into sesquiterpene oxides, thereby enhancing anti-herbivory defense (Boachon, et al., 2019) This observation in Arabidopsis was explained as a phenomenon that occurred in the plant as a result of *CYP706A3* and *AtTPS11* evolving early within the *Brassicaceae* family (Boachon, Burdloff, et al., 2019). A probable explanation for what we observe in the case of *MtTPS10* and *CYP71D62* could be that this clustering was to ensure a rapid and robust localized metabolic response after *A. euteiches* infection. In the context of metabolic response to stressors, several studies have captured the ecological relevance of cytochrome P450-terpene synthase interaction in plants (Boachon, et al., 2019; Boachon et al., 2015; Geisler et al., 2013; Liu et al., 2024). In barley, a biosynthetic gene cluster comprising genes encoding CYP89E31, CYP99A66, and CYP99A67 together with the diterpene synthases copalyl

diphosphate synthase (HvCPS2) and kaurene synthase-like (HvKSL4), gave rise to the phytoalexin 19-b-hydroxy-hordetrienoic acid (19-OH-HTA) (Liu et al., 2024). This compound was shown to possess antifungal activity against *F. graminearum* (Liu et al., 2024). Also, in oats, AsCYP51H10 oxidizes β-amyrin to produce avenacins, triterpenes with antifungal activity against the economically important fungus, *Gaeumannomyces graminis* (take-all diseases) (Geisler et al., 2013). Similarly, in Arabidopsis, the cytochrome P450 enzyme CYP76C1 modulates floral linalool emission by converting it into linalool oxides, which are less attractive to herbivores, thereby contributing to floral defense strategies (Boachon et al., 2015). Together, this evidence from barley, oats, and Arabidopsis highlights the potential role of cytochrome P450s in mediating ecologically relevant interactions. Given that the *MtTPS10* and *CYP71D62* were coexpressed following *A. euteiches* infection (Figure 2.21C), it is plausible that these new products (**5/8)** (1R,7S, E)-7-Isopropyl-4,10-dimethylenecyclodec-5-enol and (**6/7**) longifolenaldehyde could confer antimicrobial activity against *A. euteiches* (Figure 2.22B). It would therefore be valuable to investigate the biological activity of these products. In this regard, confirming the activity of *CYP71D62* on himachalol with a microsomal system is a crucial next step toward validating its enzymatic function. Given that plant cytochrome P450 enzymes are membrane-bound and require specific redox partners for activity (Laursen et al., 2021), the microsomal assay will provide a suitable environment for assessing their catalytic potential. To facilitate this, we have extracted microsomal membranes from yeast expressing CYP71D62 (data not shown). Furthermore, generating *CYP71D62* mutant lines in *M. truncatula* could provide complementary *in planta* evidence, allowing us to evaluate the impact of *CYP71D62* loss-of-function on himachalol metabolism and pathogen response. We have also obtained mutant lines of *CYP71D62* in *M. truncatula,* which can be used for future experiments.

Together, this work has identified key genes involved in the planta modification of himachalol through a combination of transcriptomic analysis, coexpression profiling, and enzyme characterization in yeast. This study lays an important groundwork for further characterization of these cytochrome P450 enzymes and their roles in plant defense.

4 Summary

Among the myriad specialized metabolites that plants employ to mediate interactions with their environment, terpenoids produced by terpene synthases (TPSs) form the largest but diverse group. The majority of these terpenoids are often species-specific metabolites with functions in responses to biotic and abiotic stressors. In *M. truncatula*, a substantial amount of information has been gathered describing the relevance of *M. truncatula*-derived terpenes produced by one specific TPS, MtTPS10. This TPS has emerged as the only reported TPS involved in *M. truncatula*'s defense against the economically important root pathogen, *A. euteiches.* The expression of *MtTPS10* is upregulated at 2 after infection of roots of *M. truncatula* with the oomycete, and its produced sesquiterpene products are reported to deter *A. euteiches* growth.

Our work showed that the induction of *MtTPS10* following the early contact with *A. euteiches* zoospores may occur due to the binding of an *A. euteiches* ligand, elicitor M, to an unknown plant receptor. Further characterization of elicitor M using a GUS reporter system and transcriptomics revealed that elicitor M and *A. euteiches* zoospores elicit the same set of stress-related genes in *M. truncatula* after 2 hpi, hinting at the notion that elicitor M may function as the PAMP initiating *MtTPS10* expression in *M. truncatula* after *A. euteiches* infection.

To determine whether evolutionary history or local environment influences the contribution of MtTPS10 to immunity in different ecotypes of *M. truncatula*, this study examined the expression of *MtTPS10* in a panel of 7 natural *M. truncatula* ecotypes and discovered differences in *MtTPS10* transcript levels following exposure to *A. euteiches* zoospores. Our work also established a correlation between *MtTPS10* expression and *A. euteiches* susceptibility, except for the ecotype 368, which accumulated no *MtTPS10* transcript but exhibited enhanced resistance to *A. euteiches,* accompanied by the release of sesquiterpene volatiles. To identify the contributing enzyme responsible for the blend of sesquiterpenoids emitted by 368 roots after *A. euteiches* infection, we employed transcriptomics and metabolomics approaches to study the response of this line 368 to *A. euteiches* infection in comparison to line Jemalong A17 as reference line. We found that the two *M. truncatula* ecotypes express different *MtTPSs, MtTPS10* and *MtTPS25*, respectively, at 2 hours after contact with *A. euteiches*. We characterized MtTPS25 based on its molecular, functional, and biological relevance and demonstrated that MtTPS25 functions as a sesquiterpene synthase, catalyzing the conversion of FPP into a blend of various sesquiterpene alcohols and olefins, with α-copaene as the primary product. The induction of *MtTPS25* is regulated by oomycetes, and its expression is root specific. Silencing of *MtTPS25* via RNAi resulted in a complete loss

of sesquiterpene volatiles emitted by wild-type roots. Furthermore, RNAi lines of *MtTPS25* showed an increased oomycete biomass compared to wild-type plants, suggesting a defensive role of the sesquiterpenes produced by MtTPS25.

Given the defensive roles of *MtTPS10* and *MtTPS25*, we bioengineered *S. tuberosum* to express these genes with the aim of conferring resistance against another important oomycete, *Phytophthora infestans*. We successfully obtained transgenic potato plants expressing either *MtTPS10* or *MtTPS25.* These plants did not show phenotypic alterations in comparison to the wild-type potato plants. Using GC-MS measurements, we also showed that the transgenic lines accumulated more metabolites compared to the wildtype. By using pathogen assays, we demonstrated that *MtTPS10* transgenic lines exhibited enhanced resistance to *P. infestans*, highlighting the functional relevance of this protein across species and its potential use for crop protection.

Finally, by using molecular tools, transcriptomics, protein expression, and metabolomics, we were able to pinpoint a cytochrome P450 gene, *CYP71D62*, as the putative agent responsible for modifying MtTPS10-derived product himachalol *in planta*. This work lays the groundwork for characterizing *CYP71D62* further to identify its implication in *M. truncatula* and *A. euteiches* interaction. Additionally, these discoveries offer valuable insights into legume resistance to *A. euteiches*, the No. 1 limiting factor in legume production.

5 Materials and Methods

5.1 Chemicals, solvents, and supplies

Chemical reagents required for respective experiments were purchased from the following chemical providers: Thermo-Fisher Scientific, Sigma-Aldrich, Merk, Bio & Sell, Qiagen, highQu GMHBH, Duchefa, Biozym, and Macherey-Nagel. Solvents were obtained from Carl Roth and Honeywell Riedel-de haën.

5.2 Organisms

5.2.1 *Escherichia coli*

The bacteria strain *E. coli* (DH10B, Invitrogen) was used to propagate plasmid vectors. Genotype: F– *mcrA* Δ(*mrr-hsdRMS-mcrBC*) φ80*lacZ*ΔM15 Δ*lacX74 recA1 endA1 araD139* Δ (*ara-leu*)7697 *galU galK* λ– *rpsL*(Str^R) *nupG*. The *E. coli* strain Rosetta was used for protein expression.

5.2.2 *Agrobacterium strains*

The *A. tumefaciens* GV3101::pMP90 (Zipfel, 2008) It was used for transit expression in *Nicotiana benthamiana. In contrast,* the *A. rhizogenes* strain ARqua1 (Quandt et al., 1993), genotype Onc+, Streptomycin+, biotype II (Keane et al., 1970) was used for the generation of hairy roots in *M. truncatula*. The strain AGL0:pTiBO542 was the *A. tumefaciens* strain used to transform potato plants.

5.2.3 *Saccharomyces cerevisiae*

The yeast strain (INV*Sc*1, Invitrogen) was used for the heterologous expression of plant proteins. Genotype: *MATa his3D1 leu2 trp1-289 ura3-52 MA*T *his3D1 leu2 trp1-289 ura3-52.*

5.2.4 *Aphanomyces euteiches*

Ae1a (obtained from INRA Rennes, France), ATCC201684, a pea isolate from Denmark, and AeRB84, a more aggressive strain from France, were kindly provided by Prof. Christophe Jacquet from Toulouse, France.

5.2.5 *Phytophthora infestans*

Prof. Sabine Rosahl of the Leibniz Institute of Plant Biochemistry kindly provided *P. infestans.*

5.2.6 *Medicago truncatula*

M. truncatula lines were obtained from the SARDI core collection and kindly provided by Jean-Marie Pros-peri, INRA Montpellier, France: 163, 368,542, 555, and 213. The reference line A17 Jemalong was obtained from AustraHort Pty Ltd., Cleveland, Queensland, Australia.

5.2.7 *Nicotiana benthamiana*

The wild-type *N. benthamiana* was used for protoplast isolation.

5.3 Microbial and plant growth conditions

5.3.1 *Escherichia coli*

For the transformation assay, *E. coli* was cultured on LB agar medium at 37 °C for 16 h. In a liquid medium, the culture was grown under continuous shaking at 200 rpm.

5.3.2 *Agrobacterium species*

Agrobacteria were cultured on LB plates at 28 °C for 2 days. In a liquid medium, the culture was grown under continuous shaking at 200 rpm for 2 days.

5.3.3 *S. cerevisiae*

Yeast strains were cultured in YPD or SCU medium at 30 °C, with shaking at 250 rpm if a liquid medium was used.

5.3.4 *Aphanomyces euteiches* growth and zoospore production

A. euteiches strain ATCC201684 was used for all infection studies (unless stated otherwise). The strain was routinely sub-cultured on 1.7 % (w/v) corn-meal agar (CMA, Sigma Aldrich, Germany) (**Table 4.1**) in the dark at 24 °C. For zoospore production, mycelial pieces from a fully-grown CMA plate (10-15 days old) were transferred to a sterile plastic pot (with lid) containing a 1:3 mixture of yeast tryptone medium (0.3% w/v yeast extract, 0.5 % w/v tryptone) and swamp water in the dark at 24°C. After 3 days of mycelial growth, the old medium was decanted, and the mycelial mats were washed 2-3 times with sterile tap water and incubated overnight in swamp water for zoospore release. The zoospores were counted using a hemocytometer, and appropriate volumes containing 10^5 zoospores and 3000 zoospores were directly applied to the roots of adult plants and seedlings on plates, respectively.

5.3.5 *Phytophthora infestans* growth and zoospore production

P. infestans was routinely cultured on oat-bean media (**Table 4.1**) at a temperature of 18°C. For zoospore release, autoclaved distilled water (10-20 ml) was added to mycelium, grown for

10- 11, and incubated in the dark at 4°C for 3-4 hours. After this period, spores are transferred into Falcon tubes through a Nylon net filter (20µm NY20 von Millipore). Cells were counted with LUNA™ automated cell counter, and a concentration of $1X10^5$ was used for infection assays.

5.3.6 *Medicago truncatula*

The germination of *M. truncatula* seeds involved a 5-minute scarification with anhydrous sulfuric acid for 5 min, followed by intensive washing with autoclaved Milli-Q water. Seeds were then placed on plant agar medium (0.7 % w/v in water) and cold-treated at 4°C in the dark for 2-3 days to break dormancy. Seedlings were transferred to either pots or plates based on the purpose of the experiment. For pot experiments, seedlings were grown at room temperature (25 °C) for 24h. Single seedlings were transferred to pots (13 cm diameter) filled with lecaton (Lamstedt Ton, Fibo Exclay) and grown in a growth chamber with a light period of 16 h at 26 °C and a dark period of 8 h at 20 °C and 40 % humidity. Plants were fertilized weekly with long-Ashton fertilizer (**Table 4.2**). For sterile cultivation of seedlings, seedlings were placed in square plates filled with 2/3 either M-medium (**Table 4.1**) for seedling assays or F-medium (**Table 4.1**) for root transformation. These plates were cultivated in growth chambers with 16 h at 26 °C and a dark period of 8 h at 20 °C and 40 % humidity.

Table 5.1:Media composition and their respective supplements

Medium type	Composition	Supplements	Reference
LB medium (*E. coli*, *A. tumefaciens/rhizogenes*)	10 g/l Tryptone, 10 g/lNaCl, 5 g/l Yeast extract, 10 g/l Micro agar, pH 7.5	50 µg/ml Carbenicillin, 50 µg/ml Gentamycin, 50 µg/ml Kanamycin, 25 µg/ml Rifampicin, 100µg/mlSpectinomycin, 50 µg/ml X-Gal	
YPD (*S. cerevisiae*)	20 g/l Peptone, 10 g/l Yeast extract, pH 6.5	20 g/l Micro agar, 2% (w/v) D(+)-glucose or D(+)-galactose	Clontech Protocols (PT3024-1)
Synthetic Dropout medium (SCU) (*S. cerevisiae*)	6.7 g/l Yeast Nitrogen Base without amino acids, 0.8-1g/dropout supplement without Uracil	20 g/L Micro agar, 2% (w/v) D(+)-glucose or D(+)-galactose	Clontech Protocols (PT3024-1)
Yeast tryptone media (*A. rhizogenes*)	5g/l Tryptone, 3g/l Yeast extract, 5 g/l Micro agar.	50 µg/mL streptomycin 50 µg/mL kanamycin	
Fahraeus media *(M. truncatula)*	$CaCl_2$ 0.9 M, $MgSO_4$ 0.5 M, KH_2PO_4 0.7 M, Na_2HPO_4 0.4 M, $C_6H_5FeO_7$ 1 M.	50 µg/mL streptomycin 50 µg/mL kanamycin	Harrison Lab Boyce-Thompson-institute

	$MnCl_2$ 1 mg/ml, $CuSO_4$ 1 mg/ml, $ZnCl_2$ 1mg/ml, H_3BO_3 1mg/ml, Na_2MoO_4 1mg/ml, Plant agar 15g\l	
M-media	$MgSO_4.7H_2O$ 7.31g, KNO_3 0.8 g, KCl 0.65 g/ml $Ca(NO_3)_2.4H_2O$ 2.88 g/ml, KH_2PO_4 250 mg/ml NaFe-EDTA 400 mg/l KI 37.5 mg/ml $ZnSO_4.7H_2O$ 132.5 mg/l H_3BO_3 75 mg/ml $CuSO_4.5H_2O$ 6.5 mg/l $Na_2MoO_4.2H_2O$ 120 µl Glycin 150 mg Nicotinic acid 25 mg Pyridoxine 5 mg Thiamine 5 mg Myo-Inositol 2.5 mg/l	(Bécard & Fortin, 1988)
2 MS media (*S. tuberosum*)	4.41 g MS salt with MES and vitamins 20g saccharose 6g plant agar pH= 5.8	Cefotaxime 250 mg/ml Kanamycin 100 mg/ml
3 MS media (*S. tuberosum*)	4.41 g MS salt with MES and vitamins 30g saccharose pH= 5.8	
GMS media Callus induction (*S. tuberosum*)	4.41 g/l MS salt (with MES and vitamins) 16 g/l glucose 6 g/l plant agar pH= 5.8	1 ml Cefotaxime 250 mg/ml 100 µl BAP 1mg/ml 5 ml NAA 1mg/ml 500 µl Kanamycin 100mg/ml
GMS media Shoot induction (*S. tuberosum*)	4.41 g/l MS salt (with MES and vitamins) 16 g/l glucose 6 g/l plant agar pH= 5.8	1 ml Cefotaxime 250 mg/ml 20 µl NAA 1mg/ml 500 µl Kanamycin 100mg/ml 20 µl GA3 1 mg/ml 2 ml Zeatinriboside 1 mg/ml
Corn-meal medium	17 g/l cornmeal	
Oat-bean medium (*P.infestans*)	34 g/l bean flour 17 g/l oat flour 8.5 g/l sucrose	

Table 5.2: Long-Ashton plant nutrient composition

compound	**Composition**

Macroelements	KNO_3 4.40 g/l $Ca(NO_3)_2.4H_2O$ 9.44 g/l Na_2HPO_4. $4H_2O$ 1.84 g/l $MgSO_4$. $7H_2O$ 7.53 g/l
Microelements (A)	$MnSO_4.4H_2O$ 2.23 g/l $MgSO_4$. $5H_2O$ 0.25 g/l $ZnSO_4.5H_2O$ 0.29 g/l H_3BO_3 3.10 g/l Nacl 5.90 g/l
Microelements (B)	$(NH_4)_6Mo_7O_{24}$. $4H_2O$ 0.88 g/l

To prepare Long-Ashton fertilizer, 10 ml of microelement A,1 ml of microelement A, 0.22 g Fe-EDTA, and the 1 L macroelements in **Table 5.2** were mixed.

5.3.7 *Solanum tuberosum*

Sterile potato plants (*Solanum tuberosum* cv De´siree´) were grown in tissue culture in a phytochamber for 3 weeks under long-day conditions (16 h light, 140 µmol photons) at 22 °C. The plants were transferred into sterilized soil and grown in a phytochamber for 3–4 weeks under long-day conditions (16 h light, 140 µmol photons) at 18–20°Cand 70% relative humidity.

5.4 Molecular Biology Methods

5.4.1 Golden Gate Cloning

Golden Gate modular cloning (MoClo System) (Engler et al., 2008) Can efficiently assemble many DNA fragments in a single step. The Golden Gate system uses the ability of type II restriction endonucleases that cut outside their recognition site sequence, allowing DNA fragments flanked by compatible restriction sites and overhangs to be digested and ligated easily. Since the ligated products lack the original type II restriction site, they will not be re-digested in a second restriction ligation reaction. Four base pairs are placed distal to the cleavage site such that recognition sites are removed after digestion, and only 4 base pair overhangs remain; these overhangs are used to assemble multiple DNA fragments in a specific unidirectional manner.

5.4.2 Construction of *MtTPS25* promoter-GUS reporter gene

Golden gate MoClo system was used to construct all vectors. The 2.0 kb promoter of *MtTPS25* was isolated from the genomic DNA of ecotype 368 via PCR using primers containing the *BpiI* sites. PCR reactions were performed, and the resulting PCR product was inserted into the level 0 vector pICH41295. After confirming the right promoter was cloned via sequencing, the level 0 vector with the *pMtTPS10* or *pMtTPS25* was fused to the GUS gene (pICH7511) with Tnos terminator in the destination vector pICH47742. The promoter-GUS construct was fused to the *DsRed* marker and cloned together in the destination vector pAGM4673, having

kanamycin as the selection marker. (Figure 4.1). All primers and vectors are available in the appendix (Table 7.2).

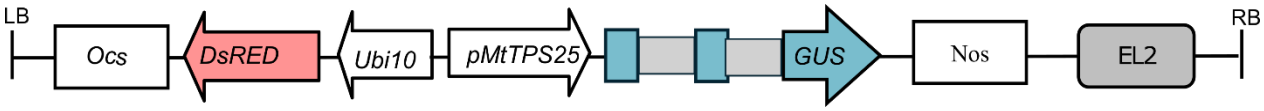

Figure 5.1: Construct of *MtTPS25* promoter GUS reporter gene.

GUS reporter gene driven by the promoter of *MtTPS25. DsRED* selection marker was used to select plants with transformed roots.

5.4.3 Generation of *MtTPS25*-RNAi constructs

The *MtTPS25* silencing construct (RNAi_*MtTPS25*) was generated using the NCBI BLAST tool to identify the best target region of the *MtTPS25* and to verify that the designed *MtTPS25* double-stranded RNA (dsRNA) trigger would not result in off-target interference. A hairpin RNA construct targeting *MtTPS25* was designed using a 750 bp sense/antisense fragment of *MtTPS25* interspaced with a 372 spacer (pAGM12285). Suitable restriction sites were introduced to both sides of the sequence to allow cloning into the appropriate Golden Gate vector, pAGM4031. Sequences were synthesized from a commercial company (Geneart-Thermo Fisher Scientific). The resulting sequence was cloned into a destination vector for expression under the control of the Ubi10 promoter. RNA transcribed from this construct produces a hairpin structure, resulting in double-stranded RNA. The anthocyanin-producing gene (*MtLAP1*) driven by *M. truncatula* root-cap-specific promoter (pMtRc) enabled the identification of co-transformed roots by the purple appearance of the root tips. The efficiency of the silencing of transformed roots was determined via RT-qPCR. The complete cassette was denoted as RNAi_*MtTPS25*. Roots of ecotype 368 were transformed using the plasmid RNAi_*MtTPS25*, following the hairy root transformation protocol.

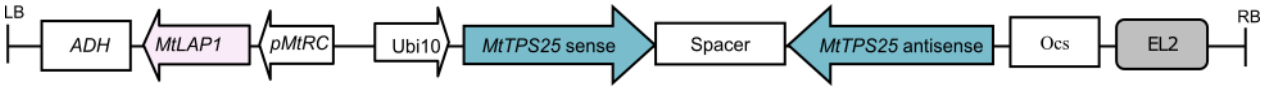

Figure 5.2: Construct of *MtTPS25*-RNAi.

Schematic representation of *MtTPS25*-RNAi construct showing Ubi10 driving the sense and anti-sense fragments of *MtTPS25* interspaced with a spacer.

5.4.4 Generation of vectors for potato transformation

The coding region of either *MtTPS10* or *MtTPS25*, together with farnesyl pyrophosphate synthase (*FPPS*) and a truncated version of *HMG-CoA* reductase (3-hydroxy-3-methyl-glutaryl-coenzyme A reductase, *tHMGCR*) from *N. benthamiana*, kindly provided by Prof. Alain Tissier and Dr. Sylvestre Marillonnet, respectively, were cloned behind the 35*S* promoter into

the level 2 vector pAGM37443. Kanamycin was used as a plant selection marker. The final constructs were denoted as pAGM1915 for *MtTPS10* and pAGM1917 for *MtTPS25.* Primers for the amplification of *MtTPS* cDNA can be found in the appendix (Table 7.2). The entire coding region of *MtTPS25* was synthesized from Geneart (Thermo Fisher Scientific).

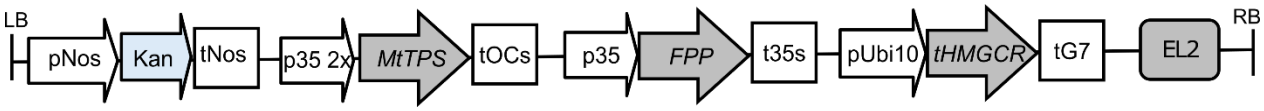

Figure 5.3:Schematic representation of the construct used for potato transformation.

All the precursor enzymes for the sesquiterpenoid pathway together with *MtTPS* were co-transformed into the Golden Gate vector pAGM37443

5.4.5 Generation of yeast expression vector

Golden Gate-compatible yeast expression vectors were used to produce plasmids for yeast engineering. For determining the products of MtTPS25, the full-length coding sequence of *MtTPS25*, farnesyl pyrophosphate synthase (*FPPS*), and a truncated version of *HMG-CoA* reductase (3-hydroxy-3-methyl-glutaryl-coenzyme A reductase, *tHMGCR*) were cloned into Golden Gate entry vector pAGM4031.In further cloning steps, each gene was fused to a synthetic galactose-inducible promoter and a terminator in a yeast level 1 expression vector using *BsaI* and T4-Ligase in restriction-ligation reaction. Different gene combinations were finally assembled into one yeast expression level M (pAGT564) vector by a restriction-ligation reaction with *BpiI* and T4-Ligase (Figure 4.4A) (Scheler *et al.*, 2016).To determine the modification of MtTPS10 by putative cytochrome P450s, the reductase ATR was incorporated into the backbone, followed by the respective cytochrome P450 enzyme (Figure 4.4B). After galactose induction, the constructs were tested for terpenoid production by GC-MS or product modification.

A

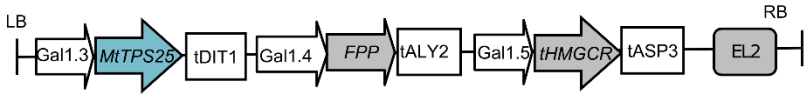

B

Figure 5.4: Construct for product expression MtTPS and CYP enzymes.

A. All the precursor enzymes for the sesquiterpenoid pathway and *MtTPS25* were co-transformed into the yeast expression vector. **B** Expression cassette for co-expression of *MtTPS10* with putative *CYP* enzymes.

5.4.6 Generation of vector for MtTPS25 protein localization

The full-length coding sequence of *MtTPS25* without stop codon cloned into the entry vector pAGM1287; this then fused to mCherry at the C-terminal under a CaMV 35S promoter using Golden Gate cloning into the destination vector pICH75055. Primers for sequence amplification can be found in the appendix (Table 7.2).

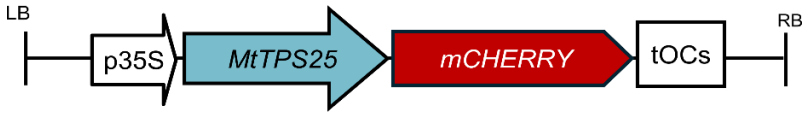

Figure 5.5: Scheme of the construct used for MtTPS25 localization.

The construct was used for transient expression in *N. benthamiana* protoplasts.

5.4.7 Polymerase Chain Reaction (PCR)

PCR is an in vitro DNA amplification method based on the ability of DNA polymerase to synthesize new strands complementary to the template. A normal PCR cycle involves three basic steps: denaturation of template DNA fragment, annealing of complementary primers, and elongation of DNA strand. The PCR reaction was performed in a thermocycler with a heated lid (C1000 Touch™ Thermal Cycler, BioRad Laboratories GmbH, Germany). All oligonucleotides were synthesized by Eurofins Genomics and are listed in appendix (Table 7.2). Different DNA polymerases were used depending on the downstream requirement of the PCR product. All PCR reactions were performed per the manufacturer's guidelines (Table. 5.3, Table. 5.4).

Table 5.3: Components of PCR reactions

KOD hot start polymerase		**highQu ALLin™ Taq DNA polymerase**	
Components	Amount	Components	Amount
10X Buffer	2.5 µl	MasterMix, 2X	12.5 µl
dNTPs (2 mM each)	2.5 µl	Forward primer (10 µM)	1 µl
Forward primer (10 µM)	0.75 µl	Reverse primer (10 µM)	1 µl
Reverse primer (10 µM)	0.75 µl	Template DNA	10-30 ng
Template DNA	10-30 ng	ddH_2O	Up to 25 µl
$MgSO_4$ (25 mM)	1.5 µl		
DNA polymerase (1U/µl)	1 µl		
ddH_2O	Up to 25 µl		

Table 5.4: Thermal programs of PCR reactions

Phase	KOD hot start polymerase		highQu ALLinTM Taq DNA polymerase		No. of cycles
Polymerase activation	95 °C	2 mins	95 °C	3 min	1
Denaturation	95 °C	20 s	95 °C	30 s	35
Annealing	Lowest primer Tm	20 s	55-65 °C	30 s	35
Extension	70 °C	20 s/Kb	72 °C	15 s/Kb	35
Final Extension	70 °C	2 mins	72 °C	5 mins	1

5.4.8 Agarose gel

PCR products were analyzed by electrophoretic separation in a 1% Agarose Gel, which was prepared by dissolving Agarose (Roth, Karlsruhe, Germany) in 1x TAE buffer (40 mM Tris-HCl pH 7.6, 20 mM acetic acid, and 1 mM EDTA), followed by brief boiling. Before casting the gel, one drop of ethidium bromide (EB, Roth) per 30 ml TAE buffer was added for DNA staining. Electrophoretic separation was performed at 100 V for 20-30 min, depending on the size of the product. A gel documentation system (FUSION FX7, Germany) was used to visualize the DNA fragments in the gel. Depending on the purity of PCR products, either PCR purification or gel extraction was performed using kit Monarch® PCR & DNA Cleanup (New England BioLabs) or Monarch® DNA Gel Extraction (New England BioLabs) according to manufacturer's instructions.

5.4.9 Isolation of plasmid DNA

Plasmid DNA was isolated from a 5 ml overnight culture of *E. coli* using NucleoSpin® Plasmid EasyPure Kit (Macherey Nagel, Germany) according to the manufacturer's instructions; the concentration was measured using Nanodrop and stored at -20 °C.

5.4.10 Isolation of genomic DNA

For genomic DNA isolation, 30-100 mg of frozen plant materials were homogenized to a fine powder using Retsch Beadmill (Retsch MM 400) and a steel bead of 7 mm at 30 Hz for 1 min. According to the manufacturer's guidelines, genomic DNA from the frozen fine powder was extracted using a NucleoSpin® Plant II kit (Macherey Nagel, Germany). The DNA concentration was measured using NanoDrop and stored at -20 °C.

5.4.11 Isolation of plasmid (miniprep)

The isolated white colonies were picked and grown overnight in culture tubes containing 5 ml LB media with suitable antibiotics at 37ºC and 200 rpm. Nucleospin® plasmid EasyPure, MACHEREY-NAGEL GmbH plasmid purification kit was used to isolate the plasmid DNA. After the plasmid extraction, restriction digestion was done with suitable restriction enzymes. Plasmid DNAs were digested (incubation at 37ºC for 1 hr 30 mins, deactivation at 65ºC for 20 mins) and run in the gel to confirm the expected bands. The correct plasmids were selected for further use, and glycerol stocks of positive colonies were prepared by mixing 500 µl of 50% sterile glycerol and 500 µl of overnight grown E. coli culture of positive colonies and immediately stored at -80ºC.

5.4.12 Isolation of plasmid (midiprep)

According to the manufacturer's guideline, the Midiprep kit (Macherey Nagel, Germany) was used to isolate plasmid DNA from a 50 ml bacterial culture. The concentration was measured using nanodrop and further concentrated using the PEG-DNA precipitation method. For this, the isolated plasmid from midiprep was mixed with PEG- solution (13 g PEG 4000, 67 mg MgCl2, 25 ml 1.2 M Na-acetate pH 5.2 in a total volume of 50 ml) in a 1:1 ratio and incubated at room temperature for 20 min followed by centrifugation at 17000×g for 20 min. The supernatant was carefully removed, and the pellet was washed with 1 ml of 70% ethanol. The pellet was then dried at 37ºC for approximately 30 min and resolved with 20 µl ddH20. The concentration of DNA was measured, and the DNA was stored at -20 ºC.

5.4.13 Isolation of RNA

RNA was isolated from 30-100 mg of frozen plant material, grounded in liquid nitrogen by mortar and pestle. RNA isolation was performed using Qiagen Plant Total RNA-Kit according to manufacturer's instructions, followed by DNase digestion using Ambion DNA-freeTM DNA Removal kit (Invitrogen, Thermo Scientific, Germany). RNA concentration was determined using a Nanodrop Spectrophotometer. RNA integrity and quality were analyzed using agarose gel electrophoresis (1% Agarose) or a bioanalyzer kit. RNA was stored at - 80 °C.

5.4.14 cDNA synthesis from mRNA

The RNA was reverse transcribed to cDNA for the quantitative real-time polymerase chain reaction (qRT-PCR) analysis. Total RNA was used to synthesize complementary DNA(cDNA) using Thermo Scientific RevertAid H minus First Strand cDNA synthesis kit according to the manufacturer's guidelines. 750 ng of RNA was used as a template with one µl of oligoDT primer and topped up to 12 µl with nuclease-free water. The reaction mixture was then

incubated at 65ºC for 5 min to denature the secondary structure of RNA. After denaturation, the samples were centrifuged and kept on ice for 2 minutes. 4 µl 5X Reaction Buffer, 1 µl RiboLock RNase Inhibitor, 2 µl of 10Mm dNTP Mix, and 1 µl Revert-Aid M-MuLV RT were added in the indicated order to the sample. The 20 µl of cDNA synthesis mixture was then incubated at 42ºC for one hour, inactivated at 80ºC for 5 min, and stored at -20ºC for further use.

5.4.15 Quantitative real-time PCR

Quantitative PCR was carried out in Hard-Shell® 96-Well PCR Plates (Bio-Rad Laboratories, www.bio-rad.com, #HSP9601) supplied with 10 µl reaction mix of 1.5 ng/µl cDNA, 1x EvaGreen QPCR Mix II (Bio&Sell, www.bio-sell.de, #BS76.580.0200) and 0.2 µM of forward and reverse primers (Appendix, Table 7.2). The reactions were run on a CFX Connect Real-Time PCR Detection System (Bio-Rad Laboratories) with denaturation (95°C for 15 min), amplification (cycles of 95°C for 15 s and 60°C for 30 s), and melt curve analysis (95°C for 10 s, 65°C heating up to 95°C with a heating rate of 0.05°C s −1). Gene expression was normalized to the housekeeping gene *MtACTIN2* for *M.truncatula* PCR and *EF1α* for potatoes using the $2^{-\Delta CT}$ method (Schmittgen & Livak, 2008) and included biological triplicates.

5.4.16 Genotyping of *Tnt1* insertion lines

The Samuel Roberts Noble Foundation´s Medicago *Tnt1* insertion mutant population is the most extensive collection of DNA-insertion mutants of all legumes. It was established from a starter parental line, containing approximately five copies of the *Tnt1* retroelement transferred into wild-type R108 by Agrobacterium tumefaciens-mediated transformation. To test whether the single plants of the ordered seeds really had the insertion in the gene of interest, a PCR screening using gene-specific primers in combination with *Tnt1* primers was used to identify *Tnt1* insertions in the genes of interest. To test the presence of the wt allele, primers of the gene of interest depicted as primer 1 and 2 in Figure 2.23A were used to test the presence of the *Tnt1* insertion, the forward primer of the gene of interest (1) was combined with a reverse primer located on the *Tnt1* sequence (3). DNA was isolated from every *Tnt1* insertion plant, and two PCR reactions were performed with primer 1+2 and primer 1+3. If both reactions showed a band, the plant had a heterozygous insertion; if there was only a band for reaction 1+2 there is no insertion in any of the alleles, and if there was a band only in reaction 1+3, it depicts a homozygous insertion of *Tnt1* in both alleles.

5.4.17 Transcriptome analysis (RNA-sequencing)

RNA quality and integrity were assessed on the Agilent 2100 Bioanalyzer system (Agilent Technologies, www.agilent.com) using the RNA 6000 Nano Kit for standard RNA sensitivity

(Agilent, #5067-1511). According to their pipeline, three biological replicates were submitted to Novogene (www.novogene.com) for mRNA paired-end short-read sequencing (150 bp length) on an Illumina NovaSeq 6000 Sequencing System and bioinformatics analysis. Reads were mapped to *M. truncatula* reference genome MedtrA17_4.0. Gene expression levels were determined using the FPKM (Fragments per kilobase per million) method. Gene expression heatmaps, principal component analysis (PCA), gene clustering, and Gene Ontology (GO) enrichment analysis were generated using the iDEP .96 and iDEP 1.1 (Ge et al., 2018) and Novomagic (www.novogene.com) software tools.

5.5 Bacteria and yeast transformation procedures

5.5.1 *Escherichia coli*

For all cloning and plasmid maintenance procedures, we used the *E. coli* strain DH10B. 200 ng or plasmid or 15 µl golden gate ligation mix was added to electrically competent cells and incubated on ice for 30 mins. Cells were immediately heat-shocked at 42 ºC for 30 s and cooled after this time on ice for 2 mins. Cells were incubated at 37 ºC with shaking at 350 rpm for 1 h in 800 µl of liquid LB medium. Afterward, an aliquot of 50 µl was plated on LB agar plates containing suitable antibiotics and X-Gal for blue-white selection of LacZ marker gene constructs. Restriction digestion and colony PCR were used to validate positively transformed *E. coli* colonies.

For the expression of MtTPS25 in *E. coli*, the ORF of *MtTPS25* was cloned with the affinity tag (His_6) in the pET28 vector, digested by SalI and XhoI. The plasmid pET28 containing the cDNA fragment was transformed into DH5α *E. coli* cells. Positively transformed colonies were transformed into the expressing strain Rosetta. A single colony was used to inoculate 100 ml containing kanamycin (50 µg/ml) and chloramphenicol (34 µg/ml). Liquid cultures of the bacteria harboring the expression constructs were grown at 37°C to an OD600 of 0.8-1.0 overnight. Then, isopropyl-β-thiogalactopyranoside (IPTG) was added to a final concentration of 1M, and the cultures were incubated for 44 h at 22°C. The cells were collected by centrifugation and disrupted by a 4 × 30 s treatment with a sonicator in chilled extraction buffer (50 mM MOPS, pH 7.0, with 5 mM $MgCl_2$, 5 mM sodium ascorbate, 0.5 mM phenylmethylsulphonyl fluoride, 5 mM dithiothreitol, and 10% [v/v] glycerol). The cell fragments were removed by centrifugation at 14,000g, and the supernatant was desalted into assay buffer (10 mm MOPSO, pH 7.0, 1 mm dithiothreitol, and 10% [v/v] glycerol) by passage through an Econopac 10DG column (Bio-Rad, Hercules, CA). The His-tagged enzymes were further purified on a nickel-nitrilotriacetate agarose column (Qiagen) according to the manufacturer's instructions. For terpene synthase activity, 100 µg/ml of MtTPS25 was assayed in TRIS buffer containing 5 mM $MgCl_2$, 5% glycerol, and 2 mM of either FPP, GPP,

or GGPP in a total volume of 500 µl. The assay was overlaid with 200 µl of hexane containing 25 µM naphthalene as internal standard. The mixture was incubated at 25 °C for 2-3 days. After this period samples were measured with GC-MS.

5.5.2 *Agrobacterium species*

Except for the AGLO strain of *A. tumefaciens* used for potato transformation, all *Agrobacterium* strains used in this work were transfected using electroporation. With this, 1µg of positively transformed plasmids was added to 50 µl of *Agrobacterium* cells and after carefully mixing the plasmid and *Agrobacterium*, the mixture was transferred to pre-chilled cuvette (VWR cuvette with 2 mm gap) and inserted into the cuvette arm of electroporator (Micropulser Electroporator, BioRad Laboratories GmbH, Munich, Germany). A pulse of 2.2 kV for approximately 5 ms was applied to cells, 250 µl LB was added to revive cells and then cultured in an Eppendorf tube at 28 °C for 2-3 h. After a resurgence in LB, cells were plated on LB agar with appropriate antibiotics and grown for 2-3 days at 28 °C. For AGL0, the heat/thaw method was used. (Höfgen & Willmitzer, 1988). 1 µg of plasmid was added to 250 ml of frozen competent cells in 2 ml Eppendorf tubes. The mixture was allowed to thaw for 10 mins, and after this time, the tubes containing the mixture were immersed in liquid nitrogen for 5 mins and heat-shocked at 37 °C for 5 mins directly from the liquid nitrogen. 1 ml of LB liquid medium was added to the mixture and incubated for 2-4 h at 28 °C. Cells were centrifuged after the incubation time at 3,000 rpm at room temperature for 3 min, the supernatant was discarded, and the pellets were resuspended in a 200 ml LB medium. The cells were spread on LB plates with appropriate antibiotics.

5.5.3 *Saccharomyces cerevisiae*

The preparation of competent cells and yeast transformation was done using the manufactory protocol of the Zymo Research Yeast transformation kit (Frozen EZ- yeast transformation II kit). Yeast cells from a glycerol stock were streaked on a YPD plate without antibiotics and grown for 2 days at 30 °C. A single colony was then used to inoculate 10 ml YPD broth and grown overnight with shaking at 30 °C until OD_{600} of 4.5 was reached. This yeast suspension served as a primary culture to inoculate 100 ml YPD broth. The new suspension was further grown in the same growing condition until a mid-log phase with an OD_{600} between 0.8-1 was reached. Cells were pelleted at 4000 rpm, and the supernatant was discarded. Cells were washed with 100 ml of frozen EZ solution 1 and re-pelleted; the supernatant was discarded, and finally, the cells were resuspended in frozen EZ solution 2. Cells were aliquoted and kept at -80 ºC. For the yeast transformation procedures, 1 µg of plasmid was added to 10 µl of the yeast-competent cells and mixed by tapping gently. 100 µl of frozen EZ solution 3 was added to the mixture and mixed by pipetting. The yeast mixture was incubated at 37 for 1 h with

intermittent mixing; after 1 h, the cells were pelleted and resuspended in 50 µl frozen EZ solution 3 and plated on SCU plates. Plates were incubated at 30 °C for 3-4 days.

5.6 Plant transformation

5.6.1 *A. rhizogenes* mediated hairy root transformation of *M. truncatula*

M. truncatula hairy roots were generated via *A. rhizogenes*-mediated root transformation. The generated hairy roots are well adapted for root-microbe and root architecture studies. Vector constructs containing disarmed T-DNA region carrying the GOI with left and right borders, plant and bacterial antibiotic marker, visualization marker, and origin of replication were transformed in ARqua1 and grown in LB agar containing kanamycin and streptomycin for 48h. Positive colonies were cultured in LB medium with antibiotics for another 24 h, and 200 µl was plated out on YT agar containing 2 mM $CaCl_2$, antibiotics, and 200 µl acetosyringone (1 mM/ml). Meanwhile, *M. truncatula* seeds were sterilized and germinated on a 0.7 % plant agar plate. The plates were kept inverted at 4 °C for 4 days and 12 °C for 1-2 days in the dark. Root transformation was performed when the seedlings were around 1 cm long and *A. rhizogenes* were fully grown. The germinated seedlings were placed in a water-filled petri plate to avoid desiccation, and the seed coat was removed. The root tip (approx. 3 mm) was cut using a sharp scalpel, scraped on the Agrobacterium lawn, and placed on 2/3 filled F- medium (Table 5.1) square plates. The roots were laid over the agar so the shoot part was in the agar-free zone and had enough space to grow. Seven seedlings were placed in a plate, and 1 ml sterile tap water was pipetted on top of agar to avoid meristem drying, and the plates were sealed with leucopore tape to allow gas exchange. The plates were covered with an aluminum foil to maintain a dark environment for roots, and incubated at an angle of 45° for 4 days, and then vertically for 1 week in a climate chamber with 16 h light phase of 20 °C and 8 h dark phase at 17 °C. The plates were cultivated for 3-4 weeks in a climate chamber with a 16 h light phase of 24 °C and an 8 h dark phase at 20 °C. After 2 weeks, 5 ml of sterile tap water was pipetted into the plates to avoid drying and maintain humidity. After 4-5 weeks of growth, roots were screened for transformation using red fluorescence emitted by constitutively expressing the DsRed module under a stereo microscope (Leica MZIII-Fluorescence microscope) or visualization of anthocyanin with the naked on the root tips. Non-transformed roots were carefully removed, and the selected transformed plants were transferred to pots filled with lecaton or fresh plates for in vitro assays. After 1 week in lecaton, roots were screened again for transformation, and transgenic plants were transferred to lecaton pots. The transgenic plants were then further grown for 1 week, followed by infection with *A. euteiches*. Plants were fertilized with LA fertilizer once per week and watered 3 times a week. While harvesting, the roots were carefully taken out of lecaton, washed in ddH_2O, and dried with paper towels. About

2 cm centerpieces of roots were stored in 50 % ethanol for staining purposes, and the rest were snap-frozen in liquid nitrogen and later stored at -80 °C until RNA extraction.

5.6.2 *S. tuberosum* leaf disk transformation

Before the leaf disk transformation of potato leaves, vector constructs harboring the T-DNA region carrying the GOI with left and right borders, plant and bacterial antibiotic marker (Figure 4.3), and origin of replication were transformed in AGLO strain of *A. tumefaciens* and grown in LB agar containing kanamycin, Gentamycin and Rifampicin for 48h. colonies were tested for the insertion of GOI via colony PCR, and positively transformed colonies were further cultured in 20 ml LB medium with antibiotics for another 48 h. The agro suspension was transferred to Falcon tubes and centrifuged for 10 mins at 5000 rpm. The supernatant was discarded, and the pellets were suspended in a filter sterilized 10 mM $MgSO_4$. This suspension was again centrifuged for 10 mins at 5000 rpm. The supernatant was discarded, and the pellets were re-suspended in 10 ml 3MS-medium and placed on ice. Under sterile conditions, transgenic potato plants were regenerated from sterile potato plant leaves (wild-type Désirée). Wild-type leaves were placed upside down on sterile filter papers socked with 3MS-Medium. For the transformation process. Petioles were detached, and leaves were gently wounded with a sharp blade by creating cuttings (3-4 times) across each leaf (cuttings should not cut through the leaves). Leaves (12-14 leaves per Petri dish, 5-6 Petri dishes per construct) were then transferred upside down into Petri dishes with 10 ml 3MS-Medium (Leaves should float). 100 µl of agrobacteria suspension with the desired gene construct was added to the Petri dishes and shaken gently for uniform dispersal of the agro. Petri dishes were wrapped with aluminum foil without sealing with parafilm and incubated in the dark for 2 days at 21°C. After incubation, leaves were gently dried off excess *Agrobacterium* on filter papers (sterile) and transferred to callus induction media (Table 5.1) with the right antibiotics. Leaves were transferred to fresh media every 14 days. After 4-6 weeks, the first calli started to emerge, and when the calli were long enough, they were transferred to shoot induction media (Table 5.1) with the appropriate antibiotics. After 2-3 weeks, shoots developed roots and were transferred to new shoot induction media. Copies of each plant were made. Sterile potato plants were grown in tissue culture in a phytochamber with long day conditions of 16 h light, 140 µmol photons at 22 ºC for 3 weeks. Gene expression analysis using RT-qPCR was done on all transgenic lines to determine positively transformed plants. Plants exhibiting the GOI were transferred to 110 mm diameter sterile pots after 3-4 weeks and grown under long-day conditions of 16 h light, 140 µmol photons at 18-20 ºC, and 70% relative humidity for 3 weeks.

5.7 Infection assays

5.7.1 Determination of *A. euteiches* biomass

Biomass of *A. euteiches* was determined from infected roots of *M. truncatula* grown in pots for 6 weeks (Infection was done when plants were 2 weeks old and further grown for an additional 4 weeks). Roots were immediately frozen in liquid nitrogen and ground to powder using mortar and pestle. RNA was extracted from frozen root tissue (70 mg) using the RNeasy mini kit (Qiagen) according to the manufacturer's instruction.A*. euteiches* biomass was determined in root tissues using RT-qPCR with *A. euteiches-specific* primers 5′-TGTCTAGGCTCGCACATCGA-3′ and 5′-AGTGCA ATATG GTTCAA CGT TT-3′ to determine 5.8s rRNA levels in the root. The 5.8s rRNA levels from one sample were determined using the mean of three technical replicates. The resulting values were converted using the formula $2^{-\Delta Ct}$.

5.7.2 Determination of *P. infestans* biomass

Infection of potato plants and determination of *P. infestans* biomass was done according to (Gorzolka et al.(2021). The abaxial side of leaves of 4–5-week-old phytochamber-grown plants was inoculated with 10 µL of a *P. infestans* zoospore suspension (1 × 105 zoospores/mL). 8 drops of spores were applied to each leaf, and 3 leaves per plant were inoculated. The leaves were covered with a plastic bag to ensure sufficient humidity for the germination of *P. infestans*. After 3 days, inoculated areas of leaves were sampled with a cork borer (size 6 mm). DNA was extracted from leaf tissues according to GenElute™ Plant Genomic DNA Miniprep Kit Protocol after adding an external DNA standard, NADPH oxidase (NOX), at a 0,001 µg/µl concentration. Samples were then subjected to RT-qPCR analyses using the *P. infestans*-specific primers PiO 5'CGT ACG GCC AAT GTA GTTCC 3' and PiO 5' TTTGCACAGTATCACGCA AGT 3'. The content of NOX was determined using the primer set 5'TCAATGCATAGGATGAAGGAATC 3' and using the primer set 5'TCAATGCATAGGATGAAGGAATC 3' and 5'TCTCTTCCTAGCTAGAGCATAAA 3'. The following program was used: Initial denaturation at 95 °C for 10 min, 40 cycles of denaturation at 95 °C for 15 s, annealing, extension, and plate read at 60 °C for 1 min and 95 °C for 15 s.

5.8 Fungal growth-inhibition assays

Assays were carried out previously as described by Geisler et al.(2013). Mycelium plugs from an actively growing colony of the *A. euteiches* oomycete were placed onto corn meal agar. Copaene (1 mg/mL stock solution) was dissolved in n-hexane, and different concentrations (50 µM, 80 µM,120 µM) were applied to filter paper discs. The discs were placed equidistant

from the oomycete plug of the inoculum. Plates were incubated at 24 °C in the dark, and growth was monitored after 1 week.

5.9 PAMPs assays

7- week-old *M. truncatula* seedlings were used for the PAMP assays. The roots of these seedlings were inoculated with Pep-13 (100 µM) or the nearly inactive analog W2A (100 µM), flg22 (100 nM), and chitin (100 nM/ml). Roots were harvested after 2 hpi and frozen in liquid nitrogen. The root samples were homogenized using mortar and pestle. RNA was extracted from 70 mg homogenized root, and the expression of *MtTPS10* was determined using RT-qPCR. Three technical replicates for each sample were used for the expression analysis.

5.10 Phylogenetic analysis

MtTPS amino acid sequences were obtained from NCBI and uniport (www.uniprot.org). Sequence alignment was performed using ClustalO-mega. (Sievers et al., 2011).The maximum likelihood tree was inferred in MEGAX (Kumar et al., 2018) The following parameters are used: 1,000 bootstrap replication, JTT model, and scale bar based on the distances of sequences.

5.11 Cell Biology Methods

5.11.1 GUS staining for promoter activity

Glucouronidase (GUS) reporter assay is the most valuable tool for studying promoter activity, where GUS is used to visualize the activity of a promoter under study. Two different kinds of carbohydrate substrates are available for GUS, namely X-Gluc (5-Bromo-4-chloro-3-indolyl-β-D- glucuronide), which on cleavage and further oxidization gives a dense blue color, and MUG (4- Methyl umbelliferyl -D-glucuronide) which on cleavage gives a fluorescent product detectable by spectrophotometer. Promoter activity was visualized using X-Gluc (Glycosynth, UK) as substrate. Transformed roots, infected with *A. euteiches* infected or not, were incubated with the staining solution (Table 5.5)under vacuum infiltration for a few minutes to allow penetration of the staining solution into the roots and then incubated for 1-2 h at 37 °C. GUS-stained roots were later embedded in PEG 1500, according to Yadav et al. (2019), and sectioned in 10 µm thick sections using a microtome. The stained root fragments and the sections were analyzed using a Stemi2000 (Zeiss) and an AxioImager (Zeiss), respectively.

Table 5.5: Composition of GUS-staining solution (in ddH_2O)

Components	concentration	Final concentration	Amount for 100 ml
NaH_2PO_4, pH 7	500 mM	100 mM	20 ml
Na_2EDTA, pH 7	250 mM	10 mM	4 ml
$K_3Fe(CN)_6$	50 mM	0.5 mM	1 ml
$K_4Fe(CN)_6$	50 mM	0.5 mM	1 ml
X-Gluc(104 mg in 2 ml DMSO)	100 mM	2 mM	2 ml
Triton X-100	10 %	0.1 %	1 ml
ddH_2O			71 ml

5.11.2 Isolation of protoplast

The third and fourth leaves of 4-week-old well-developed N. benthamiana plants were used for the protoplast isolation. The leaves were placed on white paper, and the midribs were removed carefully with the help of a sharp razor blade. Leaf laminae were cut into approximately 4 mm2 small pieces. The freshly cut pieces were placed in a Petri dish (5 cm diameter) filled with enzyme solution (Appendix, Table 7.3). The leaf pieces were vacuum infiltrated two times for 15 min. The infiltrated leaves appeared dark and transparent and sank at the bottom. After the infiltration, the leaves were incubated in the dark for 4 hours at room temperature. After 4 hours, the enzyme solution should appear green. The Petri dish was gently shaken on a shaker in the dark for 30 min to release the protoplast. The protoplast suspension (4.5 ml) was filtered using nylon mesh (100 microns) into 15 ml culture tubes on ice and centrifuged (200×g) for 1 min at 4ºC. The supernatant was carefully removed, and the pellet was re-suspended in 3 ml W5 solution (Appendix, Table 7.3), centrifuged, and resuspended in 3 ml W5 solution. The protoplasts were incubated on ice for 40 min to allow them to settle at the bottom. The supernatant was removed again, and the protoplasts were re-suspended in 2-3 ml of MMG solution (Appendix, Table 7.3) and further incubated on ice for 40 mins. The protoplast number was determined by placing 20 µl of suspension on a counting chamber and visualizing using a light microscope.

5.11.3 Protoplast transformation and microscopy

5-10 ng (approx. 2 µl) of plasmid DNA purified was added to 200 µl of protoplast suspension in a 2 ml Eppendorf tube and mixed gently. 220 µl of PEG solution was added, mixed slowly, and incubated at room temperature for 10 min. To this mixture, 880 µl of W5 solution was added and mixed carefully before centrifuging at 200×g at 4ºC for 1 min. The supernatant was removed, and the protoplasts were resuspended in 200 µl WI solution. The transformed protoplasts were incubated overnight in a horizontal position in the dark at room temperature. The following morning, they were observed by confocal laser scanning microscopy. The Zeiss LSM880 confocal microscope was used to capture fluorescent images using the following excitation or emission settings: 480 nm/660-700 for chlorophyll and 561 nm/600-660 for mCherry. Images were processed using LSM image processing software (Zeiss).

5.12 Metabolomics

5.12.1 Volatile from roots of *M. truncatula* and GC-MS-based profiling

plants were gently removed from the lecaton substrate and placed in 500 ml volumetric flasks containing a sterile, moist filter paper to keep the flask humid after Six weeks of growth. Depending on the architecture of the roots, 2-3 Sorbstar® tubings were inserted in different regions of the root. The roots were either treated with zoospores or mock-treated with swamp water for 24 hours, with each treatment having 3 replicates. The Sorbstar® tubings were collected and put in GC vials. The root volatiles emitted after *A. euteiches* treatment were adsorbed on silica tubes (Sorbstar, Restek, Germany) and later measured in thermo-desorption GC-MS (TD-20) coupled to GCMS QP2010 SE (Shimadzu, Japan), 48-Sample autosampler and QP2010 Ultra mass spectrometer with electron ionization. Here, the volatiles are first thermally desorbed from the tubes and passed through a cold trap to concentrate the volatile peaks before transferring them to GC-Column coupled to the mass spectrometer. Using split injection mode, chromatographic separation was performed on an RXI-5il MS capillary column (30m x 0.25mm, Shimadzu, Japan). The GC Column oven temperature ramp was as follows: 50 °C for 1 min, 50 to 300 °C at a rate of 15 °C min^{-1}, 300 to 320 °C at a rate of 20 °C min^{-1}, and 320 °C for 2 min. Mass spectrometry was performed in a full scan mode from 35 to 500 m/z. Data analysis was done using device-specific GCMS Postrun Analysis.

5.12.2 Yeast extracts and GC-MS-based profiling

Constructs cloned into yeast vectors were transformed into *S. cerevisiae* strain INVSc1 and plated onto the SCU selection medium. Three positive colonies were picked and inoculated into a 5 ml SCU medium containing 2% glucose and grown for 24 h at 30 °C with shaking. The cell pellet was resuspended in a fresh SCU medium containing 2% galactose to induce protein

expression. After another 24 h of growth, the whole culture was extracted with 2 ml n-hexane. Dried extracts of yeast were suspended in 200 µl n-hexane for GC-MS analysis. GC-MS analysis was conducted on Trace GC Ultra gas chromatograph (Thermo Scientific) coupled to an ATAS Optic 3 injector and an ISQ single quadrupole mass spectrometer (Thermo Scientific) with electron impact ionization. Capillary gas chromatography was performed using an HP-5ms column (30 m × 0.25 mm × 0.25 µm; Phenomenex). Samples were injected by splitless injection at a 250°C injector temperature, using a program consisting of 3 min at 40°C, followed by a 20°C min−1 ramp to 320°C, then 5 min at 320°C, with a flow rate of 1.0 mL min−1 of He as the carrier gas. Products were identified based on their retention times and electron ionization mass spectra (70 eV, m/z 50-300) and compared to those present in the NIST library. Some samples were analyzed on an Agilent 8890 using the same temperature parameters, with a capillary column (30 m × 0.25 mm × 0.25 µm, Phenomenex) and splitless injection at an injection volume of 1 µl. The MS spectra were acquired using the same parameters, which are described above.

5.12.3 Potato Extract and GC-MS based targeted profiling

For qualitative analysis of metabolites from transgenic potato leaves, leaves expressing *MtTPS10* or M*tTPS25* together with wildtype and empty vector leaves were harvested 2 weeks after transfer into pots and frozen in liquid nitrogen. Leaves were homogenized using mortar and pestle with the homogenizer (Retch). 100 mg of samples were extracted with 1 ml ethyl acetate with sonification for 1 min. The suspension was centrifuged at 14,000 g for 2 mons, and the supernatant was analyzed directly by GC-MS.

5.13 Statistical and analysis

Microsoft Excel and GraphPad Prism 9 were used for regular statistical data analysis. Based on the experiment, a student *t-test* or ANOVA was used to show statistically significant differences.

6 References

Abramovitch, R. B., Anderson, J. C., & Martin, G. B. (2006). Bacterial elicitation and evasion of plant innate immunity. *Nature Reviews. Molecular Cell Biology*, *7*(8), 601–611. https://doi.org/10.1038/nrm1984

Afrin, T., Seok, M., Terry, B. C., & Pajerowska-Mukhtar, K. M. (2020). Probing natural variation of IRE1 expression and endoplasmic reticulum stress responses in Arabidopsis accessions. *Scientific Reports*, *10*(1), 19154. https://doi.org/10.1038/s41598-020-76114-1

Aharoni, A., Jongsma, M. A., & Bouwmeester, H. J. (2005). Volatile science? Metabolic engineering of terpenoids in plants. *Trends in Plant Science*, *10*(12), 594–602. https://doi.org/10.1016/j.tplants.2005.10.005

Alagna, F., Reed, J., Calderini, O., Thimmappa, R., Cultrera, N. G. M., Cattivelli, A., Tagliazucchi, D., Mousavi, S., Mariotti, R., Osbourn, A., & Baldoni, L. (2023). OeBAS and CYP716C67 catalyze the biosynthesis of health-beneficial triterpenoids in olive (Olea europaea) fruits. *New Phytologist*, *238*(5), 2047–2063. https://doi.org/10.1111/nph.18863

Albert, I., Böhm, H., Albert, M., Feiler, C. E., Imkampe, J., Wallmeroth, N., Brancato, C., Raaymakers, T. M., Oome, S., Zhang, H., Krol, E., Grefen, C., Gust, A. A., Chai, J., Hedrich, R., Van den Ackerveken, G., & Nürnberger, T. (2015). An RLP23-SOBIR1-BAK1 complex mediates NLP-triggered immunity. *Nature Plants*, *1*, 15140. https://doi.org/10.1038/nplants.2015.140

Alfano, J. R., & Collmer, A. (2004). Type III secretion system effector proteins: Double agents in bacterial disease and plant defense. *Annual Review of Phytopathology*, *42*, 385–414. https://doi.org/10.1146/annurev.phyto.42.040103.110731

Arimura, G., Garms, S., Maffei, M., Bossi, S., Schulze, B., Leitner, M., Mithöfer, A., & Boland, W. (2007). Herbivore-induced terpenoid emission in Medicago truncatula: Concerted action of jasmonate, ethylene and calcium signaling. *Planta*, *227*(2), 453. https://doi.org/10.1007/s00425-007-0631-y

Armstrong, M. R., Whisson, S. C., Pritchard, L., Bos, J. I. B., Venter, E., Avrova, A. O., Rehmany, A. P., Böhme, U., Brooks, K., Cherevach, I., Hamlin, N., White, B., Fraser, A., Lord, A., Quail, M. A., Churcher, C., Hall, N., Berriman, M., Huang, S., … Birch, P. R. J. (2005). An ancestral oomycete locus contains late blight avirulence gene Avr3a, encoding a protein that is recognized in the host cytoplasm. *Proceedings of the National Academy of Sciences of the United States of America*, *102*(21), 7766–7771. https://doi.org/10.1073/pnas.0500113102

Attaran, E., Rostás, M., & Zeier, J. (2008). Pseudomonas syringae Elicits Emission of the Terpenoid (E,E)-4,8,12-Trimethyl-1,3,7,11-Tridecatetraene in Arabidopsis Leaves Via Jasmonate Signaling and Expression of the Terpene Synthase TPS4. *Molecular Plant-Microbe Interactions*, *21*, 1482–1497. https://doi.org/10.1094/MPMI-21-11-1482

Axtell, M. J., & Staskawicz, B. J. (2003). Initiation of RPS2-specified disease resistance in Arabidopsis is coupled to the AvrRpt2-directed elimination of RIN4. *Cell*, *112*(3), 369–377. https://doi.org/10.1016/s0092-8674(03)00036-9

Aziz, A., Gauthier, A., Bézier, A., Poinssot, B., Joubert, J.-M., Pugin, A., Heyraud, A., & Baillieul, F. (2007). Elicitor and resistance-inducing activities of β-1,4 cellodextrins in grapevine, comparison with β-1,3 glucans and α-1,4 oligogalacturonides. *Journal of Experimental Botany*, *58*(6), 1463–1472. https://doi.org/10.1093/jxb/erm008

Badis, Y., Bonhomme, M., Lafitte, C., Huguet, S., Balzergue, S., Dumas, B., & Jacquet, C. (2015). Transcriptome analysis highlights preformed defences and signalling pathways controlled by the prAe1 quantitative trait locus (QTL), conferring partial resistance to Aphanomyces euteiches in Medicago truncatula. *Molecular Plant Pathology*, *16*(9), 973–986. https://doi.org/10.1111/mpp.12253

Badreddine, I., Lafitte, C., Heux, L., Skandalis, N., Spanou, Z., Martinez, Y., Esquerré-Tugayé, M.-T., Bulone, V., Dumas, B., & Bottin, A. (2008). Cell wall chitosaccharides are essential components and exposed patterns of the phytopathogenic oomycete Aphanomyces euteiches. *Eukaryotic Cell*, *7*(11), 1980–1993. https://doi.org/10.1128/EC.00091-08

Baetz, U., & Martinoia, E. (2014). Root exudates: The hidden part of plant defense. *Trends in Plant Science*, *19*(2), 90–98. https://doi.org/10.1016/j.tplants.2013.11.006

Baldauf, S. L., Roger, A. J., Wenk-Siefert, I., & Doolittle, W. F. (2000). A Kingdom-Level Phylogeny of Eukaryotes Based on Combined Protein Data. *Science*. https://doi.org/10.1126/science.290.5493.972

Barker, D. G., Bianchi, S., Blondon, F., Dattée, Y., Duc, G., Essad, S., Flament, P., Gallusci, P., Génier, G., Guy, P., Muel, X., Tourneur, J., Dénarié, J., & Huguet, T. (1990). Medicago truncatula, a model plant for studying the molecular genetics of theRhizobium-legume symbiosis. *Plant Molecular Biology Reporter*, *8*(1), 40–49. https://doi.org/10.1007/BF02668879

Bartnicki-Garcia, S. (1968). Cell wall chemistry, morphogenesis, and taxonomy of fungi. *Annual Review of Microbiology*, *22*, 87–108. https://doi.org/10.1146/annurev.mi.22.100168.000511

Bathe, U., & Tissier, A. (2019). Cytochrome P450 enzymes: A driving force of plant diterpene diversity. *Phytochemistry*, *161*, 149–162. https://doi.org/10.1016/j.phytochem.2018.12.003

Beakes, G. W., Glockling, S. L., & Sekimoto, S. (2012). The evolutionary phylogeny of the oomycete “fungi”. *Protoplasma*, *249*(1), 3–19. https://doi.org/10.1007/s00709-011-0269-2

Bécard, G., & Fortin, J. A. (1988). Early events of vesicular–arbuscular mycorrhiza formation on Ri T-DNA transformed roots. *New Phytologist*, *108*(2), 211–218. https://doi.org/10.1111/j.1469-8137.1988.tb03698.x

Bennett, R. N., & Wallsgrove, R. M. (1994). Secondary metabolites in plant defence mechanisms. *New Phytologist*, *127*(4), 617–633. https://doi.org/10.1111/j.1469-8137.1994.tb02968.x

Bi, W., Liu, J., Li, Y., He, Z., Chen, Y., Zhao, T., Liang, X., Wang, X., Meng, X., Dou, D., & Xu, G. (2024). CRISPR/Cas9-guided editing of a novel susceptibility gene in potato improves Phytophthora resistance without growth penalty. *Plant Biotechnology Journal*, *22*(1), 4–6. https://doi.org/10.1111/pbi.14175

Boachon, B., Burdloff, Y., Ruan, J.-X., Rojo, R., Junker, R. R., Vincent, B., Nicolè, F., Bringel, F., Lesot, A., Henry, L., Bassard, J.-E., Mathieu, S., Allouche, L., Kaplan, I., Dudareva, N., Vuilleumier, S., Miesch, L., André, F., Navrot, N., … Werck-Reichhart, D. (2019). A Promiscuous CYP706A3 Reduces Terpene Volatile Emission from Arabidopsis Flowers, Affecting Florivores and the Floral Microbiome. *The Plant Cell*, *31*(12), 2947–2972. https://doi.org/10.1105/tpc.19.00320

Boachon, B., Junker, R. R., Miesch, L., Bassard, J.-E., Höfer, R., Caillieaudeaux, R., Seidel, D. E., Lesot, A., Heinrich, C., Ginglinger, J.-F., Allouche, L., Vincent, B., Wahyuni, D. S. C., Paetz, C., Beran, F., Miesch, M., Schneider, B., Leiss, K., & Werck-Reichhart, D. (2015). CYP76C1 (Cytochrome P450)-Mediated Linalool Metabolism and the Formation of Volatile and Soluble Linalool Oxides in Arabidopsis Flowers: A Strategy for Defense against Floral Antagonists[OPEN]. *The Plant Cell*, *27*(10), 2972–2990. https://doi.org/10.1105/tpc.15.00399

Boachon, B., Lynch, J. H., Ray, S., Yuan, J., Caldo, K. M. P., Junker, R. R., Kessler, S. A., Morgan, J. A., & Dudareva, N. (2019). Natural fumigation as a mechanism for volatile transport between flower organs. *Nature Chemical Biology*, *15*(6), 583–588. https://doi.org/10.1038/s41589-019-0287-5

Boisson-Dernier, A., Chabaud, M., Garcia, F., Bécard, G., Rosenberg, C., & Barker, D. G. (2001). Agrobacterium rhizogenes-transformed roots of Medicago truncatula for the study of nitrogen-fixing and endomycorrhizal symbiotic associations. *Molecular Plant-Microbe Interactions: MPMI*, *14*(6), 695–700. https://doi.org/10.1094/MPMI.2001.14.6.695

Boland, W., & Garms, S. (2010). Induced volatiles of Medicago truncatula: Molecular diversity and mechanistic aspects of a multiproduct sesquiterpene synthase from M.

truncatula. *Flavour and Fragrance Journal*, *25*, 114–116. https://doi.org/10.1002/ffj.1979

Boller, T., & Felix, G. (2009). A renaissance of elicitors: Perception of microbe-associated molecular patterns and danger signals by pattern-recognition receptors. *Annual Review of Plant Biology*, *60*, 379–406. https://doi.org/10.1146/annurev.arplant.57.032905.105346

Boncan, D. A. T., Tsang, S. S. K., Li, C., Lee, I. H. T., Lam, H.-M., Chan, T.-F., & Hui, J. H. L. (2020). Terpenes and Terpenoids in Plants: Interactions with Environment and Insects. *International Journal of Molecular Sciences*, *21*(19), 7382. https://doi.org/10.3390/ijms21197382

Bonhomme, M., André, O., Badis, Y., Ronfort, J., Burgarella, C., Chantret, N., Prosperi, J.-M., Briskine, R., Mudge, J., Debéllé, F., Navier, H., Miteul, H., Hajri, A., Baranger, A., Tiffin, P., Dumas, B., Pilet-Nayel, M.-L., Young, N. D., & Jacquet, C. (2014). High-density genome-wide association mapping implicates an F-box encoding gene in Medicago truncatula resistance to Aphanomyces euteiches. *The New Phytologist*, *201*(4), 1328–1342. https://doi.org/10.1111/nph.12611

Booth, J. K., Yuen, M. M. S., Jancsik, S., Madilao, L. L., Page, J. E., & Bohlmann, J. (2020). Terpene Synthases and Terpene Variation in Cannabis sativa1[OPEN]. *Plant Physiology*, *184*(1), 130–147. https://doi.org/10.1104/pp.20.00593

Bos, R., Koulman, A., Woerdenbag, H. J., Quax, W. J., & Pras, N. (2002). Volatile components from Anthriscus sylvestris (L.) Hoffm. *Journal of Chromatography A*, *966*(1), 233–238. https://doi.org/10.1016/S0021-9673(02)00704-5

Bostock, R. M., Pye, M. F., & Roubtsova, T. V. (2014). Predisposition in Plant Disease: Exploiting the Nexus in Abiotic and Biotic Stress Perception and Response. *Annual Review of Phytopathology*, *52*(Volume 52, 2014), 517–549. https://doi.org/10.1146/annurev-phyto-081211-172902

Bozsoki, Z., Cheng, J., Feng, F., Gysel, K., Vinther, M., Andersen, K. R., Oldroyd, G., Blaise, M., Radutoiu, S., & Stougaard, J. (2017). Receptor-mediated chitin perception in legume roots is functionally separable from Nod factor perception. *Proceedings of the National Academy of Sciences of the United States of America*, *114*(38), E8118–E8127. https://doi.org/10.1073/pnas.1706795114

Brock, N. L., Ravella, S. R., Schulz, S., & Dickschat, J. S. (2013). A detailed view of 2-methylisoborneol biosynthesis. *Angewandte Chemie (International Ed. in English)*, *52*(7), 2100–2104. https://doi.org/10.1002/anie.201209173

Brunner, F., Rosahl, S., Lee, J., Rudd, J. J., Geiler, C., Kauppinen, S., Rasmussen, G., Scheel, D., & Nürnberger, T. (2002). Pep-13, a plant defense-inducing pathogen-

associated pattern from Phytophthora transglutaminases. *The EMBO Journal*, *21*(24), 6681–6688. https://doi.org/10.1093/emboj/cdf667

Camborde, L. (2020). *Functional characterization of different candidate effectors from the root rot oomycete Aphanomyces euteiches* [Phdthesis, Université Paul Sabatier - Toulouse III]. https://theses.hal.science/tel-03208760

Carelli, M., Biazzi, E., Panara, F., Tava, A., Scaramelli, L., Porceddu, A., Graham, N., Odoardi, M., Piano, E., Arcioni, S., May, S., Scotti, C., & Calderini, O. (2011). Medicago truncatula CYP716A12 is a multifunctional oxidase involved in the biosynthesis of hemolytic saponins. *The Plant Cell*, *23*(8), 3070–3081. https://doi.org/10.1105/tpc.111.087312

Cascone, P., Iodice, L., Maffei, M. E., Bossi, S., Arimura, G.-I., & Guerrieri, E. (2015). Tobacco overexpressing β-ocimene induces direct and indirect responses against aphids in receiver tomato plants. *Journal of Plant Physiology*, *173*, 28–32. https://doi.org/10.1016/j.jplph.2014.08.011

Chae, L., Kim, T., Nilo-Poyanco, R., & Rhee, S. Y. (2014). Genomic signatures of specialized metabolism in plants. *Science (New York, N.Y.)*, *344*(6183), 510–513. https://doi.org/10.1126/science.1252076

Chang, J. H., Urbach, J. M., Law, T. F., Arnold, L. W., Hu, A., Gombar, S., Grant, S. R., Ausubel, F. M., & Dangl, J. L. (2005). A high-throughput, near-saturating screen for type III effector genes from Pseudomonas syringae. *Proceedings of the National Academy of Sciences of the United States of America*, *102*(7), 2549–2554. https://doi.org/10.1073/pnas.0409660102

Charkowski, A., Sharma, K., Parker, M. L., Secor, G. A., & Elphinstone, J. (2020). Bacterial diseases of potato. *The Potato Crop: Its Agricultural, Nutritional and Social Contribution to Humankind*, 351–388.

Chen, D., Ye, H., & Li, G. (2000). Expression of a chimeric farnesyl diphosphate synthase gene in Artemisia annua L. transgenic plants via Agrobacterium tumefaciens-mediated transformation. *Plant Science: An International Journal of Experimental Plant Biology*, *155*(2), 179–185. https://doi.org/10.1016/s0168-9452(00)00217-x

Chen, F., Ro, D.-K., Petri, J., Gershenzon, J., Bohlmann, J., Pichersky, E., & Tholl, D. (2004). Characterization of a Root-Specific Arabidopsis Terpene Synthase Responsible for the Formation of the Volatile Monoterpene 1,8-Cineole. *Plant Physiology*, *135*(4), 1956–1966. https://doi.org/10.1104/pp.104.044388

Chen, F., Tholl, D., Bohlmann, J., & Pichersky, E. (2011). The family of terpene synthases in plants: A mid-size family of genes for specialized metabolism that is highly diversified throughout the kingdom. *The Plant Journal: For Cell and Molecular Biology*, *66*(1), 212–229. https://doi.org/10.1111/j.1365-313X.2011.04520.x

Chen, F., Tholl, D., D'Auria, J. C., Farooq, A., Pichersky, E., & Gershenzon, J. (2003). Biosynthesis and emission of terpenoid volatiles from Arabidopsis flowers. *The Plant Cell*, *15*(2), 481–494. https://doi.org/10.1105/tpc.007989

Chinchilla, D., Zipfel, C., Robatzek, S., Kemmerling, B., Nürnberger, T., Jones, J. D. G., Felix, G., & Boller, T. (2007). A flagellin-induced complex of the receptor FLS2 and BAK1 initiates plant defence. *Nature*, *448*(7152), 497–500. https://doi.org/10.1038/nature05999

Chisholm, S. T., Coaker, G., Day, B., & Staskawicz, B. J. (2006). Host-Microbe Interactions: Shaping the Evolution of the Plant Immune Response. *Cell*, *124*(4), 803–814. https://doi.org/10.1016/j.cell.2006.02.008

Christianson, D. W. (2006). Structural Biology and Chemistry of the Terpenoid Cyclases. *Chemical Reviews*, *106*(8), 3412–3442. https://doi.org/10.1021/cr050286w

Christianson, D. W. (2017). Structural and Chemical Biology of Terpenoid Cyclases. *Chemical Reviews*, *117*(17), 11570–11648. https://doi.org/10.1021/acs.chemrev.7b00287

Colditz, F., Nyamsuren, O., Niehaus, K., Eubel, H., Braun, H.-P., & Krajinski, F. (2004). Proteomic approach: Identification of Medicago truncatula proteins induced in roots after infection with the pathogenic oomycete Aphanomyces euteiches. *Plant Molecular Biology*, *55*(1), 109–120. https://doi.org/10.1007/s11103-004-0499-1

Cook, D. R. (1999). *Medicago truncatula*—A model in the making! *Current Opinion in Plant Biology*, *2*(4), 301–304. https://doi.org/10.1016/S1369-5266(99)80053-3

Cooke, D. E. L., Drenth, A., Duncan, J. M., Wagels, G., & Brasier, C. M. (2000). A Molecular Phylogeny of *Phytophthora* and Related Oomycetes. *Fungal Genetics and Biology*, *30*(1), 17–32. https://doi.org/10.1006/fgbi.2000.1202

Coomber, A., Saville, A., & Ristaino, J. B. (2024). Evolution of Phytophthora infestans on its potato host since the Irish potato famine. *Nature Communications*, *15*(1), 6488. https://doi.org/10.1038/s41467-024-50749-4

Dangl, J. L., & Jones, J. D. (2001). Plant pathogens and integrated defence responses to infection. *Nature*, *411*(6839), 826–833. https://doi.org/10.1038/35081161

Degen, T., Dillmann, C., Marion-Poll, F., & Turlings, T. C. J. (2004). High genetic variability of herbivore-induced volatile emission within a broad range of maize inbred lines. *Plant Physiology*, *135*(4), 1928–1938. https://doi.org/10.1104/pp.104.039891

Degenhardt, J., & Gershenzon, J. (2000). Demonstration and characterization of (E)-nerolidol synthase from maize: A herbivore-inducible terpene synthase participating in (3E)-4,8-dimethyl-1,3,7-nonatriene biosynthesis. *Planta*, *210*(5), 815–822. https://doi.org/10.1007/s004250050684

Degenhardt, J., Hiltpold, I., Köllner, T. G., Frey, M., Gierl, A., Gershenzon, J., Hibbard, B. E., Ellersieck, M. R., & Turlings, T. C. J. (2009). Restoring a maize root signal that attracts insect-killing nematodes to control a major pest. *Proceedings of the National Academy of Sciences of the United States of America*, *106*(32), 13213–13218. https://doi.org/10.1073/pnas.0906365106

Dick, M. W., Vick, M. C., Gibbings, J. G., Hedderson, T. A., & Lopez Lastra, C. C. (1999). 18S rDNA for species of Leptolegnia and other Peronosporomycetes: Justification for the subclass taxa Saprolegniomycetidae and Peronosporomycetidae and division of the Saprolegniaceae sensu lato into the Leptolegniaceae and Saprolegniaceae. *Mycological Research*, *103*(9), 1119–1125. https://doi.org/10.1017/S0953756299008643

Djébali, N., Jauneau, A., Ameline-Torregrosa, C., Chardon, F., Jaulneau, V., Mathé, C., Bottin, A., Cazaux, M., Pilet-Nayel, M.-L., Baranger, A., Aouani, M. E., Esquerré-Tugayé, M.-T., Dumas, B., Huguet, T., & Jacquet, C. (2009). Partial resistance of Medicago truncatula to Aphanomyces euteiches is associated with protection of the root stele and is controlled by a major QTL rich in proteasome-related genes. *Molecular Plant-Microbe Interactions: MPMI*, *22*(9), 1043–1055. https://doi.org/10.1094/MPMI-22-9-1043

Dodds, P. N., Chen, J., & Outram, M. A. (2024a). Pathogen perception and signaling in plant immunity. *The Plant Cell*, koae020. https://doi.org/10.1093/plcell/koae020

immunity. *The Plant Cell*, *36*(5), 1465–1481. https://doi.org/10.1093/plcell/koae020

Dreher, D., Yadav, H., Zander, S., & Hause, B. (2017). Is there genetic variation in mycorrhization of Medicago truncatula? *PeerJ*, *5*, e3713. https://doi.org/10.7717/peerj.3713

Driller, R., Janke, S., Fuchs, M., Warner, E., Mhashal, A. R., Major, D. T., Christmann, M., Brück, T., & Loll, B. (2018). Towards a comprehensive understanding of the structural dynamics of a bacterial diterpene synthase during catalysis. *Nature Communications*, *9*(1), 3971. https://doi.org/10.1038/s41467-018-06325-8

Dudareva, N., Negre, F., Nagegowda, D. A., & Orlova, I. (2006). Plant Volatiles: Recent Advances and Future Perspectives. *Critical Reviews in Plant Sciences*, *25*(5), 417–440. https://doi.org/10.1080/07352680600899973

Dudareva, N., & Pichersky, E. (2000). Biochemical and Molecular Genetic Aspects of Floral Scents1. *Plant Physiology*, *122*(3), 627–634. https://doi.org/10.1104/pp.122.3.627

Dudareva, N., Pichersky, E., & Gershenzon, J. (2004). Biochemistry of plant volatiles. *Plant Physiology*, *135*(4), 1893–1902. https://doi.org/10.1104/pp.104.049981

Engler, C., Kandzia, R., & Marillonnet, S. (2008). A one pot, one step, precision cloning method with high throughput capability. *PloS One*, *3*(11), e3647. https://doi.org/10.1371/journal.pone.0003647

Eschen-Lippold, L., Rothe, G., Stumpe, M., Göbel, C., Feussner, I., & Rosahl, S. (2007). Reduction of divinyl ether-containing polyunsaturated fatty acids in transgenic potato plants. *Phytochemistry*, *68*(6), 797–801. https://doi.org/10.1016/j.phytochem.2006.12.010

Fellbrich, G., Romanski, A., Varet, A., Blume, B., Brunner, F., Engelhardt, S., Felix, G., Kemmerling, B., Krzymowska, M., & Nürnberger, T. (2002). NPP1, a Phytophthora-associated trigger of plant defense in parsley and Arabidopsis. *The Plant Journal: For Cell and Molecular Biology*, *32*(3), 375–390. https://doi.org/10.1046/j.1365-313x.2002.01454.x

Fewell, A. M., & Roddick, J. G. (1993). Interactive antifungal activity of the glycoalkaloids α-solanine and α-chaconine. *Phytochemistry*, *33*(2), 323–328. https://doi.org/10.1016/0031-9422(93)85511-O

Finn, R. D., Coggill, P., Eberhardt, R. Y., Eddy, S. R., Mistry, J., Mitchell, A. L., Potter, S. C., Punta, M., Qureshi, M., Sangrador-Vegas, A., Salazar, G. A., Tate, J., & Bateman, A. (2016). The Pfam protein families database: Towards a more sustainable future. *Nucleic Acids Research*, *44*(D1), D279-285. https://doi.org/10.1093/nar/gkv1344

Fisher, M. C., Henk, D. A., Briggs, C. J., Brownstein, J. S., Madoff, L. C., McCraw, S. L., & Gurr, S. J. (2012). Emerging fungal threats to animal, plant and ecosystem health. *Nature*, *484*(7393), 186–194. https://doi.org/10.1038/nature10947

Fones, H. N., Bebber, D. P., Chaloner, T. M., Kay, W. T., Steinberg, G., & Gurr, S. J. (2020). Threats to global food security from emerging fungal and oomycete crop pathogens. *Nature Food*, *1*(6), 332–342. https://doi.org/10.1038/s43016-020-0075-0

Freeman. (2008). An Overview of Plant Defenses against Pathogens and Herbivores. *The Plant Health Instructor*. https://doi.org/10.1094/PHI-I-2008-0226-01

Frey, M., Bathe, U., Meink, L., Balcke, G. U., Schmidt, J., Frolov, A., Soboleva, A., Hassanin, A., Davari, M. D., Frank, O., Schlagbauer, V., Dawid, C., & Tissier, A. (2024). Combinatorial biosynthesis in yeast leads to over 200 diterpenoids. *Metabolic Engineering*, *82*, 193–200. https://doi.org/10.1016/j.ymben.2024.02.006

Fry, W. E. (2016). Phytophthora infestans: New Tools (and Old Ones) Lead to New Understanding and Precision Management. *Annual Review of Phytopathology*, *54*, 529–547. https://doi.org/10.1146/annurev-phyto-080615-095951

Fry, W. E., Birch, P. R. J., Judelson, H. S., Grünwald, N. J., Danies, G., Everts, K. L., Gevens, A. J., Gugino, B. K., Johnson, D. A., Johnson, S. B., McGrath, M. T., Myers, K. L., Ristaino, J. B., Roberts, P. D., Secor, G., & Smart, C. D. (2015). Five Reasons

to Consider Phytophthora infestans a Reemerging Pathogen. *Phytopathology*, *105*(7), 966–981. https://doi.org/10.1094/PHYTO-01-15-0005-FI

Fu, C., Hernandez, T., Zhou, C., & Wang, Z.-Y. (2015). Alfalfa (Medicago sativa L.). *Methods in Molecular Biology (Clifton, N.J.)*, *1223*, 213–221. https://doi.org/10.1007/978-1-4939-1695-5_17

Gamir, J., Darwiche, R., Van't Hof, P., Choudhary, V., Stumpe, M., Schneiter, R., & Mauch, F. (2017). The sterol-binding activity of PATHOGENESIS-RELATED PROTEIN 1 reveals the mode of action of an antimicrobial protein. *The Plant Journal: For Cell and Molecular Biology*, *89*(3), 502–509. https://doi.org/10.1111/tpj.13398

Garmier, M., Gentzbittel, L., Wen, J., Mysore, K. S., & Ratet, P. (2017). Medicago truncatula: Genetic and Genomic Resources. *Current Protocols in Plant Biology*, *2*(4), 318–349. https://doi.org/10.1002/cppb.20058

Garms, S., Köllner, T. G., & Boland, W. (2010). A multiproduct terpene synthase from Medicago truncatula generates cadalane sesquiterpenes via two different mechanisms. *The Journal of Organic Chemistry*, *75*(16), 5590–5600. https://doi.org/10.1021/jo100917c

Gaulin, E., Dramé, N., Lafitte, C., Torto-Alalibo, T., Martinez, Y., Ameline-Torregrosa, C., Khatib, M., Mazarguil, H., Villalba-Mateos, F., Kamoun, S., Mazars, C., Dumas, B., Bottin, A., Esquerré-Tugayé, M.-T., & Rickauer, M. (2006). Cellulose binding domains of a Phytophthora cell wall protein are novel pathogen-associated molecular patterns. *The Plant Cell*, *18*(7), 1766–1777. https://doi.org/10.1105/tpc.105.038687

Gaulin, E., Jacquet, C., Bottin, A., & Dumas, B. (2007). Root rot disease of legumes caused by Aphanomyces euteiches. *Molecular Plant Pathology*, *8*(5), 539–548. https://doi.org/10.1111/j.1364-3703.2007.00413.x

Ge, S. X., Son, E. W., & Yao, R. (2018). iDEP: An integrated web application for differential expression and pathway analysis of RNA-Seq data. *BMC Bioinformatics*, *19*(1), 534. https://doi.org/10.1186/s12859-018-2486-6

Gebhardt, C., & Valkonen, J. P. (2001). Organization of genes controlling disease resistance in the potato genome. *Annual Review of Phytopathology*, *39*, 79–102. https://doi.org/10.1146/annurev.phyto.39.1.79

Geisler, K., Hughes, R. K., Sainsbury, F., Lomonossoff, G. P., Rejzek, M., Fairhurst, S., Olsen, C.-E., Motawia, M. S., Melton, R. E., Hemmings, A. M., Bak, S., & Osbourn, A. (2013). Biochemical analysis of a multifunctional cytochrome P450 (CYP51) enzyme required for synthesis of antimicrobial triterpenes in plants. *Proceedings of the National Academy of Sciences of the United States of America*, *110*(35), E3360-3367. https://doi.org/10.1073/pnas.1309157110

Gershenzon, J., & Dudareva, N. (2007). The function of terpene natural products in the natural world. *Nature Chemical Biology*, *3*(7), 408–414. https://doi.org/10.1038/nchembio.2007.5

Gomez, S. K., Cox, M. M., Bede, J. C., Inoue, K., Alborn, H. T., Tumlinson, J. H., & Korth, K. L. (2005). Lepidopteran herbivory and oral factors induce transcripts encoding novel terpene synthases in Medicago truncatula. *Archives of Insect Biochemistry and Physiology*, *58*(2), 114–127. https://doi.org/10.1002/arch.20037

Gómez-Gómez, L., & Boller, T. (2000). FLS2: An LRR Receptor–like Kinase Involved in the Perception of the Bacterial Elicitor Flagellin in Arabidopsis. *Molecular Cell*, *5*(6), 1003–1011. https://doi.org/10.1016/S1097-2765(00)80265-8

Goossens, J., De Geyter, N., Walton, A., Eeckhout, D., Mertens, J., Pollier, J., Fiallos-Jurado, J., De Keyser, A., De Clercq, R., Van Leene, J., Gevaert, K., De Jaeger, G., Goormachtig, S., & Goossens, A. (2016). Isolation of protein complexes from the model legume Medicago truncatula by tandem affinity purification in hairy root cultures. *The Plant Journal: For Cell and Molecular Biology*, *88*(3), 476–489. https://doi.org/10.1111/tpj.13258

Gorzolka, K., Perino, E. H. B., Lederer, S., Smolka, U., & Rosahl, S. (2021a). Lysophosphatidylcholine 17:1 from the Leaf Surface of the Wild Potato Species Solanum bulbocastanum Inhibits Phytophthora infestans. *Journal of Agricultural and Food Chemistry*, *69*(20), 5607–5617. https://doi.org/10.1021/acs.jafc.0c07199

Gorzolka, K., Perino, E. H. B., Lederer, S., Smolka, U., & Rosahl, S. (2021b). Lysophosphatidylcholine 17:1 from the Leaf Surface of the Wild Potato Species Solanum bulbocastanum Inhibits Phytophthora infestans. *Journal of Agricultural and Food Chemistry*, *69*(20), 5607–5617. https://doi.org/10.1021/acs.jafc.0c07199

Graham, P. H., & Vance, C. P. (2003). Legumes: Importance and Constraints to Greater Use. *Plant Physiology*, *131*(3), 872–877. https://doi.org/10.1104/pp.017004

Griffith, J. M., Davis, A. J., & Grant, B. R. (1992). Target Sites of Fungicides to Control Oomycetes. In *Target Sites of Fungicide Action*. CRC Press.

Gruner, K., Esser, T., Acevedo-Garcia, J., Freh, M., Habig, M., Strugala, R., Stukenbrock, E., Schaffrath, U., & Panstruga, R. (2020). Evidence for Allele-Specific Levels of Enhanced Susceptibility of Wheat mlo Mutants to the Hemibiotrophic Fungal Pathogen Magnaporthe oryzae pv. Triticum. *Genes*, *11*(5), Article 5. https://doi.org/10.3390/genes11050517

Guo, J., Ma, X., Cai, Y., Ma, Y., Zhan, Z., Zhou, Y. J., Liu, W., Guan, M., Yang, J., Cui, G., Kang, L., Yang, L., Shen, Y., Tang, J., Lin, H., Ma, X., Jin, B., Liu, Z., Peters, R. J., … Huang, L. (2016). Cytochrome P450 promiscuity leads to a bifurcating biosynthetic

pathway for tanshinones. *The New Phytologist*, *210*(2), 525–534. https://doi.org/10.1111/nph.13790

Gust, A. A., Willmann, R., Desaki, Y., Grabherr, H. M., & Nürnberger, T. (2012). Plant LysM proteins: Modules mediating symbiosis and immunity. *Trends in Plant Science*, *17*(8), 495–502. https://doi.org/10.1016/j.tplants.2012.04.003

Hacquard, S., Spaepen, S., Garrido-Oter, R., & Schulze-Lefert, P. (2017). Interplay Between Innate Immunity and the Plant Microbiota. *Annual Review of Phytopathology*, *55*(Volume 55, 2017), 565–589. https://doi.org/10.1146/annurev-phyto-080516-035623

Hamberger, B., & Bak, S. (2013). Plant P450s as versatile drivers for evolution of species-specific chemical diversity. *Philosophical Transactions of the Royal Society of London. Series B, Biological Sciences*, *368*(1612), 20120426. https://doi.org/10.1098/rstb.2012.0426

Haq, I. U., Khan, N. A., & Sarwar, M. K. (2022). Predictive Models for Plant Disease Assessment. In I. Ul Haq & S. Ijaz (Eds.), *Trends in Plant Disease Assessment* (pp. 225–239). Springer Nature. https://doi.org/10.1007/978-981-19-5896-0_12

Hassanali, A., Herren, H., Khan, Z. R., Pickett, J. A., & Woodcock, C. M. (2008). Integrated pest management: The push-pull approach for controlling insect pests and weeds of cereals, and its potential for other agricultural systems including animal husbandry. *Philosophical Transactions of the Royal Society of London. Series B, Biological Sciences*, *363*(1491), 611–621. https://doi.org/10.1098/rstb.2007.2173

Hause, B., & Fester, T. (2005). Molecular and cell biology of arbuscular mycorrhizal symbiosis. *Planta*, *221*(2), 184–196. https://doi.org/10.1007/s00425-004-1436-x

Haverkort, A. J., Boonekamp, P. M., Hutten, R. C. B., Jacobsen, E., Lotz, L. a. P., Kessel, G. J. T., Visser, R. G. F., & Vossen, E. A. G. van der. (2008). Societal Costs of Late Blight in Potato and Prospects of Durable Resistance Through Cisgenic Modification. *Potato Research*, *51*(1), 47–57. https://doi.org/10.1007/s11540-008-9089-y

Heese, A., Hann, D. R., Gimenez-Ibanez, S., Jones, A. M. E., He, K., Li, J., Schroeder, J. I., Peck, S. C., & Rathjen, J. P. (2007). The receptor-like kinase SERK3/BAK1 is a central regulator of innate immunity in plants. *Proceedings of the National Academy of Sciences of the United States of America*, *104*(29), 12217–12222. https://doi.org/10.1073/pnas.0705306104

Hendrickson, H., Islam, M., Wabo, G. F., & Mafu, S. (2024). Biochemical analysis of the TPS-a subfamily in Medicago truncatula. *Frontiers in Plant Science*, *15*. https://doi.org/10.3389/fpls.2024.1349009

Herde, M., Gärtner, K., Köllner, T. G., Fode, B., Boland, W., Gershenzon, J., Gatz, C., & Tholl, D. (2008). Identification and regulation of TPS04/GES, an Arabidopsis

geranyllinalool synthase catalyzing the first step in the formation of the insect-induced volatile C16-homoterpene TMTT. *The Plant Cell*, *20*(4), 1152–1168. https://doi.org/10.1105/tpc.106.049478

Höfgen, R., & Willmitzer, L. (1988). Storage of competent cells for Agrobacterium transformation. *Nucleic Acids Research*, *16*(20), 9877. https://doi.org/10.1093/nar/16.20.9877

Holopainen, J. K., & Gershenzon, J. (2010). Multiple stress factors and the emission of plant VOCs. *Trends in Plant Science*, *15*(3), 176–184. https://doi.org/10.1016/j.tplants.2010.01.006

Hossain, Z., Zhao, S., Luo, X., Liu, K., Li, L., & Hubbard, M. (2024). Deciphering Aphanomyces euteiches-pea-biocontrol bacterium interactions through untargeted metabolomics. *Scientific Reports*, *14*(1), 8877. https://doi.org/10.1038/s41598-024-52949-w

Huang, A. C., & Osbourn, A. (2019). Plant terpenes that mediate below-ground interactions: Prospects for bioengineering terpenoids for plant protection. *Pest Management Science*, *75*(9), 2368–2377. https://doi.org/10.1002/ps.5410

Huang, M., Abel, C., Sohrabi, R., Petri, J., Haupt, I., Cosimano, J., Gershenzon, J., & Tholl, D. (2010). Variation of herbivore-induced volatile terpenes among Arabidopsis ecotypes depends on allelic differences and subcellular targeting of two terpene synthases, TPS02 and TPS03. *Plant Physiology*, *153*(3), 1293–1310. https://doi.org/10.1104/pp.110.154864

Hughes, T., & Grau, C. (2007). Aphanomyces root rot or common root rot of legumes. *The Plant Health Instructor*. https://doi.org/10.1094/PHI-I-2007-0418-01

Iqbal, Z., Iqbal, M. S., Hashem, A., Abd_Allah, E. F., & Ansari, M. I. (2021). Plant Defense Responses to Biotic Stress and Its Interplay With Fluctuating Dark/Light Conditions. *Frontiers in Plant Science*, *12*. https://doi.org/10.3389/fpls.2021.631810

Ivanov, A. A., Ukladov, E. O., & Golubeva, T. S. (2021). Phytophthora infestans: An Overview of Methods and Attempts to Combat Late Blight. *Journal of Fungi*, *7*(12), 1071. https://doi.org/10.3390/jof7121071

Jansky, S. H., Charkowski, A. O., Douches, D. S., Gusmini, G., Richael, C., Bethke, P. C., Spooner, D. M., Novy, R. G., De Jong, H., De Jong, W. S., Bamberg, J. B., Thompson, A. L., Bizimungu, B., Holm, D. G., Brown, C. R., Haynes, K. G., Sathuvalli, V. R., Veilleux, R. E., Miller Jr., J. C., … Jiang, J. (2016). Reinventing Potato as a Diploid Inbred Line–Based Crop. *Crop Science*, *56*(4), 1412–1422. https://doi.org/10.2135/cropsci2015.12.0740

Jia, Q., & Chen, F. (2016). Catalytic Functions of the Isoprenyl Diphosphate Synthase Superfamily in Plants: A Growing Repertoire. *Molecular Plant*, *9*(2), 189–191. https://doi.org/10.1016/j.molp.2015.12.020

Jones, J. D. G., & Dangl, J. L. (2006). The plant immune system. *Nature*, *444*(7117), Article 7117. https://doi.org/10.1038/nature05286

Jones, J. D. G., Staskawicz, B. J., & Dangl, J. L. (2024). The plant immune system: From discovery to deployment. *Cell*, *187*(9), 2095–2116. https://doi.org/10.1016/j.cell.2024.03.045

Judelson, H. S. (2017). Metabolic Diversity and Novelties in the Oomycetes. *Annual Review of Microbiology*, *71*, 21–39. https://doi.org/10.1146/annurev-micro-090816-093609

Judelson, H. S., & Blanco, F. A. (2005). The spores of Phytophthora: Weapons of the plant destroyer. *Nature Reviews. Microbiology*, *3*(1), 47–58. https://doi.org/10.1038/nrmicro1064

Kaku, H., Nishizawa, Y., Ishii-Minami, N., Akimoto-Tomiyama, C., Dohmae, N., Takio, K., Minami, E., & Shibuya, N. (2006). Plant cells recognize chitin fragments for defense signaling through a plasma membrane receptor. *Proceedings of the National Academy of Sciences*, *103*(29), 11086–11091. https://doi.org/10.1073/pnas.0508882103

Kamoun, S. (2001). Nonhost resistance to Phytophthora: Novel prospects for a classical problem. *Current Opinion in Plant Biology*, *4*(4), 295–300. https://doi.org/10.1016/s1369-5266(00)00176-x

Kamoun, S., Furzer, O., Jones, J. D. G., Judelson, H. S., Ali, G. S., Dalio, R. J. D., Roy, S. G., Schena, L., Zambounis, A., Panabières, F., Cahill, D., Ruocco, M., Figueiredo, A., Chen, X.-R., Hulvey, J., Stam, R., Lamour, K., Gijzen, M., Tyler, B. M., … Govers, F. (2015). The Top 10 oomycete pathogens in molecular plant pathology. *Molecular Plant Pathology*, *16*(4), 413–434. https://doi.org/10.1111/mpp.12190

Kappers, I. F., Aharoni, A., van Herpen, T. W. J. M., Luckerhoff, L. L. P., Dicke, M., & Bouwmeester, H. J. (2005). Genetic engineering of terpenoid metabolism attracts bodyguards to Arabidopsis. *Science (New York, N.Y.)*, *309*(5743), 2070–2072. https://doi.org/10.1126/science.1116232

Karunanithi, P. S., & Zerbe, P. (2019). Terpene Synthases as Metabolic Gatekeepers in the Evolution of Plant Terpenoid Chemical Diversity. *Frontiers in Plant Science*, *10*, 1166. https://doi.org/10.3389/fpls.2019.01166

Keeling, C. I., & Bohlmann, J. (2006). Diterpene resin acids in conifers. *Phytochemistry*, *67*(22), 2415–2423. https://doi.org/10.1016/j.phytochem.2006.08.019

pathogens. *The New Phytologist*, *170*(4), 657–675. https://doi.org/10.1111/j.1469-8137.2006.01716.x

Kelly, S., Radutoiu, S., & Stougaard, J. (2017). Legume LysM receptors mediate symbiotic and pathogenic signalling. *Current Opinion in Plant Biology*, *39*, 152–158. https://doi.org/10.1016/j.pbi.2017.06.013

Kieu, N. P., Lenman, M., Wang, E. S., Petersen, B. L., & Andreasson, E. (2021). Mutations introduced in susceptibility genes through CRISPR/Cas9 genome editing confer increased late blight resistance in potatoes. *Scientific Reports*, *11*(1), 4487. https://doi.org/10.1038/s41598-021-83972-w

Kigathi, R. N., Weisser, W. W., Reichelt, M., Gershenzon, J., & Unsicker, S. B. (2019). Plant volatile emission depends on the species composition of the neighboring plant community. *BMC Plant Biology*, *19*(1), 58. https://doi.org/10.1186/s12870-018-1541-9

Kilian, J., Peschke, F., Berendzen, K. W., Harter, K., & Wanke, D. (2012). Prerequisites, performance and profits of transcriptional profiling the abiotic stress response. *Biochimica Et Biophysica Acta*, *1819*(2), 166–175. https://doi.org/10.1016/j.bbagrm.2011.09.005

Kim, D. S., & Hwang, B. K. (2012). The pepper MLO gene, CaMLO2, is involved in the susceptibility cell-death response and bacterial and oomycete proliferation. *The Plant Journal: For Cell and Molecular Biology*, *72*(5), 843–855. https://doi.org/10.1111/tpj.12003

Kliebenstein, D. J. (2014). Orchestration of plant defense systems: Genes to populations. *Trends in Plant Science*, *19*(4), 250–255. https://doi.org/10.1016/j.tplants.2014.01.003

Köllner, T. G., Schnee, C., Gershenzon, J., & Degenhardt, J. (2004). The Variability of Sesquiterpenes Emitted from Two Zea mays Cultivars Is Controlled by Allelic Variation of Two Terpene Synthase Genes Encoding Stereoselective Multiple Product Enzymes. *The Plant Cell*, *16*(5), 1115–1131. https://doi.org/10.1105/tpc.019877

Kovacevic, N., Pavlovic, M., Menkovic, N., Tzakou, O., & Couladis, M. (2002). Composition of the essential oil from roots and rhizomes of Valeriana pancicii Halácsy & Bald. *Flavour and Fragrance Journal*, *17*(5), 355–357. https://doi.org/10.1002/ffj.1100

Kumar, S., & Rzhetsky, A. (1996). Evolutionary relationships of eukaryotic kingdoms. *Journal of Molecular Evolution*, *42*(2), 183–193. https://doi.org/10.1007/BF02198844

Kumar, S., Stecher, G., Li, M., Knyaz, C., & Tamura, K. (2018). MEGA X: Molecular Evolutionary Genetics Analysis across Computing Platforms. *Molecular Biology and Evolution*, *35*(6), 1547–1549. https://doi.org/10.1093/molbev/msy096

Kunze, G., Zipfel, C., Robatzek, S., Niehaus, K., Boller, T., & Felix, G. (2004). The N terminus of bacterial elongation factor Tu elicits innate immunity in Arabidopsis plants. *The Plant Cell*, *16*(12), 3496–3507. https://doi.org/10.1105/tpc.104.026765

Kurdyukov, S., Mathesius, U., Nolan, K. E., Sheahan, M. B., Goffard, N., Carroll, B. J., & Rose, R. J. (2014). The 2HA line of Medicago truncatulahas characteristics of an epigenetic mutant that is weakly ethylene insensitive. *BMC Plant Biology*, *14*(1), 174. https://doi.org/10.1186/1471-2229-14-174

Kusch, S., & Panstruga, R. (2017). mlo-Based Resistance: An Apparently Universal 'Weapon' to Defeat Powdery Mildew Disease. *Molecular Plant-Microbe Interactions: MPMI*, *30*(3), 179–189. https://doi.org/10.1094/MPMI-12-16-0255-CR

Küster, H. (2013). Medicago truncatula. In S. Maloy & K. Hughes (Eds.), *Brenner's Encyclopedia of Genetics (Second Edition)* (pp. 335–337). Academic Press. https://doi.org/10.1016/B978-0-12-374984-0.00915-3

Lacombe, S., Rougon-Cardoso, A., Sherwood, E., Peeters, N., Dahlbeck, D., van Esse, H. P., Smoker, M., Rallapalli, G., Thomma, B. P. H. J., Staskawicz, B., Jones, J. D. G., & Zipfel, C. (2010). Interfamily transfer of a plant pattern-recognition receptor confers broad-spectrum bacterial resistance. *Nature Biotechnology*, *28*(4), 365–369. https://doi.org/10.1038/nbt.1613

Latijnhouwers, M., Wit, P. J. G. M. de, & Govers, F. (2003). Oomycetes and fungi: Similar weaponry to attack plants. *Trends in Microbiology*, *11*(10), 462–469. https://doi.org/10.1016/j.tim.2003.08.002

Laursen, T., Lam, H. Y. M., Sørensen, K. K., Tian, P., Hansen, C. C., Groves, J. T., Jensen, K. J., & Christensen, S. M. (2021). Membrane anchoring facilitates colocalization of enzymes in plant cytochrome P450 redox systems. *Communications Biology*, *4*(1), 1–9. https://doi.org/10.1038/s42003-021-02604-1

Lavy, M., Zuker, A., Lewinsohn, E., Larkov, O., Ravid, U., Vainstein, A., & Weiss, D. (2002). Linalool and linalool oxide production in transgenic carnation flowers expressing the Clarkia breweri linalool synthase gene. *Molecular Breeding*, *9*(2), 103–111. https://doi.org/10.1023/A:1026755414773

Leclerc, M. C., Guillot, J., & Deville, M. (2000). Taxonomic and phylogenetic analysis of Saprolegniaceae (Oomycetes) inferred from LSU rDNA and ITS sequence comparisons. *Antonie van Leeuwenhoek*, *77*(4), 369–377. https://doi.org/10.1023/A:1002601211295

Lee, W. Y. W., Cheung, C. C. M., Liu, K. W. K., Fung, K. P., Wong, J., Lai, P. B. S., & Yeung, J. H. K. (2010). Cytotoxic Effects of Tanshinones from Salvia miltiorrhiza on Doxorubicin-Resistant Human Liver Cancer Cells. *Journal of Natural Products*, *73*(5), 854–859. https://doi.org/10.1021/np900792p

Leesutthiphonchai, W., Vu, A. L., Ah-Fong, A. M. V., & Judelson, H. S. (2018). How Does Phytophthora infestans Evade Control Efforts? Modern Insight Into the Late Blight

Disease. *Phytopathology®*, *108*(8), 916–924. https://doi.org/10.1094/PHYTO-04-18-0130-IA

Leitner, M., Boland, W., & Mithöfer, A. (2005). Direct and indirect defences induced by piercing-sucking and chewing herbivores in Medicago truncatula. *The New Phytologist*, *167*(2), 597–606. https://doi.org/10.1111/j.1469-8137.2005.01426.x

Leitner, M., Kaiser, R., Hause, B., Boland, W., & Mithöfer, A. (2010). Does mycorrhization influence herbivore-induced volatile emission in Medicago truncatula? *Mycorrhiza*, *20*(2), 89–101. https://doi.org/10.1007/s00572-009-0264-z

Leppyanen, I. V., Shakhnazarova, V. Y., Shtark, O. Y., Vishnevskaya, N. A., Tikhonovich, I. A., & Dolgikh, E. A. (2018). Receptor-Like Kinase LYK9 in Pisum sativum L. Is the CERK1-Like Receptor that Controls Both Plant Immunity and AM Symbiosis Development. *International Journal of Molecular Sciences*, *19*(1), Article 1. https://doi.org/10.3390/ijms19010008

Lesburg, C. A., Zhai, G., Cane, D. E., & Christianson, D. W. (1997). Crystal structure of pentalenene synthase: Mechanistic insights on terpenoid cyclization reactions in biology. *Science (New York, N.Y.)*, *277*(5333), 1820–1824. https://doi.org/10.1126/science.277.5333.1820

Lewinsohn, E., Schalechet, F., Wilkinson, J., Matsui, K., Tadmor, Y., Nam, K. H., Amar, O., Lastochkin, E., Larkov, O., Ravid, U., Hiatt, W., Gepstein, S., & Pichersky, E. (2001). Enhanced levels of the aroma and flavor compound S-linalool by metabolic engineering of the terpenoid pathway in tomato fruits. *Plant Physiology*, *127*(3), 1256–1265.

Lichtenthaler, H. K. (1999). THE 1-DEOXY-D-XYLULOSE-5-PHOSPHATE PATHWAY OF ISOPRENOID BIOSYNTHESIS IN PLANTS. *Annual Review of Plant Biology*, *50*(Volume 50, 1999), 47–65. https://doi.org/10.1146/annurev.arplant.50.1.47

Lin, J., Wang, D., Chen, X., Köllner, T. G., Mazarei, M., Guo, H., Pantalone, V. R., Arelli, P., Stewart, C. N., Wang, N., & Chen, F. (2017). An (E,E)-α-farnesene synthase gene of soybean has a role in defence against nematodes and is involved in synthesizing insect-induced volatiles. *Plant Biotechnology Journal*, *15*(4), 510–519. https://doi.org/10.1111/pbi.12649

Little, D. B., & Croteau, R. B. (2002). Alteration of product formation by directed mutagenesis and truncation of the multiple-product sesquiterpene synthases delta-selinene synthase and gamma-humulene synthase. *Archives of Biochemistry and Biophysics*, *402*(1), 120–135. https://doi.org/10.1016/S0003-9861(02)00068-1

Liu, Y., Esposto, D., Mahdi, L. K., Porzel, A., Stark, P., Hussain, H., Scherr-Henning, A., Isfort, S., Bathe, U., Acosta, I. F., Zuccaro, A., Balcke, G. U., & Tissier, A. (2024). Hordedane diterpenoid phytoalexins restrict Fusarium graminearum infection but

enhance Bipolaris sorokiniana colonization of barley roots. *Molecular Plant*, *17*(8), 1307–1327. https://doi.org/10.1016/j.molp.2024.07.006

Lohmann, G. V., Shimoda, Y., Nielsen, M. W., Jørgensen, F. G., Grossmann, C., Sandal, N., Sørensen, K., Thirup, S., Madsen, L. H., Tabata, S., Sato, S., Stougaard, J., & Radutoiu, S. (2010). Evolution and regulation of the Lotus japonicus LysM receptor gene family. *Molecular Plant-Microbe Interactions: MPMI*, *23*(4), 510–521. https://doi.org/10.1094/MPMI-23-4-0510

Lopes Fischer, N., Naseer, N., Shin, S., & Brodsky, I. E. (2020). Effector-triggered immunity and pathogen sensing in metazoans. *Nature Microbiology*, *5*(1), 14–26. https://doi.org/10.1038/s41564-019-0623-2

Loreto, F., Bagnoli, F., & Fineschi, S. (2009). One species, many terpenes: Matching chemical and biological diversity. *Trends in Plant Science*, *14*(8), 416–420. https://doi.org/10.1016/j.tplants.2009.06.003

Lücker, J., Bouwmeester, H. J., Schwab, W., Blaas, J., van der Plas, L. H., & Verhoeven, H. A. (2001). Expression of Clarkia S-linalool synthase in transgenic petunia plants results in the accumulation of S-linalyl-beta-D-glucopyranoside. *The Plant Journal: For Cell and Molecular Biology*, *27*(4), 315–324. https://doi.org/10.1046/j.1365-313x.2001.01097.x

Ma, Y., Cui, G., Chen, T., Ma, X., Wang, R., Jin, B., Yang, J., Kang, L., Tang, J., Lai, C., Wang, Y., Zhao, Y., Shen, Y., Zeng, W., Peters, R. J., Qi, X., Guo, J., & Huang, L. (2021). Expansion within the CYP71D subfamily drives the heterocyclization of tanshinones synthesis in Salvia miltiorrhiza. *Nature Communications*, *12*(1), 685. https://doi.org/10.1038/s41467-021-20959-1

Mackay, T. F. C., & Anholt, R. R. H. (2022). Gregor Mendel's legacy in quantitative genetics. *PLoS Biology*, *20*(7), e3001692. https://doi.org/10.1371/journal.pbio.3001692

Mackey, D., Belkhadir, Y., Alonso, J. M., Ecker, J. R., & Dangl, J. L. (2003). Arabidopsis RIN4 is a target of the type III virulence effector AvrRpt2 and modulates RPS2-mediated resistance. *Cell*, *112*(3), 379–389. https://doi.org/10.1016/s0092-8674(03)00040-0

Mackey, D., Holt, B. F., Wiig, A., & Dangl, J. L. (2002). RIN4 interacts with Pseudomonas syringae type III effector molecules and is required for RPM1-mediated resistance in Arabidopsis. *Cell*, *108*(6), 743–754. https://doi.org/10.1016/s0092-8674(02)00661-x

Magnani, R. F., Volpe, H. X. L., Luvizotto, R. A. G., Mulinari, T. A., Agostini, T. T., Bastos, J. K., Ribeiro, V. P., Carmo-Sousa, M., Wulff, N. A., Peña, L., & Leal, W. S. (2025). α-Copaene is a potent repellent against the Asian Citrus Psyllid Diaphorina citri. *Scientific Reports*, *15*(1), 3564. https://doi.org/10.1038/s41598-025-86369-1

Martins, D., Araújo, S. de S., Rubiales, D., & Vaz Patto, M. C. (2020). Legume Crops and Biotrophic Pathogen Interactions: A Continuous Cross-Talk of a Multilayered Array of

Defense Mechanisms. *Plants (Basel, Switzerland)*, *9*(11), 1460. https://doi.org/10.3390/plants9111460

Mélida, H., Sandoval-Sierra, J. V., Diéguez-Uribeondo, J., & Bulone, V. (2013). Analyses of Extracellular Carbohydrates in Oomycetes Unveil the Existence of Three Different Cell Wall Types. *Eukaryotic Cell*, *12*(2), 194–203. https://doi.org/10.1128/EC.00288-12

Mengiste, T. (2012). Plant immunity to necrotrophs. *Annual Review of Phytopathology*, *50*, 267–294. https://doi.org/10.1146/annurev-phyto-081211-172955

Miller, B., Madilao, L. L., Ralph, S., & Bohlmann, J. (2005). Insect-induced conifer defense. White pine weevil and methyl jasmonate induce traumatic resinosis, de novo formed volatile emissions, and accumulation of terpenoid synthase and putative octadecanoid pathway transcripts in Sitka spruce. *Plant Physiology*, *137*(1), 369–382. https://doi.org/10.1104/pp.104.050187

Mithöfer, A., Fliegmann, J., Daxberger, A., Ebel, C., Neuhaus-Url, G., Bhagwat, A. A., Keister, D. L., & Ebel, J. (2001). Induction of H2O2 synthesis by β-glucan elicitors in soybean is independent of cytosolic calcium transients. *FEBS Letters*, *508*(2), 191–195. https://doi.org/10.1016/S0014-5793(01)03054-X

Muchlinski, A., Jia, M., Tiedge, K., Fell, J. S., Pelot, K. A., Chew, L., Davisson, D., Chen, Y., Siegel, J., Lovell, J. T., & Zerbe, P. (2021). Cytochrome P450-catalyzed biosynthesis of furanoditerpenoids in the bioenergy crop switchgrass (Panicum virgatum L.). *The Plant Journal: For Cell and Molecular Biology*, *108*(4), 1053–1068. https://doi.org/10.1111/tpj.15492

Murphy, K. M., Dowd, T., Khalil, A., Char, S. N., Yang, B., Endelman, B. J., Shih, P. M., Topp, C., Schmelz, E. A., & Zerbe, P. (2023). A dolabralexin-deficient mutant provides insight into specialized diterpenoid metabolism in maize. *Plant Physiology*, *192*(2), 1338–1358. https://doi.org/10.1093/plphys/kiad150

Nagegowda, D. A. (2010). Plant volatile terpenoid metabolism: Biosynthetic genes, transcriptional regulation and subcellular compartmentation. *FEBS Letters*, *584*(14), 2965–2973. https://doi.org/10.1016/j.febslet.2010.05.045

Nandety, R. S., Wen, J., & Mysore, K. S. (2023). *Medicago truncatula* resources to study legume biology and symbiotic nitrogen fixation. *Fundamental Research*, *3*(2), 219–224. https://doi.org/10.1016/j.fmre.2022.06.018

Nars, A., Lafitte, C., Chabaud, M., Drouillard, S., Mélida, H., Danoun, S., Costaouëc, T. L., Rey, T., Benedetti, J., Bulone, V., Barker, D. G., Bono, J.-J., Dumas, B., Jacquet, C., Heux, L., Fliegmann, J., & Bottin, A. (2013). Aphanomyces euteiches Cell Wall Fractions Containing Novel Glucan-Chitosaccharides Induce Defense Genes and

Nuclear Calcium Oscillations in the Plant Host Medicago truncatula. *PLOS ONE*, *8*(9), e75039. https://doi.org/10.1371/journal.pone.0075039

Nasim, Z., Karim, N., Susila, H., & Ahn, J. H. (2025). Natural variation in *FLOWERING LOCUS C* and *FLOWERING LOCUS M* underlies the weak temperature sensitivity of the Arabidopsis accession Ellershausen. *Current Plant Biology*, *41*, 100444. https://doi.org/10.1016/j.cpb.2025.100444

Newman, J. D., & Chappell, J. (1999). Isoprenoid biosynthesis in plants: Carbon partitioning within the cytoplasmic pathway. *Critical Reviews in Biochemistry and Molecular Biology*, *34*(2), 95–106. https://doi.org/10.1080/10409239991209228

Niderman, T., Genetet, I., Bruyère, T., Gees, R., Stintzi, A., Legrand, M., Fritig, B., & Mösinger, E. (1995). Pathogenesis-related PR-1 proteins are antifungal. Isolation and characterization of three 14-kilodalton proteins of tomato and of a basic PR-1 of tobacco with inhibitory activity against Phytophthora infestans. *Plant Physiology*, *108*(1), 17–27. https://doi.org/10.1104/pp.108.1.17

Nietzschmann, L., Gorzolka, K., Smolka, U., Matern, A., Eschen-Lippold, L., Scheel, D., & Rosahl, S. (2019). Early Pep-13-induced immune responses are SERK3A/B-dependent in potato. *Scientific Reports*, *9*(1), 18380. https://doi.org/10.1038/s41598-019-54944-y

Nieuwenhuizen, N. J., Wang, M. Y., Matich, A. J., Green, S. A., Chen, X., Yauk, Y.-K., Beuning, L. L., Nagegowda, D. A., Dudareva, N., & Atkinson, R. G. (2009). Two terpene synthases are responsible for the major sesquiterpenes emitted from the flowers of kiwifruit (Actinidia deliciosa). *Journal of Experimental Botany*, *60*(11), 3203–3219. https://doi.org/10.1093/jxb/erp162

Nützmann, H.-W., Huang, A., & Osbourn, A. (2016). Plant metabolic clusters – from genetics to genomics. *New Phytologist*, *211*(3), 771–789. https://doi.org/10.1111/nph.13981

Nützmann, H.-W., & Osbourn, A. (2014). Gene clustering in plant specialized metabolism. *Current Opinion in Biotechnology*, *26*, 91–99. https://doi.org/10.1016/j.copbio.2013.10.009

Oldroyd, G. E. D. (2013). Speak, friend, and enter: Signalling systems that promote beneficial symbiotic associations in plants. *Nature Reviews. Microbiology*, *11*(4), 252–263. https://doi.org/10.1038/nrmicro2990

Paquin, B., Laforest, M. J., Forget, L., Roewer, I., Wang, Z., Longcore, J., & Lang, B. F. (1997). The fungal mitochondrial genome project: Evolution of fungal mitochondrial genomes and their gene expression. *Current Genetics*, *31*(5), 380–395. https://doi.org/10.1007/s002940050220

Parker, M. T., Zhong, Y., Dai, X., Wang, S., & Zhao, P. (2014). Comparative genomic and transcriptomic analysis of terpene synthases in Arabidopsis and Medicago. *IET Systems Biology*, *8*(4), 146–153. https://doi.org/10.1049/iet-syb.2013.0032

Peleg-Grossman, S., Golani, Y., Kaye, Y., Melamed-Book, N., & Levine, A. (2009). NPR1 Protein Regulates Pathogenic and Symbiotic Interactions between Rhizobium and Legumes and Non-Legumes. *PLoS ONE*, *4*(12), e8399. https://doi.org/10.1371/journal.pone.0008399

Petersen, A. B., & Rosendahl, Sø. (2000). Phylogeny of the *Peronosporomycetes* (*Oomycota*) based on partial sequences of the large ribosomal subunit (LSU rDNA). *Mycological Research*, *104*(11), 1295–1303. https://doi.org/10.1017/S0953756200003075

Phillips, M. A., & Croteau, R. B. (1999). Resin-based defenses in conifers. *Trends in Plant Science*, *4*(5), 184–190. https://doi.org/10.1016/s1360-1385(99)01401-6

Pichersky, E., & Gershenzon, J. (2002). The formation and function of plant volatiles: Perfumes for pollinator attraction and defense. *Current Opinion in Plant Biology*, *5*(3), 237–243. https://doi.org/10.1016/s1369-5266(02)00251-0

Pilet-Nayel, M.-L., Prospéri, J.-M., Hamon, C., Lesné, A., Lecointe, R., Le Goff, I., Hervé, M., Deniot, G., Delalande, M., Huguet, T., Jacquet, C., & Baranger, A. (2009). AER1, a major gene conferring resistance to Aphanomyces euteiches in Medicago truncatula. *Phytopathology*, *99*(2), 203–208. https://doi.org/10.1094/PHYTO-99-2-0203

Preston, G. M., Studholme, D. J., & Caldelari, I. (2005). Profiling the secretomes of plant pathogenic Proteobacteria. *FEMS Microbiology Reviews*, *29*(2), 331–360. https://doi.org/10.1016/j.femsre.2004.12.004

Quenouille, J., Vassilakos, N., & Moury, B. (2013). otato virus: A major crop pathogen that has provided major insights into the evolution of viral pathogenicity. *Molecular Plant Pathology*, *14*(5), 439–452. https://doi.org/10.1111/mpp.12024

Ralston, L., Kwon, S. T., Schoenbeck, M., Ralston, J., Schenk, D. J., Coates, R. M., & Chappell, J. (2001). Cloning, heterologous expression, and functional characterization of 5-epi-aristolochene-1,3-dihydroxylase from tobacco (Nicotiana tabacum). *Archives of Biochemistry and Biophysics*, *393*(2), 222–235. https://doi.org/10.1006/abbi.2001.2483

Rasmann, S., Köllner, T. G., Degenhardt, J., Hiltpold, I., Toepfer, S., Kuhlmann, U., Gershenzon, J., & Turlings, T. C. J. (2005). Recruitment of entomopathogenic nematodes by insect-damaged maize roots. *Nature*, *434*(7034), 732–737. https://doi.org/10.1038/nature03451

Regina. (2021, October 18). Potato diseases & common pests. *Plantura*. https://plantura.garden/uk/vegetables/potatoes/potato-diseases

Rehmany, A. P., Gordon, A., Rose, L. E., Allen, R. L., Armstrong, M. R., Whisson, S. C., Kamoun, S., Tyler, B. M., Birch, P. R. J., & Beynon, J. L. (2005). Differential recognition of highly divergent downy mildew avirulence gene alleles by RPP1 resistance genes from two Arabidopsis lines. *The Plant Cell*, *17*(6), 1839–1850. https://doi.org/10.1105/tpc.105.031807

Rey, T., Nars, A., Bonhomme, M., Bottin, A., Huguet, S., Balzergue, S., Jardinaud, M.-F., Bono, J.-J., Cullimore, J., Dumas, B., Gough, C., & Jacquet, C. (2013). NFP, a LysM protein controlling Nod factor perception, also intervenes in edicago truncatula resistance to pathogens. *New Phytologist*, *198*(3), 875–886. https://doi.org/10.1111/nph.12198

Riethmüller, A., Weiß, M., & Oberwinkler, F. (2000). Phylogenetic studies of Saprolegniomycetidae and related groups based on nuclear large subunit ribosomal DNA sequences. *Canadian Journal of Botany*, *77*(12), 1790–1800. https://doi.org/10.1139/b99-163

Ristaino, J. B., Cooke, D. E. L., Acuña, I., & Muñoz, M. (2020). CHAPTER 6: The Threat of Late Blight to Global Food Security. In *Emerging Plant Diseases and Global Food Security* (pp. 101–132). The American Phytopathological Society. https://doi.org/10.1094/9780890546383.006

Robert, C. A. M., Erb, M., Hiltpold, I., Hibbard, B. E., Gaillard, M. D. P., Bilat, J., Degenhardt, J., Cambet-Petit-Jean, X., Turlings, T. C. J., & Zwahlen, C. (2013). Genetically engineered maize plants reveal distinct costs and benefits of constitutive volatile emissions in the field. *Plant Biotechnology Journal*, *11*(5), 628–639. https://doi.org/10.1111/pbi.12053

Ronfort, J., Bataillon, T., Santoni, S., Delalande, M., David, J. L., & Prosperi, J.-M. (2006). Microsatellite diversity and broad scale geographic structure in a model legume: Building a set of nested core collection for studying naturally occurring variation in Medicago truncatula. *BMC Plant Biology*, *6*(1), 28. https://doi.org/10.1186/1471-2229-6-28

Roux, M., Schwessinger, B., Albrecht, C., Chinchilla, D., Jones, A., Holton, N., Malinovsky, F. G., Tör, M., de Vries, S., & Zipfel, C. (2011). The Arabidopsis leucine-rich repeat receptor-like kinases BAK1/SERK3 and BKK1/SERK4 are required for innate immunity to hemibiotrophic and biotrophic pathogens. *The Plant Cell*, *23*(6), 2440–2455. https://doi.org/10.1105/tpc.111.084301

Rynkiewicz, M. J., Cane, D. E., & Christianson, D. W. (2001). Structure of trichodiene synthase from Fusarium sporotrichioides provides mechanistic inferences on the terpene cyclization cascade. *Proceedings of the National Academy of Sciences of*

the United States of America, *98*(24), 13543–13548. https://doi.org/10.1073/pnas.231313098

Sapir-Mir, M., Mett, A., Belausov, E., Tal-Meshulam, S., Frydman, A., Gidoni, D., & Eyal, Y. (2008). Peroxisomal Localization of Arabidopsis Isopentenyl Diphosphate Isomerases Suggests That Part of the Plant Isoprenoid Mevalonic Acid Pathway Is Compartmentalized to Peroxisomes. *Plant Physiology*, *148*(3), 1219–1228. https://doi.org/10.1104/pp.108.127951

Scheler, U., Brandt, W., Porzel, A., Rothe, K., Manzano, D., Božić, D., Papaefthimiou, D., Balcke, G. U., Henning, A., Lohse, S., Marillonnet, S., Kanellis, A. K., Ferrer, A., & Tissier, A. (2016). Elucidation of the biosynthesis of carnosic acid and its reconstitution in yeast. *Nature Communications*, *7*(1), 12942. https://doi.org/10.1038/ncomms12942

Schmelz, E. A., Huffaker, A., Sims, J. W., Christensen, S. A., Lu, X., Okada, K., & Peters, R. J. (2014a). Biosynthesis, elicitation and roles of monocot terpenoid phytoalexins. *The Plant Journal: For Cell and Molecular Biology*, *79*(4), 659–678. https://doi.org/10.1111/tpj.12436

Schmelz, E. A., Huffaker, A., Sims, J. W., Christensen, S. A., Lu, X., Okada, K., & Peters, R. J. (2014b). Biosynthesis, elicitation and roles of monocot terpenoid phytoalexins. *The Plant Journal: For Cell and Molecular Biology*, *79*(4), 659–678. https://doi.org/10.1111/tpj.12436

Schmittgen, T. D., & Livak, K. J. (2008). Analyzing real-time PCR data by the comparative C(T) method. *Nature Protocols*, *3*(6), 1101–1108. https://doi.org/10.1038/nprot.2008.73

Schnee, C., Köllner, T. G., Held, M., Turlings, T. C. J., Gershenzon, J., & Degenhardt, J. (2006). The products of a single maize sesquiterpene synthase form a volatile defense signal that attracts natural enemies of maize herbivores. *Proceedings of the National Academy of Sciences of the United States of America*, *103*(4), 1129–1134. https://doi.org/10.1073/pnas.0508027103

Schrepfer, P., Buettner, A., Goerner, C., Hertel, M., van Rijn, J., Wallrapp, F., Eisenreich, W., Sieber, V., Kourist, R., & Brück, T. (2016). Identification of amino acid networks governing catalysis in the closed complex of class I terpene synthases. *Proceedings of the National Academy of Sciences*, *113*(8), E958–E967. https://doi.org/10.1073/pnas.1519680113

Scott, W. W. (1961). A monograph of the genus Aphanomyces. *Technical Bulletin. Virginia Agricultural Experiment Station*, *151*. https://www.cabdirect.org/cabdirect/abstract/19621102474

Seki, H., Sawai, S., Ohyama, K., Mizutani, M., Ohnishi, T., Sudo, H., Fukushima, E. O., Akashi, T., Aoki, T., Saito, K., & Muranaka, T. (2011). Triterpene functional genomics in licorice for identification of CYP72A154 involved in the biosynthesis of glycyrrhizin. *The Plant Cell*, *23*(11), 4112–4123. https://doi.org/10.1105/tpc.110.082685

Sievers, F., Wilm, A., Dineen, D., Gibson, T. J., Karplus, K., Li, W., Lopez, R., McWilliam, H., Remmert, M., Söding, J., Thompson, J. D., & Higgins, D. G. (2011). Fast, scalable generation of high-quality protein multiple sequence alignments using Clustal Omega. *Molecular Systems Biology*, *7*, 539. https://doi.org/10.1038/msb.2011.75

Smýkal, P., von Wettberg, E. J. B., & McPhee, K. (2020). Legume Genetics and Biology: From Mendel's Pea to Legume Genomics. *International Journal of Molecular Sciences*, *21*(9), Article 9. https://doi.org/10.3390/ijms21093336

Song, Y., Nolan, K. E., & Rose, R. J. (2013). Stable transformation of Medicago truncatula cv. Jemalong for gene analysis using Agrobacterium tumefaciens. *Methods in Molecular Biology (Clifton, N.J.)*, *1069*, 203–214. https://doi.org/10.1007/978-1-62703-613-9_14

Starks, C. M., Back, K., Chappell, J., & Noel, J. P. (1997). Structural basis for cyclic terpene biosynthesis by tobacco 5-epi-aristolochene synthase. *Science (New York, N.Y.)*, *277*(5333), 1815–1820. https://doi.org/10.1126/science.277.5333.1815

Steele, C. L., Crock, J., Bohlmann, J., & Croteau, R. (1998). Sesquiterpene Synthases from Grand Fir (*Abies grandis*). *Journal of Biological Chemistry*, *273*(4), 2078–2089. https://doi.org/10.1074/jbc.273.4.2078

Stevens, R. (1992). Dictionary of terpenoids, J. D. Connolly and R. A. Hill, Chapman & Hall, London, 1991. Three volumes containing 2156 pages, price £985.00. ISBN 0–412–25770-X. *Flavour and Fragrance Journal*, *7*(4), 242–243. https://doi.org/10.1002/ffj.2730070418

Stokstad, E. (2019). The new potato. *Science*, *363*(6427), 574–577. https://doi.org/10.1126/science.363.6427.574

Strange, R. N., & Scott, P. R. (2005). Plant disease: A threat to global food security. *Annual Review of Phytopathology*, *43*, 83–116. https://doi.org/10.1146/annurev.phyto.43.113004.133839

Sun, Y., Li, L., Macho, A. P., Han, Z., Hu, Z., Zipfel, C., Zhou, J.-M., & Chai, J. (2013). Structural basis for flg22-induced activation of the Arabidopsis FLS2-BAK1 immune complex. *Science (New York, N.Y.)*, *342*(6158), 624–628. https://doi.org/10.1126/science.1243825

Tadege, M., Wen, J., He, J., Tu, H., Kwak, Y., Eschstruth, A., Cayrel, A., Endre, G., Zhao, P. X., Chabaud, M., Ratet, P., & Mysore, K. S. (2008). Large-scale insertional mutagenesis using the Tnt1 retrotransposon in the model legume Medicago

truncatula. *The Plant Journal*, *54*(2), 335–347. https://doi.org/10.1111/j.1365-313X.2008.03418.x

Talakayala, A., Ankanagari, S., & Garladinne, M. (2022). CRISPR-Cas genome editing system: A versatile tool for developing disease resistant crops. *Plant Stress*, *3*, 100056. https://doi.org/10.1016/j.stress.2022.100056

Tang, H., Krishnakumar, V., Bidwell, S., Rosen, B., Chan, A., Zhou, S., Gentzbittel, L., Childs, K. L., Yandell, M., Gundlach, H., Mayer, K. F., Schwartz, D. C., & Town, C. D. (2014). An improved genome release (version Mt4.0) for the model legume Medicago truncatula. *BMC Genomics*, *15*(1), 312. https://doi.org/10.1186/1471-2164-15-312

Tao, Y., Xie, Z., Chen, W., Glazebrook, J., Chang, H.-S., Han, B., Zhu, T., Zou, G., & Katagiri, F. (2003). Quantitative nature of Arabidopsis responses during compatible and incompatible interactions with the bacterial pathogen Pseudomonas syringae. *The Plant Cell*, *15*(2), 317–330. https://doi.org/10.1105/tpc.007591

Thimmappa, R., Geisler, K., Louveau, T., O'Maille, P., & Osbourn, A. (2014). Triterpene Biosynthesis in Plants. *Annual Review of Plant Biology*, *65*(Volume 65, 2014), 225–257. https://doi.org/10.1146/annurev-arplant-050312-120229

Tholl, D. (2006). Terpene synthases and the regulation, diversity and biological roles of terpene metabolism. *Current Opinion in Plant Biology*, *9*(3), 297–304. https://doi.org/10.1016/j.pbi.2006.03.014

Tholl, D., Chen, F., Petri, J., Gershenzon, J., & Pichersky, E. (2005). Two sesquiterpene synthases are responsible for the complex mixture of sesquiterpenes emitted from Arabidopsis flowers. *The Plant Journal: For Cell and Molecular Biology*, *42*(5), 757–771. https://doi.org/10.1111/j.1365-313X.2005.02417.x

Timney, B. L., Raveh, B., Mironska, R., Trivedi, J. M., Kim, S. J., Russel, D., Wente, S. R., Sali, A., & Rout, M. P. (2016). Simple rules for passive diffusion through the nuclear pore complex. *Journal of Cell Biology*, *215*(1), 57–76. https://doi.org/10.1083/jcb.201601004

van Dijk, M., Morley, T., Rau, M. L., & Saghai, Y. (2021). A meta-analysis of projected global food demand and population at risk of hunger for the period 2010–2050. *Nature Food*, *2*(7), 494–501. https://doi.org/10.1038/s43016-021-00322-9

Vandemark, G. J., Kraft, J. M., Larsen, R. C., Gritsenko, M. A., & Boge, W. L. (2000). A PCR-Based Assay by Sequence-Characterized DNA Markers for the Identification and Detection of Aphanomyces euteiches. *Phytopathology*, *90*(10), 1137–1144. https://doi.org/10.1094/PHYTO.2000.90.10.1137

Wang, L., Lui, A. C. W., Lam, P. Y., Liu, G., Godwin, I. D., & Lo, C. (2020). Transgenic expression of flavanone 3-hydroxylase redirects flavonoid biosynthesis and alleviates

anthracnose susceptibility in sorghum. *Plant Biotechnology Journal*, *18*(11), 2170–2172. https://doi.org/10.1111/pbi.13397

Wang, Q., Liu, J., & Zhu, H. (2018). Genetic and Molecular Mechanisms Underlying Symbiotic Specificity in Legume-Rhizobium Interactions. *Frontiers in Plant Science*, *9*. https://doi.org/10.3389/fpls.2018.00313

Wang, R., & Brattain, M. G. (2007). The maximal size of protein to diffuse through the nuclear pore is larger than 60kDa. *FEBS Letters*, *581*(17), 3164–3170. https://doi.org/10.1016/j.febslet.2007.05.082

Wang, Y., Tyler, B. M., & Wang, Y. (2019). Defense and Counterdefense During Plant-Pathogenic Oomycete Infection. *Annual Review of Microbiology*, *73*, 667–696. https://doi.org/10.1146/annurev-micro-020518-120022

Watanabe, K. (2015). Potato genetics, genomics, and applications. *Breeding Science*, *65*(1), 53–68. https://doi.org/10.1270/jsbbs.65.53

Whisson, S. C., Boevink, P. C., Moleleki, L., Avrova, A. O., Morales, J. G., Gilroy, E. M., Armstrong, M. R., Grouffaud, S., van West, P., Chapman, S., Hein, I., Toth, I. K., Pritchard, L., & Birch, P. R. J. (2007). A translocation signal for delivery of oomycete effector proteins into host plant cells. *Nature*, *450*(7166), 115–118. https://doi.org/10.1038/nature06203

Whittington, D. A., Wise, M. L., Urbansky, M., Coates, R. M., Croteau, R. B., & Christianson, D. W. (2002). Bornyl diphosphate synthase: Structure and strategy for carbocation manipulation by a terpenoid cyclase. *Proceedings of the National Academy of Sciences of the United States of America*, *99*(24), 15375–15380. https://doi.org/10.1073/pnas.232591099

Wilson, R. F. (2008). Soybean: Market Driven Research Needs. In G. Stacey (Ed.), *Genetics and Genomics of Soybean* (pp. 3–15). Springer. https://doi.org/10.1007/978-0-387-72299-3_1

Win, J., Morgan, W., Bos, J., Krasileva, K. V., Cano, L. M., Chaparro-Garcia, A., Ammar, R., Staskawicz, B. J., & Kamoun, S. (2007). Adaptive evolution has targeted the C-terminal domain of the RXLR effectors of plant pathogenic oomycetes. *The Plant Cell*, *19*(8), 2349–2369. https://doi.org/10.1105/tpc.107.051037

Wright, E., & Wang, Z.-Y. (2015). Medicago truncatula transformation using cotyledonary explants. *Methods in Molecular Biology (Clifton, N.J.)*, *1223*, 35–41. https://doi.org/10.1007/978-1-4939-1695-5_3

Wu, L., Chang, K.-F., Conner, R. L., Strelkov, S., Fredua-Agyeman, R., Hwang, S.-F., & Feindel, D. (2018). *Aphanomyces euteiches*: A Threat to Canadian Field Pea Production. *Engineering*, *4*(4), 542–551. https://doi.org/10.1016/j.eng.2018.07.006

Wu, L., Chang, K.-F., Conner, R., Strelkov, S., Fredua-Agyeman, R., Hwang, S., & Feindel, D. (2018c). Aphanomyces euteiches: A Threat to Canadian Field Pea Production. *Engineering*, *4*. https://doi.org/10.1016/j.eng.2018.07.006

Xu, S., Kreitzer, C., McGale, E., Lackus, N. D., Guo, H., Köllner, T. G., Schuman, M. C., Baldwin, I. T., & Zhou, W. (2020). Allelic differences of clustered terpene synthases contribute to correlated intraspecific variation of floral and herbivory-induced volatiles in a wild tobacco. *New Phytologist*, *228*(3), 1083–1096. https://doi.org/10.1111/nph.16739

Yadav, H., Dreher, D., Athmer, B., Porzel, A., Gavrin, A., Baldermann, S., Tissier, A., & Hause, B. (2019). Medicago TERPENE SYNTHASE 10 Is Involved in Defense Against an Oomycete Root Pathogen. *Plant Physiology*, *180*(3), 1598–1613. https://doi.org/10.1104/pp.19.00278

Yamada, Y., Kuzuyama, T., Komatsu, M., Shin-Ya, K., Omura, S., Cane, D. E., & Ikeda, H. (2015). Terpene synthases are widely distributed in bacteria. *Proceedings of the National Academy of Sciences of the United States of America*, *112*(3), 857–862. https://doi.org/10.1073/pnas.1422108112

Yang, C., Halitschke, R., O'Connor, S. E., & Baldwin, I. T. (2024). Roles of three cytochrome P450 monooxygenases in triterpene biosynthesis and their potential impact on growth and development. *Plant Physiology*, *196*(2), 1407–1425. https://doi.org/10.1093/plphys/kiae399

Yoshida, K., Schuenemann, V. J., Cano, L. M., Pais, M., Mishra, B., Sharma, R., Lanz, C., Martin, F. N., Kamoun, S., Krause, J., Thines, M., Weigel, D., & Burbano, H. A. (2013). The rise and fall of the Phytophthora infestans lineage that triggered the Irish potato famine. *eLife*, *2*, e00731. https://doi.org/10.7554/eLife.00731

Young, N. D., Debellé, F., Oldroyd, G. E. D., Geurts, R., Cannon, S. B., Udvardi, M. K., Benedito, V. A., Mayer, K. F. X., Gouzy, J., Schoof, H., Van de Peer, Y., Proost, S., Cook, D. R., Meyers, B. C., Spannagl, M., Cheung, F., De Mita, S., Krishnakumar, V., Gundlach, H., … Roe, B. A. (2011). The Medicago genome provides insight into the evolution of rhizobial symbioses. *Nature*, *480*(7378), 520–524. https://doi.org/10.1038/nature10625

Zhan, J., Thrall, P. H., & Burdon, J. J. (2014). Achieving sustainable plant disease management through evolutionary principles. *Trends in Plant Science*, *19*(9), 570–575. https://doi.org/10.1016/j.tplants.2014.04.010

Zhang, M., & Zhang, S. (2022). Mitogen-activated protein kinase cascades in plant signaling. *Journal of Integrative Plant Biology*, *64*(2), 301–341. https://doi.org/10.1111/jipb.13215

Zhang, S., Kondorosi, É., & Kereszt, A. (2019). An anthocyanin marker for direct visualization of plant transformation and its use to study nitrogen-fixing nodule development. *Journal of Plant Research*, *132*(5), 695–703. https://doi.org/10.1007/s10265-019-01126-6

Zhou, F., & Pichersky, E. (2020). More is better: The diversity of terpene metabolism in plants. *Current Opinion in Plant Biology*, *55*, 1–10. https://doi.org/10.1016/j.pbi.2020.01.005

Zhou, W., Kügler, A., McGale, E., Haverkamp, A., Knaden, M., Guo, H., Beran, F., Yon, F., Li, R., Lackus, N., Köllner, T. G., Bing, J., Schuman, M. C., Hansson, B. S., Kessler, D., Baldwin, I. T., & Xu, S. (2017). Tissue-Specific Emission of (E)-α-Bergamotene Helps Resolve the Dilemma When Pollinators Are Also Herbivores. *Current Biology: CB*, *27*(9), 1336–1341. https://doi.org/10.1016/j.cub.2017.03.017

Zipfel, C. (2008). Pattern-recognition receptors in plant innate immunity. *Current Opinion in Immunology*, *20*(1), 10–16. https://doi.org/10.1016/j.coi.2007.11.003

Zipfel, C., Kunze, G., Chinchilla, D., Caniard, A., Jones, J. D. G., Boller, T., & Felix, G. (2006). Perception of the bacterial PAMP EF-Tu by the receptor EFR restricts Agrobacterium-mediated transformation. *Cell*, *125*(4), 749–760. https://doi.org/10.1016/j.cell.2006.03.037

Zipfel, C., Robatzek, S., Navarro, L., Oakeley, E. J., Jones, J. D. G., Felix, G., & Boller, T. (2004). Bacterial disease resistance in Arabidopsis through flagellin perception. *Nature*, *428*(6984), 764–767. https://doi.org/10.1038/nature02485

Zitnick-Anderson, K., Porter, L. D., Hanson, L. E., & Pasche, J. S. (2021). Identification, Laboratory, Greenhouse, and Field Handling of Aphanomyces euteiches on Pea (Pisum sativum). *Plant Health Progress*, *22*(3), 392–403. https://doi.org/10.1094/PHP-01-21-0011-FI

7 Appendix

7.1 Boiled elicitor M induces *MtTPS10*

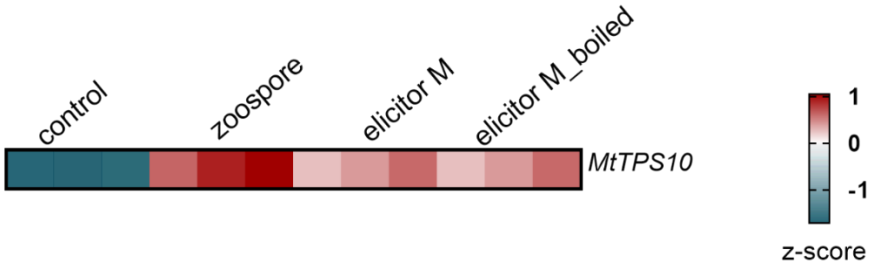

Figure 7.1: Boiled elicitor M induces *MtTPS10.*

Heatmap of the expression profile of *MtTPS10* in *M. truncatula* roots after elicitor treatments. FPKM values of three independent biological replicates of each treatment were transformed into a Z-score.

7.2 *N*-acetyl glucosamine is not a PAMP of *A. euteiches*

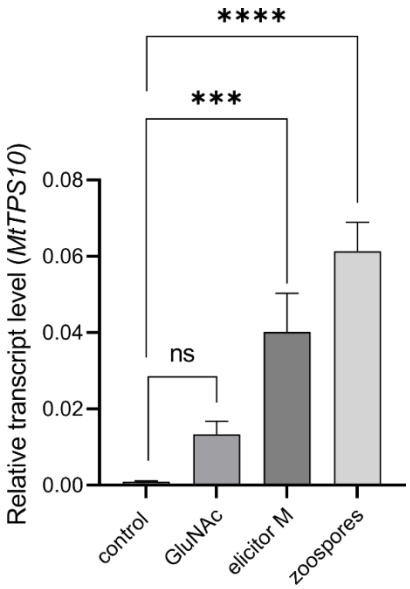

Figure 7.2: *N*-acetyl glucosamine does not induce *MtTPS10.*

MtTPS10 transcript accumulation in *M. truncatula* roots treated with GlcNAc, elicitor M, and zoospores. Expression levels of *MtTPS10* were measured in the root tissue of 7-day-old *M. truncatula* plants via RT-RT-qPCR and were normalized to the housekeeping gene *MtActin2*. Statistical significance was determined by One-Way ANOVA followed by Tukey HSD ($p<0.05$). Bars represent mean +/- SD (n = 3), **P < 0.01, ***P < 0.001; ****P < 0.0001.

7.3 Amplification of the coding sequence of *MtTPS10* from *M.truncatula* ecotypes

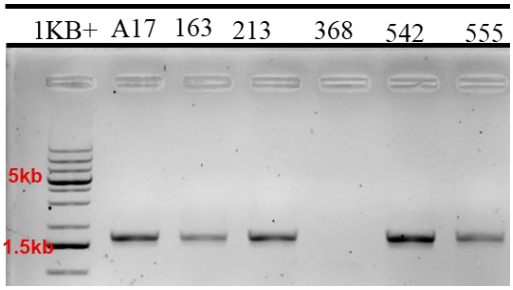

Figure 7.3: CDS of *MtTPS10* transcript is absent in 368.

A gel showing the CDS of *MtTPS10* amplified from all 6 ecotypes of *M. truncatula.* The length of *MtTPS10* is 1.65 kb. A 1 kb plus DNA ladder was used. Highlighted in red are the sizes of 5 kb and 1.5 kb DNA.

7.4 Amino acid alignment of MtTPS10 from all ecotypes

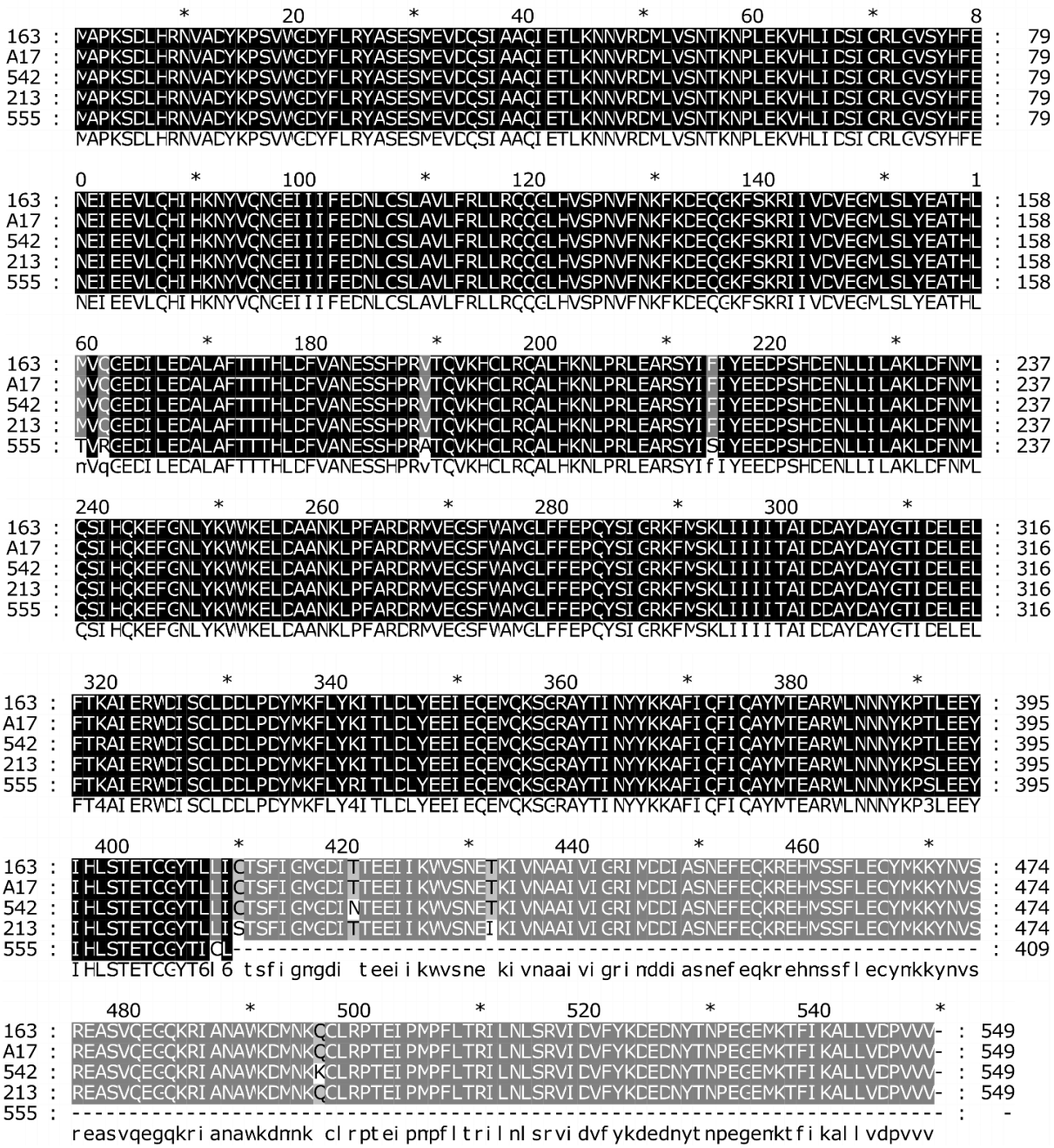

Figure 7.4: Amino acid alignment of *MtTPS10* from 5 *M. truncatula* ecotypes.

Amino acids shaded in black indicate conserved regions in all sequences, and gray areas are amino acids conserved in either three or four sequences. Dashes were inserted in gaps for optimal alignment.

7.5 Terpene volatile emission from *M. truncatula* ecotypes

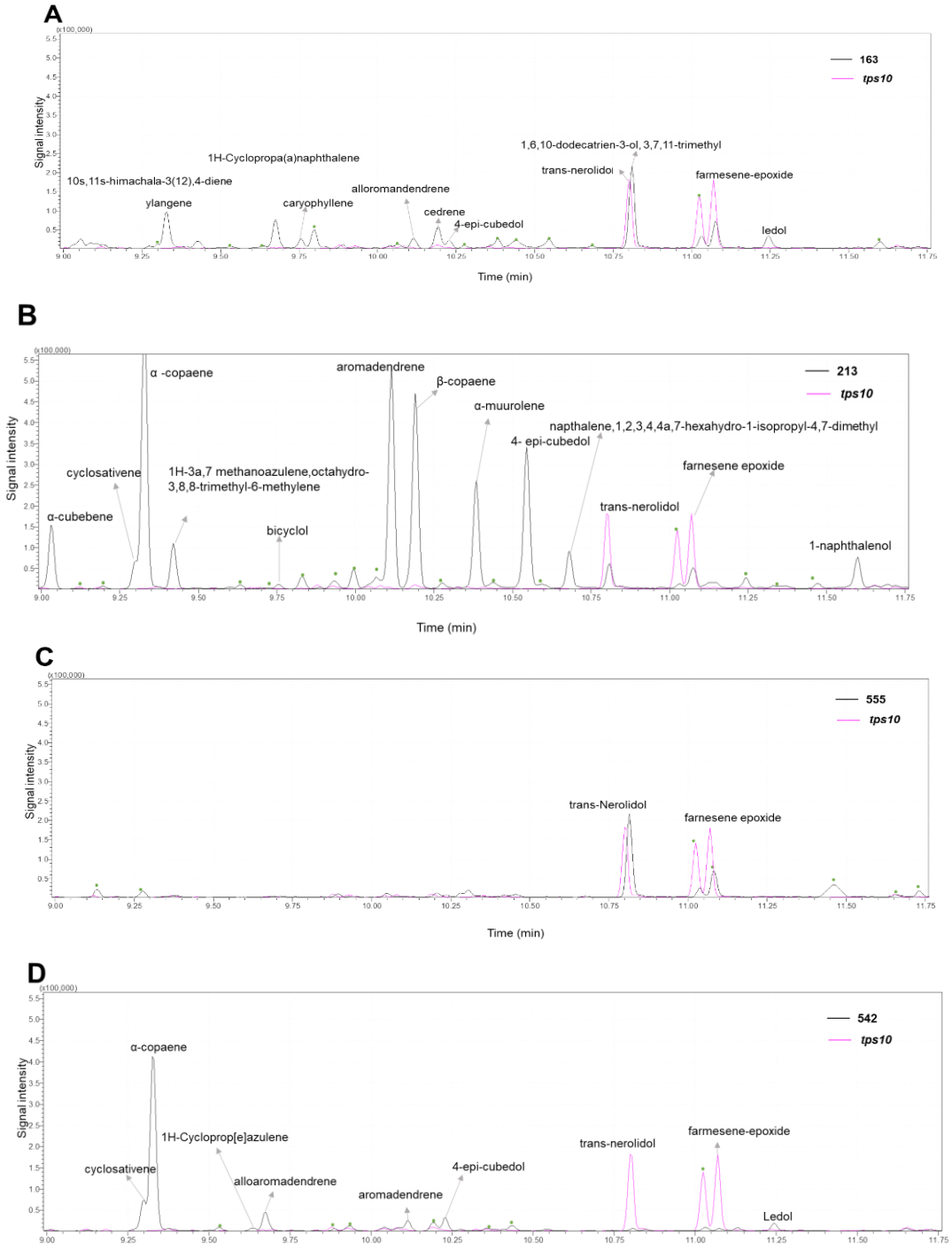

Figure 7.5: Volatiles were collected from infected roots of *M. truncatula* ecotypes after *A. euteiches* infection.

A-D. Volatiles collected from ecotypes 163,213,542, and 555, respectively. Green dots represent unknown compounds. Pink peaks are volatiles measured from the *tps10* mutant. The chromatogram shows the relative intensity of extracted ion chromatogram (*m/z* 93,105,161 and 204).

7.6 Promoter analysis of *pMtTPS10*^{A17} and *pMtTPS10*^{368}

A

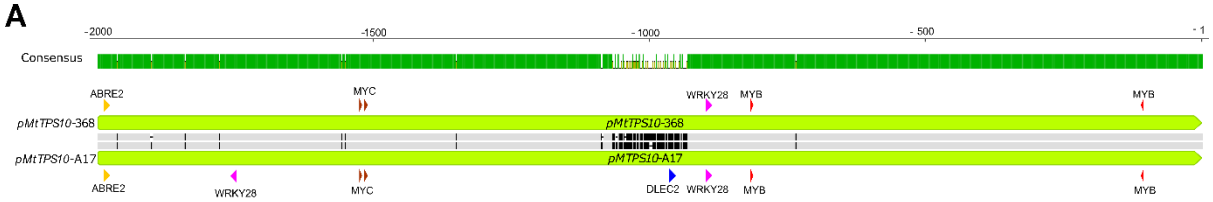

B

Sequence	Strand	BE	BF	BF name	Species
CTTACGTGGCGC	+	ABRE2	UNF	Unknown nuclear factor	*Hordeum vulgare*
GTCACGTCAGCG	+	DLEC2	MAT2	Adenosylmethionine synthetase 2	*Phaseolus vulgaris*
CATTTG	+	MYC	-	Unknown	*A. thaliana*
CATTTG	+	MYC	-	Unknown	*A. thaliana*
CAACCA	+	MYB	-	Unknown	*A. thaliana*
CAACCA	-	MYB	-	Unknown	*A. thaliana*
TTTGTGACTATT	+	WRKY28	ICS1	Arabidopsis isochrorismate synthase 1	*A. thaliana*
TTTGTGACTATT	+	WRKY28	ICS1	Arabidopsis isochrorismate synthase 1	*A. thaliana*

Figure 7.6: Alignment of *pMtTPS10* from A17 and 368.

A. 2 kb alignment of *pMtTPS10* from A17 and 368. **B.** Binding elements (BE) and associated binding factors (BF) predicted by Nsite v6.2014, Softberry Inc (softberry.com) and PlantCARE (bioinformatics.psb.ugent.be). Areas with vertical black lines represent sequence variation in these areas. Binding elements are represented by different colours and with respective names.

7.7 Promoter analysis of *pMtTPS25*^{A17} and *pMtTPS25*^{368}

A

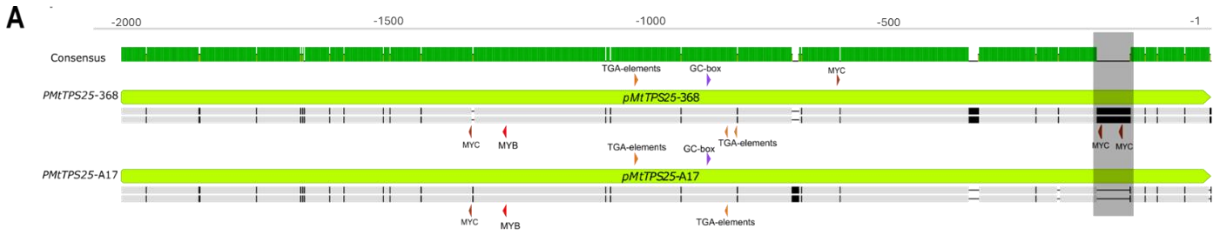

B

Sequence	Strand	BE	BF	BF name	Species
CATTTG	-	MYC	-	Unknown	*A. thaliana*
CATTTG	+	MYC	-	Unknown	*A. thaliana*
CATTTG	-	MYC	-	Unknown	*A. thaliana*
CATTTG	-	MYC	-	Unknown	*A. thaliana*
CAACAG	-	MYB	-	Unknown	*N.tabacum*
AACGAC	+	TGA-elements	-	Unknown	*Brassica oleracea*
TTGCTG	-	TGA-elements	-	Unknown	*Brassica oleracea*
TTGCTG	-	TGA-elements	-	Unknown	*Brassica oleracea*
GGGCGGG	+	GC-box	-	Unknown	*Triticum aestivum*

Figure 7.7: Alignment of *pMtTPS25* from A17 and 368.

A. 2 kb alignment of *pMtTPS10* from A17 and 368. **B.** Zoom in of sequence deletion in *pMtTPS25*^{A17} from highlighted gray area in **A.** Binding elements (BE) and associated binding factors (BF) were predicted by Nsite v6.2014, Softberry Inc (softberry.com) and PlantCARE (bioinformatics.psb.ugent.be). Dashes represent deleted nucleotides. Areas with vertical black lines represent sequence variation in these areas. Binding elements are represented by different colours and with respective names.

7.8 Molecular characterization of *MtTPS25*

```
Mtr_4g092010       EERIELTKPLSLIYIIDDIFDFYGNIDELTLFTDAVKRWDLSA-IEQLPDCMKVCFKALY 357
Mtr_2g010960       DQRIELTKVISLVYVIDDIFDVYGTLDQLTLFVDLVTRWKLAD-TEELPDFVKICLSFIY 315
Mtr_3g052120       NERVELTKPISLVYIIDDIFDVHGTLDQLTLFTEAVNRWEMDG-AENLPNFMKVSLSSLY 311
Mtr_6g064980       EQRIELTKPISLIYVIDDIFDVHGTLDQLTIFTDAIKRWEITG-TEQLPNFMKISLNALY 311
Mtr_2g082010       IARKIVAKLISVISLVDDTYDAYGTVEELELFTQAIQRWDISL-IQSLPECMQVVFNTIV 363
Mtr_2g082060       TSRKIVGKLVACISLLDDTYDAYGTVEELELFTQAIQRWDFSL-IQSLPKCMKVVFNTIV 359
Mtr_2g081980       TARKMVGKLVTCVSLLDDTYDAYGTVEELELFTEAMQRWDINV-IQSLPESMKVVFNSIV 351
Mtr_4g081460       FGRRIMTKVISLASVIDDIYDVYGTIEELQLFTQAIERWDISC-MDFLPQYMKFCYKAVL 357
Medtr5g094620      TGRKIMSKLIAILAVVDDTYDAYGTIGELELFTKAIERWDISC-LNNLPDYMRFLYKVIL 332
Medtr5g073260      TTRIIMMKQIITMTVIDDTYDAYGTIGELELFTEAIERLDISC-LDNLPDYMRFLYGIIL 347
Medtr5g073200      IGRKFMSKLIIIITAIDDAYDAYGTIDELELFTKAIERWDISC-LDDLPDYMKFLYKITL 344
Mtr_4g048460       RARKMLPKINVMLSLIDDTYDAYGTIEELERFTNAIERWDISC-LDDLPEYMKISYTALL 356
Medtr6g039440      QARKMLSKVNAILSFIDDTYDSYGTIDELELFTEAIERWDIDA-LNNLPDYMKLLYKSFW 348
Medtr6g008560      QARKMMIKVITLLSIIDDTYDAYGSIDELELFTKAIERWDISS-MDGLPNYMKLIYISVL 352
Mtr_2g089120       NCRIELTKTICILLVMDDIFDTYGTLDELVLFTKAIKRWDLDA-MDQLPEYMKICYMALY 361
Mtr_2g089130       NCRIELTKTICILDVIDDIFDNYGTLEDLVLFTKAIKRWDLDG-MEQLPEYMKICYMALY 361
Mtr_7g010710       SLRKWLTKVIIFVLVIDDVYDIHASFEELKPFTTAFQRWDAKE-IEDLPDYMKFCFNALQ 349
Mtr_4g045810       NIRKGLTKVCSLITLIDDIYDVYGTLDELELFTTAVESWDINA-IQILPEYMKIFFLALY 376
Mtr_2g065450       YYRKEMTKVNALITSIDDVYDVYGTLEELQLFTKAIDRWDLSA-MEFLPYYMKICFHALY 386
Mtr_3g058160       DSRLALAKSTVLVTVVDDFFDVGSSEEEQLNIIQLFKIWDVDVDTVCCSEAVKIIFSAMR 366
Mtr_2g012870       YIRMLVAKSAIIITVADDFFDEIGSLNELEILTDAIQRWDA----IGLSSHSKVIFDALD 549
Mtr_2g012900       YVRMFLAKSAIIITVADDFFDSIGSLNELQILTDAVQRWDT----RGLSSHSKVIFDALD 563
                     *  : *        ** :*  ..  :   :   .   .           :.
```

Figure 7.8: Amino acid sequence alignment of all 22 *M. truncatula* TPS-encoding genes containing the characteristic sequence motifs of the TPS family DDXXD.

Amino sequence showing only the DDXXD conserved region in 22 *M. truncatula*. Dashes indicate gaps inserted for optimal alignment. The region highlighted in blue is the highly conserved DDXXD motif. Asterix marks conserved amino acids.

7.9 Molecular characterization of *MtTPS25*

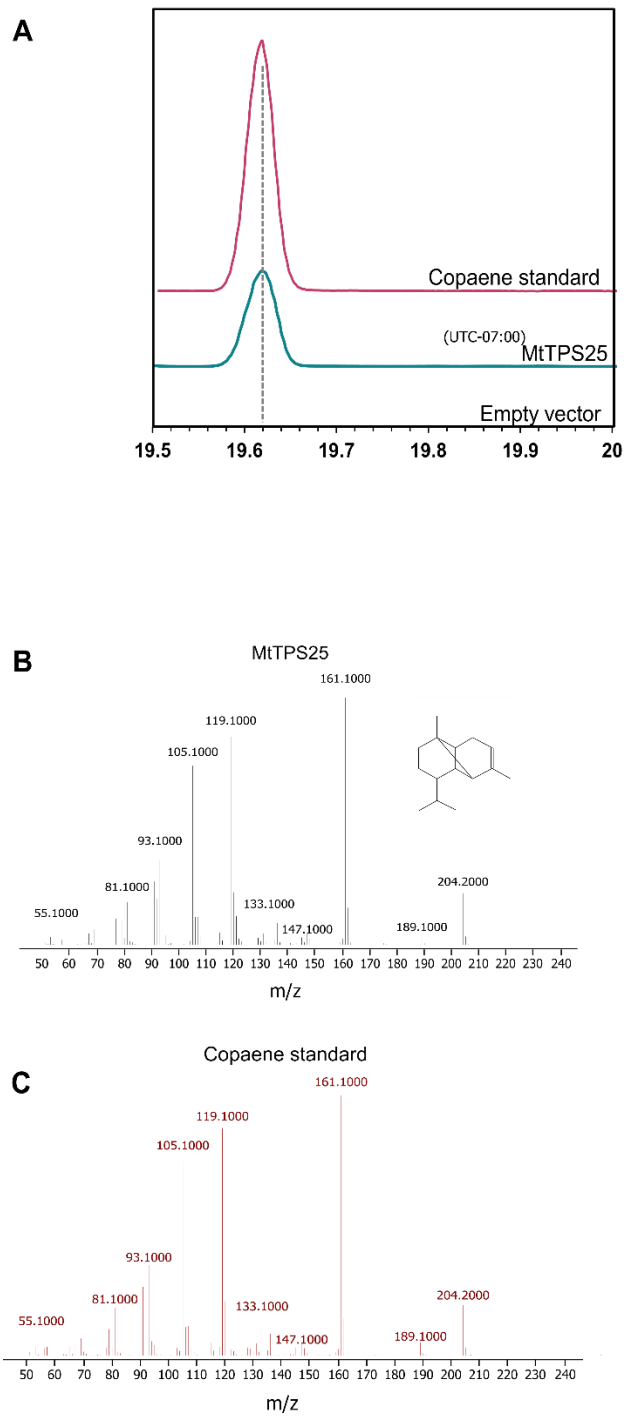

Figure 7.9: Yeast-extracted α-copaene compared to an authentic standard of α-copaene.

A. aligned extracted ion chromatogram for α-copaene (m/z 204.2). **B**. GC-MS spectra of MtTPS25 and **C**. GC-MS spectra of α-copaene standard.

7.10 Total number of transgenic potato plants expressing *MtTPS*

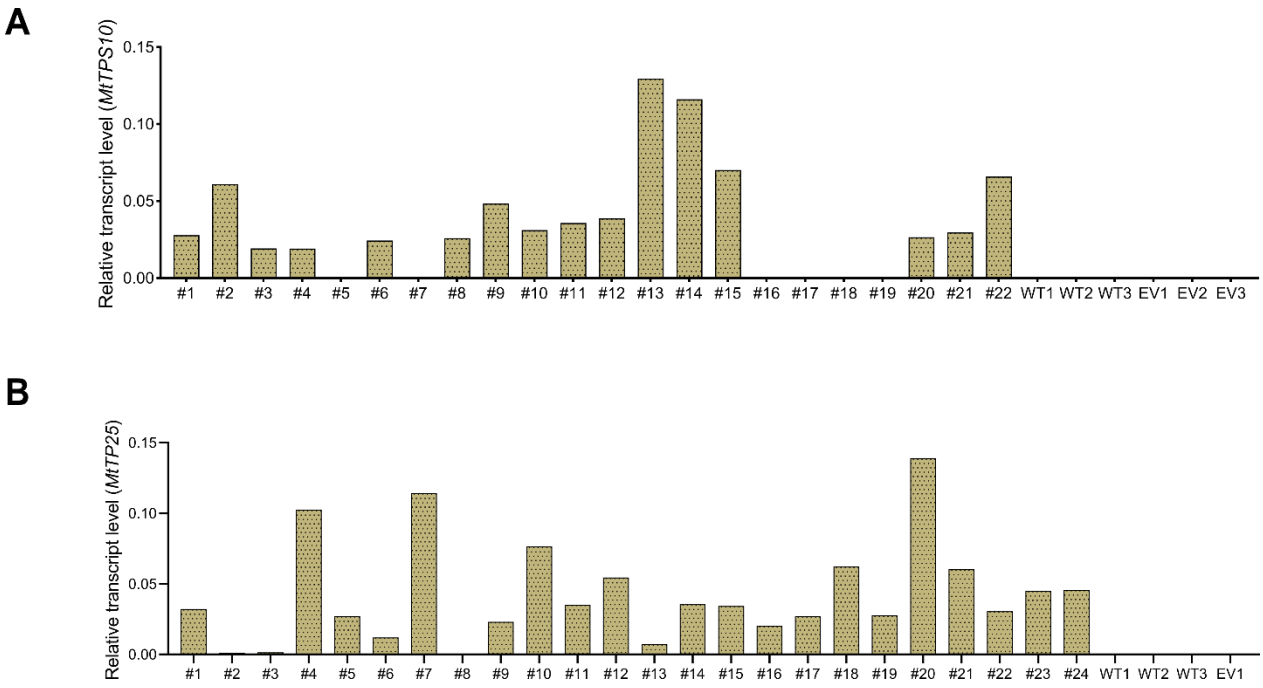

Figure 7.10: Complete number of transgenic potato plants expressing *MtTPS10* and *MtTPS25*.

A. Plants expressing *MtTPS10*. **B**. plants expressing *MtTPS25* . Numvers

7.11 Sequence similarity of MtTPS7 and MtTPS25

Figure 7.11: Amino acid alignment of MtTPS7 and MtTPS25.

Alignment of MtTPS7 and MtTPS25 exhibited 44% similarity in amino acid sequence according to NCBI blastp.

7.12 Expression of MtTPS10 after himachalol treatment.

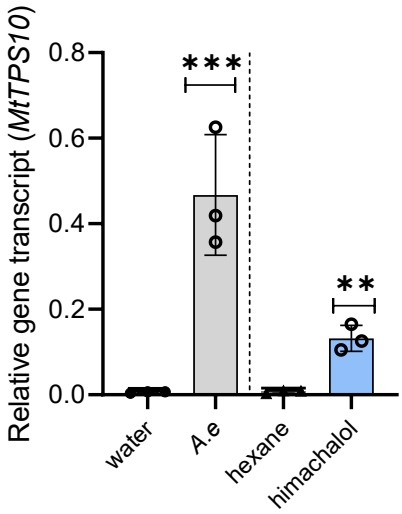

Figure 7.12: Expression of *MtTPS10* in the roots of one-week-old *M. truncatula* seedlings after application of himachalol, compared to roots treated with zoospores. Roots were treated for 2 h, treatment with water and solvent served as controls for incubation with zoospores and himachalol, respectively.Bars represent mean +/- SD (n = 3), *P < 0.05 and ***P < 0.001 according to Student's *t*-test

Table 7.1 cloning constructs

Plasmid	Purpose	Feature	Reference
pAGT564	Golden Gate Cloning	LacZ, empty vector	(Scheler *et al.*, 2016)
	Cloning	GGPPs	Dr. Martin Dippe
	Cloning	GPPs	Dr. Martin Dippe
pAGM1011	Golden Gate Cloning	ATR1	Dr. Sylvester Marillonnet
pAGM19821	Golden Gate Cloning	trHMGR	Dr. Sylvester Marillonnet
pAGH59	Protein expression in yeast	FPP:HMGCR: MtTPS10	(Yadav et al., 2019)
pAGH1501	Protein expression in yeast	FPP:HMGCR: MtTPS25	this thesis
pAGH1498	Protein expression in yeast	FPP:HMGCR: MtTPS10:ATR1: CYP71D62	this thesis
pAGH1499	Protein expression in yeast	FPP:HMGCR: MtTPS10:ATR1: CYP71D61	this thesis
pAGH1760	Protein expression in yeast	FPP:HMGCR: MtTPS10:ATR1: CYP71D63	this thesis
pAGH1287	Protein expression in yeast	Stable yeast expressing MtTPS10 products	this thesis
pAGH293	Golden Gate Cloning	*pMtTPS10*:GUS from A17	this thesis
pAGH1497	Golden Gate Cloning	*pMtTPS10*:GUS from 368	this thesis
pAGH1810	Golden Gate Cloning	*pMtTPS25*:GUS from A17	this thesis
pAGH1799	Golden Gate Cloning	*pMtTPS25*:GUS from 368	this thesis
pAGH1801	Golden Gate Cloning	*MtTPS25*_RNAi	this thesis
pAGH1915	Golden Gate Cloning	Potato transformation with *MtTPS10*	this thesis
pAGH1801	Golden Gate Cloning	Potato transformation with *MtTPS25*	this thesis
pAGH1919	Golden Gate Cloning	Localization of MtTPS25	this thesis

Table 7.2 Primers used in the thesis

Gene	Application	Direction	Sequence
MtTPS10	RT-qPCR	Forward	GGCAGGATAATGGATGACATTGC

		Reverse	GCATTCCAAGAATGAGGACATATG
MtActin2	RT-qPCR	Forward	ACTCACACCGTCACCAGAATCC
		Reverse	TCAATGTGCCTGCCATGTATGT
MtTPS25	RT-qPCR	Forward	CAACCTTCACACCATCTCAGTGC
		Reverse	TCCTTCAACATCAGTGGCAAGTT
MtTPS25	Localization	Forward	TTGAAGACAAAATGAATTCCTCTGGAGCT TTAGCAC
		Reverse	TTGAAGACAACGAAAATTGGCACCGGATC TACAAGC
Mtr_3g093980	RT-qPCR	Forward	TGCCTTCTCACCCCTTAGGA
		Reverse	TCTTGCCATGAGCATCAGCC
Mtr_3g083130	RT-qPCR	Forward	GCGATCATATCGGATATGTTCACG
		Reverse	TCTTGTTGTCAAAGGTACGACGC
Mtr_3g118390	RT-qPCR	Forward	CCCCAGTCACCTAAGCCATC
		Reverse	CACGATCTGCACTGGAAGGA
Mtr_5g075450	RT-qPCR	Forward	CGCCGTACCGGAAAGTCTG
		Reverse	GGCGAAACGACCAAGAGGA
Mtr_8g028568	RT-qPCR	Forward	CTGCTTCTGCCATCACACCA
		Reverse	CCCCTTGGATATGGTGACCC
Mtr_2g040510	RT-qPCR	Forward	TGCTCAAGTGTGCTACTGGG
		Reverse	TGATGGTCTGTCCCTCGGAT
CYP71D61	RT-qPCR	Forward	CGACGATCACAAAAGCATTCACA
		Reverse	CGCCCATAACACAGTCGTTGA
CYP71D62	RT-qPCR	Forward	TGATAGCACAAGACATCATCGAC
		Reverse	TTCGGTACCAGCAAGGAACA
MtTPS6	RT-qPCR	Forward	TGATAGCACAAGACATCATCGAC
		Reverse	TTCGGTACCAGCAAGGAACA
pMtTPS10	cloning	Forward	TTGGTCTCAACATGGAGCACCAAAATGCT TACGTGGCG
	Part A	Reverse	TTGGTCTCAACAAGTAGGCTAATAGACTG ATGATAACTAC
		Forward	TTGGTCTCAACATCTACGCCTGGGAGTTT AGATAACATTG
	Part B	Reverse	TTGGTCTCAACAACATTCTTCAAATTAATC AAAGGTGTTATAATAAGTGGCTC
pMtTPS25	cloning	Forward	TTGAAGACAAGGAGTCAATATCATTCAAC AACATTCAATTAATTAACAATCAGC
		Reverse	TTGAAGACAACATTATCATATAACTTGTTT AAATGGAATTCTTTTTTGGTTTGCG
MtTPS10	CDS	Forward	TTCAAAACCTTAGAGTTGAAAAAAGAGAGCC
		Reverse	GAAAGTTCACACATGACATGTTTTCTTTATTC
Mtcyp71d62		Primer 1	ATGGAGCTTCAAAATCCTTTTTCGAATATC
		Primer 2	TTAAAGACGACGAGTAGTAGGAATTAAAC
		Tnt1	CAGTGAACGAGCAGAACCTGTG
MtTPS6		Forward	GGTTATGGGTGAGAGTAGTG
		Reverse	CTCACGATCATTCAGTGTAG
*Ae*_5.8s rRNA		Forward	TGTCTAGGCTCGCACATCGA
		Reverse	AGTGCAATATGCGTTCAACGTTT
moclor	Sequencing	Forward	AGCGAGGAAGCGGAAGAGCG
		Reverse	GCCACCTGACGTCTAAGAAACC

EF1α	Housekeeping gene	Forward	ACTGCCCAGGTCATCATCA
		Reverse	GCACTGGAGCATATCCGTTT
P.infestans		Forward	CGTACGGCCAATGTAATTCC
		Reverse	TTTGCACAGTATCACGCAAGT

Table 7.3: Buffers used for protoplast isolation and transformation

W5									
Component	Stock conc.	Final conc.	50 ml	100 ml	200 ml	400 ml	500 ml		
NaCl	5 M	154 mM	1.54	3.08	6.16	12.32	15.4	ml	
$CaCl_2$	1 M	125 mM	6.25	12.5	25	50	62.5	ml	
KCl	0.1 M	5 mM	2.5	5	10	20	25	ml	
MES pH 5.7	0.2 M	2 mM	0.5	1	2	4	5	ml	
H_2O			39.21	78.42	156.84	313.68	392.1	ml	
WI									
Component	Stock conc.	Final conc.	5 ml	10 ml	15 ml	20 ml	30 ml	40 ml	
Mannitol	0.8 M	0.5 mM	3.15	6.3	9.45	12.6	18.9	25.2	ml
KCl	0.1 M	20 mM	1	2	3	4	6	8	ml
MES pH 5.7	0.2 M	4 mM	0.1	0.2	0.3	0.4	0.6	0.8	ml
H_2O			0.75	1.5	2.25	3	4.5	6	ml
MMG									
Component	Stock conc.	Final conc.	5 ml	10 ml	15 ml	20 ml	30 ml	40 ml	
Mannitol	0.8 M	0.4 M	2.5	5	7.5	10	15	20	ml
$MgCl_2$	0.15 M	15 mM	0.5	1	1.5	2	3	4	ml
MES pH 5.7	0.2 M	4 mM	0.1	0.2	0.3	0.4	0.6	0.8	ml
H_2O			1.9	3.8	5.7	7.6	11.4	15.2	ml
PEG									
Component	Stock conc.	Final conc.	5 ml	10 ml	15 ml	20 ml	30 ml	40 ml	
Mannitol	0.8 M	0.2 mM	1.25	2.5	3.75	5	7.5	10	ml
$CaCl_2$	1 M	0.1 mM	0.5	1	1.5	2	3	4	ml
PEG	Solid	40%	2	4	6	8	12	16	g
H_2O			1.5	3	4.5	6	9	12	ml
Enzyme solution									

Component	Stock conc.	Final conc.	5 ml	10 ml	15 ml	20 ml	30 ml	40 ml	
Mannitol	0.8 M	0.4 M	2.5	5	7.5	10	15	20	ml
KCl	0.1 M	20 mM	1	2	3	4	6	8	ml
MES pH 5.7	0.2 M	20 mM	0.5	1	1.5	2	3	4	ml
H_2O			0.95	1.9	2.85	3.8	5.7	7.6	ml
Cellulase R10		1.50%	75	150	225	300	450	600	mg
Macroenzyme R10		0.40%	20	40	60	80	120	160	mg
$CaCl_2$	1 M	10 mM	50	100	150	200	300	400	µl
BSA	0.1g/ml	1 mg/ml	50	100	150	200	300	400	µl

8 Acknowledgement

I would like to express my sincere gratitude to my supervisor, Prof. Dr. Bettina Hause, for her invaluable guidance, feedback, and support throughout my research. Her extensive knowledge and experience were instrumental in the completion of this thesis. I am grateful to her for providing emotional support during the challenging times of my PhD. I appreciate that she consistently strives to create a sound and worry-free environment for research.

I am also highly grateful to my co-supervisors, Prof. Dr. Alain Tissier and Prof. Sabine Rosahl, for their insightful suggestions and encouragement over the years. Their critical questions and comments pushed me to refine my thinking and brought greater depth to this work. I would also like to thank Dr. Sylvester Marillonnet, who has contributed immensely to the success of my research by consistently offering scientific advice, particularly regarding Golden Gate cloning.

I would like to thank the SZB PhD students for fostering a collaborative research environment. Their encouragement and willingness to share ideas created an atmosphere that was both intellectually enriching and personally rewarding. Special thanks to my students, Asmita Baral, Paola Diana Ochoa, and Alex Hattenbach, for their immense contributions to my research. Their hard work and dedication significantly advanced the progress of this work. I extend my appreciation to Dr. Yaming Liu and Dr. Alejandro Brand for their assistance with the GC-MS. To Dr. Arianna Schnabel for her help with microsomal extraction. To Ranjit Bharal for his constant support in the lab. To Dr. Jörg Ziegler and Dr. Manish Raorane for providing GC-MS machines for my measurements when the one I was using malfunctioned. To Dr. Martin Dippe and his technician, Nicole Hünecke, for their assistance with enzyme assays. To Dr. Khansa Mekkoui, who taught me all the basics in the lab and helped me adjust to the new working environment. To Hagen Stellmach for his help with microscopy and for all his encouragement and support during my PhD. Also, to Mandy Puffeld and Lena Braun for their support and immense contribution to the potato project. Mandy became a good friend during my work in IPB and I am grateful for her support and kindness, and the occasional food tips from her.

Aside from research, I had the opportunity to meet amazing people who have equally contributed to my professional growth at IPB. I would like to thank Dr. Alejandro Brand, who became a dear friend and always lent a sympathetic ear to all my problems and complaints and offered valuable advice. I am also thankful that he took time out of his busy schedule to read through my thesis and offered valuable additions. Special thanks to Rajit Baral, who also became a buddy, for whom I will forever be grateful. He was always supportive throughout my research and offered his time to read my thesis and was always ready to make time to help me. Thank you so much, Ranjit.

I want to thank Dr. Yaming Liu, who provided an excellent template for all my yeast experiments. Although he left after some time, he would constantly check in to find out how I was faring with the project. I also express my gratitude to Dr. Henna Yadav, who created an excellent foundation for my research in IPB. Also, a big thanks goes to Jayanth Gopinatha, for always being ready to help me troubleshoot my cloning. I also express my gratitude to Dr. Sarlita Dwiani for her constant encouragement throughout my writing and even to the day of printing.

I extend my heartfelt thanks to my Sunday fellowship group, with special appreciation to Prof. Imming and Cornelia Imming for graciously welcoming us to their home on Sundays. I am continually inspired and enriched by the profound insights they offer in the Scriptures.
Last but not least, I would like to thank my parents; without them, I would not be here today. They have always believed in me and supported every decision I made. A big thank you to my sister, who made my business her business and supported me through thick and thin.

Lastly, I thank God Almighty for the gift of life and His blessings throughout my life.

9 Curriculum vitae

Name	Esther Armah Harding
Gender	Female
Place of birth	Accra, Ghana
Nationality	Ghanaian

Education

Jan 2021-Till date	Ph.D. candidate at Leibniz Institute of Plant Biochemistry (IPB), Halle, Germany. **Thesis Title:** Dissecting gene metabolite relationship in the *Medicago truncatula* terpenome after *Aphanomyces euteiches* infection.
2017-2021	Master of Science in Crop Protection at the University of Göttingen, Germany. **Thesis Title:** Fungal trichothecenes and hydroxamic acid in the infection of maize with *Fusarium graminearum.*
2012-2016	Bachelor of Science at the University of Ghana. **Thesis Title:** Molecular and morphological characterization of *Solanum lycopersicum* accessions.

Scientific activities

Botanik-Tagum 2024, Germany: Selected for oral presentation 'Dissecting gene metabolite relationship in the *Medicago truncatula* terpenome after *Aphanomyces euteiches* infection'.

International Plant Immunity conference 2024, Germany: Selected for poster presentation ' Root terpenoids, the hidden part of plant defense in the case of *Medicago truncatula* and *Aphanomyces euteiches*.

TERPNET 2022, USA: Selected for oral presentation ' Root terpenoids, the hidden part of plant defense in the case of *Medicago truncatula* and *Aphanomyces euteiches.*

Supervision roles

06.2023-09.2023	**Bachelor thesis supervised at IPB** **Title:** Validation of differentially expressed genes in two *Medicago truncatula* ecotypes after *Aphanomyces euteiches* infection.
09.2021-12.2022	**Bachelor's thesis supervised at IPB**

	Title: Gene expression analysis in the roots of *M. truncatula* after *A. euteiches* infection.
09.2022-03.2023	**Master thesis supervised at IPB**
	Title: Cell specificity and systemic induction of *MtTPS10* in defense of *M.truncatula* roots against *A. euteiches*.
2025-Till date	**Internship at IPB**
	Title: The Role of Sesquiterpenoids in Plant Defense against Pathogens.
2025-Till date	**Bachelor Thesis supervised at IPB**
	Title: Assessing the possible terpenoid tradeoff before and after pathogen infection in *MtTPS* overexpression potato plants.

Work experience

08.2018-10-2018	**Intern at the Julius Kuhn Institute (JKI).** Germany, Dossenheim **Title:** Understanding the Interaction of Indigenous *Cacopsylla species* with *Pandora fungus.*
2016-2017	**Research assistant at University of Ghana**
08.2013-09.2013	**Intern at the Noguchi Memorial Institute of Medical Research, Ghana** **Title:** Characterization and identification of tropical diseases in Africa.

10 Eidesstattliche Erklärung

Hiermit erkläre ich, dass ich die vorliegende wissenschaftliche Arbeit selbständig und ohnefremde Hilfe angefertigt habe. Ich erkläre, dass ich keine anderen als die von mir angegebenen. Quellen und Hilfsmittel benutzt habe und die den Werken wörtlich und inhaltlich entnommenen Stellen als solche kenntlich gemacht habe. Ich versichere weiterhin, dass ich mich erstmals mit dieser Arbeit um die Erlangung des Doktorgrades bewerbe. Diese Arbeit wurde an keiner anderen Fakultät oder Universität zur Begutachtung eingereicht.

Esther Armah Harding

Halle (Saale)